

# Functional role of a polysialic acid- carrying proteolytic fragment of the neural cell adhesion molecule NCAM in the nervous system

## DISSERTATION

Zur Erlangung des Doktorgrades der  
Naturwissenschaften (*doctor rerum naturalium*)

des Departments Biologie  
der Fakultät für Mathematik, Informatik und Naturwissenschaften  
an der Universität Hamburg

Vorgelegt von  
NINAWESTPHAL  
Hamburg, 2017

Diese Arbeit wurde am Zentrum für Molekulare Neurobiologie Hamburg (ZMNH), im Institut für Biosynthese Neuraler Strukturen durchgeführt.

Gutachter: Frau Prof. Dr. M. Schachner

Herr Prof. Dr. T. Burmester

Tag der Disputation: 07.03.2017

# Contents

---

Statement of Contribution .....	I
1. Introduction .....	1
1.1 Structure, isoforms and proteolytic processing of NCAM .....	2
1.2. N-glycosylation of NCAM and attachment of polysialic acid .....	3
1.3 Functions of polysialylated NCAM in the central nervous system .....	5
1.4 Interaction of PSA and/or NCAM with other molecules.....	6
1.5 PSA-NCAM- mediated downstream signalling .....	7
1.5.1 Fyn and focal adhesion kinase (FAK) dependent signal transduction .....	8
1.5.2 Fibroblast growth factor (FGF)-receptor mediated signal transduction.....	8
1.5.3 Protein kinase C (PKC) and MARCKS-dependent signal transduction .....	9
2. Rationale and Aim of the study .....	11
3. Material .....	12
3.1 Animals .....	12
3.2 Cell lines.....	12
3.3 Primers .....	12
3.4 Antibodies .....	13
3.5 Reagents .....	15
3.6 Inhibitors .....	17
3.7 Buffers and solutions.....	17
4. Methods .....	22
4. 1 Primary cell culture / cell lines.....	22
4. 2 Cell surface biotinylation and cell treatment.....	22
4. 3 Preparation of mouse brain tissue sections and coronal brain slices .....	23
4. 4 Polyethylene glycol precipitation of chicken NCAM antibody from egg yolk .....	24
4. 5 Preparation of cytoplasmic fraction and microsome fractions .....	24
4. 6 Subcellular protein fractionation .....	25
4. 7 Isolation of PSA-carrying proteins by immunoprecipitation (IP) and N-glycan digestion .....	26

4. 8 <i>In vitro</i> translocation and nuclear import assay .....	27
4. 9 S-nitrosylation assay .....	28
4. 10 Protein determination and precipitation .....	29
4. 11 Sodium dodecyl sulfate polyacrylamide gelelectrophoresis (SDS-PAGE) and immunoblot analysis ....	30
4. 12 Enzyme-linked immunosorbent assay (ELISA) .....	30
4. 13 Measurement of nitric oxide levels .....	31
4. 14 Proximity ligation assay .....	32
4. 15 Immunoelectron microscopy .....	33
4. 16 RNA isolation and microarray analysis.....	34
4. 17 Quantitativ real-time polymerase chain reaction (qRT-PCR) .....	35
4. 18 Statistical analysis .....	37
5. Results .....	39
5. 1 Nuclear import of a PSA-carrying proteolytic NCAM fragment in cultured cerebellar neurons .....	39
5.2 PSA co-localizes with histone H1 in nuclei of wildtype cerebellar neurons .....	43
5.3 Detection of nuclear PSA by immunoelectron microscopy .....	45
5.4 The nuclear PSA-carrying NCAM fragment is generated by matrix-metalloproteases MMP-2 and MMP-9 upon treatment with NCAM antibody .....	46
5.5 The PSA-carrying NCAM fragment is transported from the plasma membrane to the nucleus via late endosomes .....	48
5.6 The PSA-carrying NCAM fragment is released from endosomes into the cytoplasm in a calmodulin-dependent manner .....	50
5.7 Binding of PSA-NCAM to PC4 and cofilin in nuclei of dissociated cerebellar neurons and cerebellar tissue.....	53
5.7.1 PC4 and cofilin contribute to the translocation of the PSA-carrying NCAM fragment from the cytoplasm into the nucleus.....	57
5.9 NCAM antibody, FGF-2 and the MARCKS-derived ED peptide trigger phosphorylation of MARCKS and induce the generation and nuclear import of the PSA-NCAM fragment .....	58
5.10 The generation of the PSA-carrying NCAM fragment is induced by different pathways which require activation of the FGF-receptor .....	60
5.10.1 The FGF-2- and NCAM antibody-induced generation and nuclear import of the PSA-carrying NCAM fragment depends on calmodulin-induced NO synthesis and NO-mediated activation MMP-9 ....	61
5.10.2 MARCKS-ED peptide-induced generation and nuclear import of the PSA-carrying NCAM fragment requires FGF-receptor-mediated PKC-, PLC-, PLD-, and PI3K-dependent activation of MMP-2 .....	65
5.11 Nuclear PSA-NCAM is involved in the circadian rhythm <i>in vitro</i> and <i>in vivo</i> .....	69

5.11.1 Nuclear import of the PSA-NCAM fragment affects mRNA expression of the clock-related genes CLOCK and Per-1 in cerebellar neurons .....	69
5.11.2 Nuclear PSA-NCAM fragment levels in the cerebellum and suprachiasmatic nucleus are associated with reduced expression of clock-related genes .....	72
5.12 PSA-carrying NCAM co-localizes with histone H1 <i>in vivo</i> during the light/dark cycle .....	76
5.13 The effect of the PSA-lacking NCAM and PSA-carrying NCAM fragments on the gene expression of distinct genes.....	80
5.13.1 Nuclear NCAM regulates the expression of Lrp2 and $\alpha$ -synuclein whereas nuclear PSA-NCAM regulates the expression of Nr2f6 .....	80
5.13. Nuclear PSA-NCAM regulates the expression of Nr2f6 differentially during the circadian rhythm <i>in vitro</i> and <i>in vivo</i> .....	88
6. Discussion .....	91
5.1 PSA-carrying NCAM is cleaved at the plasma membrane by MMP-2 and/or MMP-9 upon treatment of cerebellar neurons with surrogate NCAM ligands.....	91
5.2 The PSA binding partners BDNF and histone H1 do not induce the generation and the nuclear import of the PSA-carrying NCAM fragment.....	93
5.3 The generation and nuclear import of the PSA-carrying NCAM fragment is triggered by FGF-2 and by myristoylated alanine-rich C-kinase substrate (MARCKS-ED peptide through a FGF-receptor mediated signaling cascade .....	94
5.3.1 Generation of the transmembrane PSA-NCAM fragment through a FGF-receptor- mediated calmodulin/NOS-dependent signaling pathway upon treatment of cerebellar neurons with NCAM antibody or FGF-2 .....	96
5.3.2 Generation of the transmembrane PSA-NCAM fragment through the FGF-receptor-mediated PLD/PI3K signaling cascade upon treatment of cerebellar neurons with MARCKS-ED peptide.....	97
5.4 Translocation of the transmembrane PSA-carrying NCAM fragment from the endosomes into the cytoplasm is calmodulin-dependent whereas PC4 and cofilin are involved in the import of the fragment into the nucleus .....	99
5.5 Nuclear PSA-NCAM plays a role in the circadian rhythm and is involved in the gene expression of the clock-related genes Per-1, CLOCK and Nr2f6.....	101
5.6 Nuclear PSA-lacking NCAM is involved in the gene expression of Lrp2 and $\alpha$ -synuclein.....	102
7. Summary .....	104
8. Zusammenfassung .....	106
9. Abbreviations .....	108
10. References .....	111
11. Acknowledgements .....	121

**STATEMENT OF CONTRIBUTION**

---

A part of this work is published in *Molecular and Cellular Neuroscience*:

**Westphal, N.**; Kleene, R.; Lutz, D.; Theis, T.; Schachner, M. (2016) Polysialic acid enters the cell nucleus attached to a fragment of the neural cell adhesion molecule NCAM to regulate the circadian rhythm in mouse brain. *Molecular and Cellular Neuroscience* 74, pp. 114-127.

Contributions of the authors to this work are indicated within the figure legends.

## 1. INTRODUCTION

---

The development and proper functioning of the nervous system requires the concerted formation of contacts between neural cells, glial cells and the extracellular matrix (ECM). Cell adhesion molecules are cell surface proteins which play important roles for the organization of these connections and for the formation of neural networks which control cognition, emotion, behavior as well as motor and sensory functions (Benson *et al.*, 2001). Cell adhesion molecules belong to several families of cell surface glycoproteins. Members of the cadherin family, selectin family and integrin family mediate cell-cell interactions and/or cell-ECM adhesions in a calcium-dependent manner, whereas members of the Ig superfamily promote calcium-independent cell adhesions. These cell adhesion molecules are involved in regulation of cell surface receptors and cellular dynamics, in attraction and repulsion of cells, in signal transduction from the cell surface into the cell interior and in communication between cells (Maness and Schachner, 2007; Shapiro *et al.*, 2007).

Interestingly, cell adhesion molecules and, in addition, cell surface receptors are not only present at the plasma membrane, but also have been found in the nucleus (Hart and West, 2009). In the nucleus, they play an important role in cell signaling, proliferation and differentiation. Moreover there is strong evidence that these nuclear glycoproteins function as transcription regulators (Planque *et al.*, 2006). Examples for nuclear cell surface glycoproteins are: The proteoglycan syndecan (Brockstedt *et al.*, 2002), the fibroblast growth factor (FGF) (Zong *et al.*, 2009), fibroblast growth factor receptor (FGFR) (Reilly and Maher, 2001), the epidermal growth factor receptor (EGFR) (Wang and Hung, 2012), and transmembrane fragments of the neural cell adhesion molecule (NCAM) and of the cell adhesion molecule L1 (L1) (Kleene *et al.*, 2010a; Lutz *et al.*, 2012).

For the transmembrane proteoglycan syndecan and FGF a tubulin-dependent nuclear import during the cell cycle has been shown (Brockstedt *et al.*, 2002; Zong *et al.*, 2009). The nuclear import of the FGF-receptor whas been shown by a different mechanism and is dependent on importin- $\beta$  (Reilly and Maher, 2001). A well-studied receptor for the trafficking within the different cell compartments after endocytosis at the plasma membrane is EGFR. EGFR is involved in the regulation of transcription and was found to act as signal transmitter after recruitment from the cell surface into the cell nucleus (Wang and Hung, 2012). In the nucleus, growth factors and cell surface receptors seem to regulate gene transcription (Planque *et al.*, 2006). Proteolytic transmembrane fragments of NCAM and L1 are imported

into the cell nucleus and are involved in neurite outgrowth upon treatment of cultured neurons with function-triggering antibodies as ligands (Kleene *et al.*, 2010a; Lutz *et al.*, 2012). In addition exogenous forms of growth factors are reported to shuttle within the cell compartments (Klingenberg *et al.*, 2000).

### 1.1 Structure, isoforms and proteolytic processing of NCAM

NCAM is a member of the immunoglobulin (Ig) superfamily and exists in three major isoforms: NCAM120, NCAM140 and NCAM180. These isoforms differ in their molecular masses and derive from a single gene by alternative splicing of certain exons. All three isoforms have an extracellular domain consisting of five Ig-domains and two fibronectin type III (FNIII) homologous repeats (**Figure 1**) (Cunningham *et al.*, 1987). NCAM140 and NCAM180 contain a transmembrane domain and intracellular domains which differ in an additional sequence stretch in NCAM180. In contrast to NCAM140 and NCAM180, NCAM120 lacks a cytoplasmic domain and is linked to the plasma membrane by a glycosylphosphatidylinositol (GPI) (He *et al.*, 1986; Cunningham *et al.*, 1987).

NCAM120 kDa is predominantly expressed by glial cells (Bhat and Silberberg, 1988), while NCAM140 is expressed by neurons and glia cells. NCAM 180 is only expressed by neurons and it is predominantly found at postsynaptic densities (Persohn *et al.*, 1989; Saffell *et al.*, 1995), while neuronal NCAM140 localizes at growth cones of axons and dendrites and on axon shafts. NCAM is also present in non-neuronal tissue like muscle, kidney, sex organs, pancreas and liver (Kolkova *et al.*, 2010).

The proteolytic cleavage of NCAM140 and NCAM180 in their extracellular domains generates soluble NCAM forms with molecular masses of 110 -190 kDa (He *et al.*, 1986; Probstmeier *et al.*, 1994). An extracellular shedding of NCAM140 and/or NCAM180 by the serine protease plasmin has been shown upon activation of plasminogen in rat and mouse brain homogenates by the tissue-type plasminogen activator (tPA). Furthermore, the proteolysis of NCAM was demonstrated in mouse brain after injection of tPA into the lateral cerebral ventricle of the hippocampus (Endo *et al.*, 1998, 1999), indicating that plasmin cleaves NCAM under *in vivo* conditions. Previous *in vitro* studies showed that NCAM140 and NCAM180, but not the GPI-anchored NCAM120, are cleaved at the plasma membrane by ADAM (a disintegrin and metalloprotease) 17 (also known as tumor necrosis factor alpha converting enzyme (TACE)) resulting in a soluble extracellular 110 kDa NCAM fragment (Kalus *et al.*, 2006). ADAM17/TACE-mediated cleavage of NCAM is required for NCAM-



induced promotion of neurite outgrowth. In contrast to NCAM140 and NCAM180, the NCAM120 is cleaved by phosphatidylinositol-specific phospholipase C to generate a soluble NCAM form (He *et al.*, 1986). It is noteworthy to mention, that calcium-dependent proteolysis of NCAM180 in its intracellular domain by calpain has been reported (Covault *et al.*, 1991; Sheppard *et al.*, 1991).

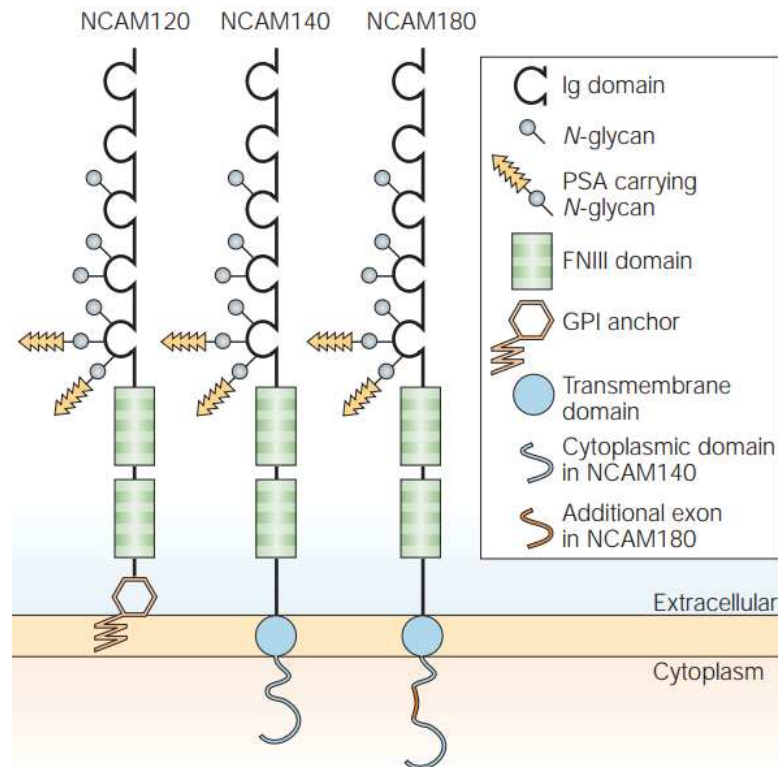


**Figure 1: Isoforms of the neural cell-adhesion molecule (NCAM).** The glycosylphosphatidylinositol (GPI)-anchored NCAM120 and the transmembrane NCAM140 and NCAM180 consist of five immunoglobulin (Ig)-like domains and two fibronectin type III repeats (FNIII). The cytoplasmic domains of NCAM140 and NCAM180 differ in length owing to the presence of an additional sequence in NCAM180 which results from alternative splicing (Kleene and Schachner, 2004).

## 1.2. N-glycosylation of NCAM and attachment of polysialic acid

The NCAM core protein undergoes N-glycosylation in the endoplasmic reticulum (ER) and Golgi complex (Finne *et al.*, 1982; Kiss and Rougon, 1997; Maness and Schachner, 2007). Six potential N-glycosylation sites at the asparagine (Asn) residues of the asparagine-X-serine/threonine (Asn-X-Ser/Thr) motif are present in the third, fourth and fifth Ig domains of murine NCAM (Figure 2) (Albach *et al.*, 2004). A homopolymer of up to 100  $\alpha$ -2,8-linked N-acetyl-neuraminic acid (sialic acid) residues (named polysialic acid or PSA) is attached by the polysialyltransferases ST8SiaII and/or ST8SiaIV to the N-glycans at the fifth and sixth N-glycosylation site in the fifth Ig domain of the extracellular domain of NCAM (Nelson *et al.*,

1995; Mühlenhoff *et al.*, 1998; Geyer *et al.*, 2001; von der Ohe *et al.*, 2002). Of note, all three isoforms can be post-translational modified by glycosylation with PSA. Besides polysialylation of NCAM, polysialylation of the synaptic cell adhesion molecule synCAM and of neuropilin 2 has been reported (Werneburg *et al.*, 2005; Curreli *et al.*, 2007).

PSA is a highly negatively charged molecule due to the carboxyl groups of the sialic acid residues and it decreases the homophilic and heterophilic interactions of NCAM due to its electric force and its huge hydration volume, which occupies a large space. Furthermore, polysialylation changes the adhesive properties of NCAM to repulsive properties (Johnson *et al.*, 2005).

The expression of NCAM starts during the closure of the neural tube and increases until the adulthood, while the expression of polysialylated NCAM starts to increase during early embryonic development, reaches its maximum in early postnatal stages and decreases to very low levels in later stages (Kurosawa *et al.*, 1997; Oltmann-Norden *et al.*, 2008). Polysialylated NCAM140 and NCAM180 but not NCAM120 were detectable at early embryonic stages (Probstmeier *et al.*, 1994).

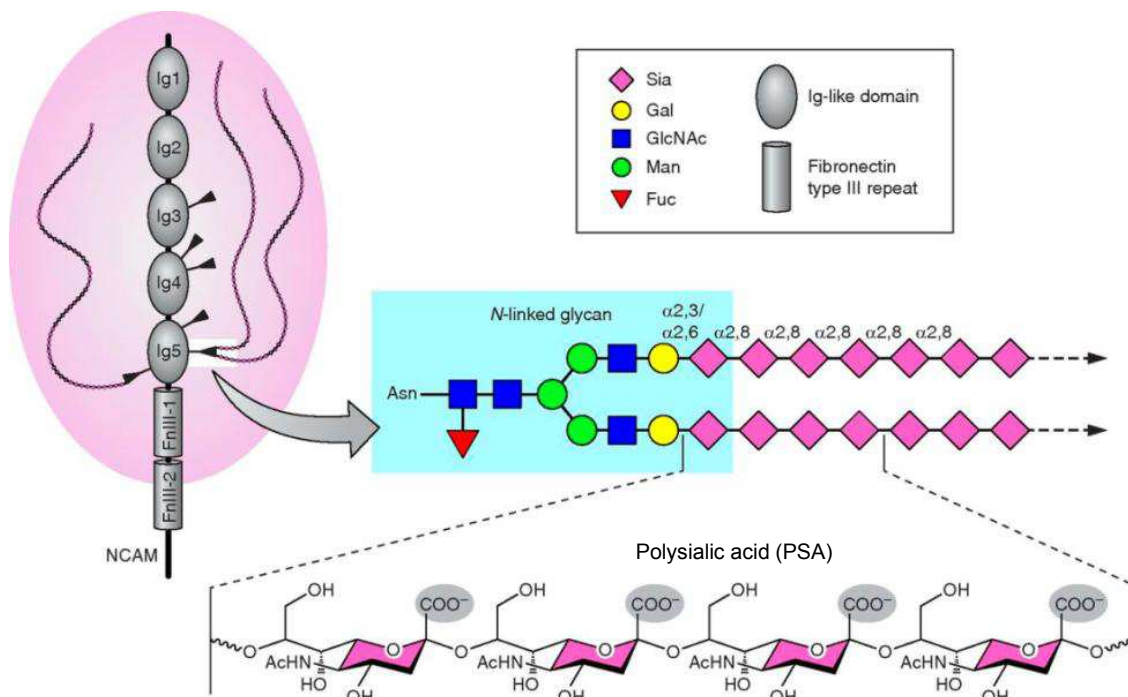


**Figure 2: Schematic representation of polysialylated NCAM.** The cell adhesion molecule NCAM consisting of five immunoglobulin-like modules (Ig1 – Ig5) and two fibronectin-type III repeats (FnIII-1 and FnIII-2), contains six N-glycosylation sites in Ig3, Ig4 and Ig5 (black arrowheads). The two N-glycosylation sites located in the fifth Ig domain can be polysialylated. The PSA chain comprises up to 100 monomers and is linked to a terminal  $\alpha 2,3$  or  $\alpha 2,6$  linked sialic acid residue of complex N-glycans forming polyanions (negatively charged carboxyl groups are highlighted with gray spheres) (modified from Schnaar *et al.*, 2014).

### 1.3 Functions of polysialylated NCAM in the central nervous system

During development PSA-NCAM plays an important role in the regulation of dynamic cellular processes, e.g. differentiation and migration of neuronal precursor cells, axonal outgrowth, synaptogenesis, physiological and morphological synaptic plasticity, and control of the circadian rhythm (Angata *et al.*, 2004; Oltmann-Norden, 2008; Bonfanti and Theodosis 2009). In mice, the levels of polysialylated NCAM decrease during the first 3-4 postnatal weeks, while the levels of non-polysialylated NCAM concomitantly increase. In the adulthood, the expression of PSA-NCAM is restricted to brain regions which are associated with persistent neural plasticity, remodeling of neural connections or neuronal regeneration (Chuong and Edelman, 1984; Gascon *et al.*, 2007; Oltmann-Norden, 2008). In adult mammals, PSA-NCAM is upregulated after injury of the central and peripheral nervous system and enhances axon regrowth in the peripheral nervous system and sprouting in the central nervous system, indicating an important role of PSA-NCAM in regeneration in the adulthood (Kleene and Schachner, 2004; Franz *et al.*, 2005; El Maarouf and Rutishauser 2010).

The presence of PSA on immature neurons in the hippocampus of mice and rats during development indicates that PSA-NCAM plays an important role in the de novo synthesis of neurons from stem cells (Rutishauser, 2008). In the adulthood, PSA-NCAM is involved in the regulation of cell proliferation and differentiation during neurogenesis after injury (Seki, 2008). While the distribution of PSA-NCAM in certain brain regions is not well studied so far, the physiological functions of PSA-NCAM have been intensively examined in brain regions associated with learning and memory like hippocampus, amygdala, the piriform cortex and neocortex (Rutishauser, 2008; Brennaman *et al.*, 2011). NCAM-deficient and ST8SiaIV-deficient mice show morphological abnormalities and impairment of long term potentiation (LTP) in the hippocampus (Muller *et al.*, 1996, 2000). Furthermore, altered spatial learning and memory was observed in rats after injection of PSA-digesting endosialidase (Endo) N into the hippocampus (Becker *et al.*, 1996). Since deficits in learning and memory are linked to schizophrenia and other psychiatric disorders like bipolar disorder and autism spectrum disorder, it is conceivable that PSA-NCAM plays a role in the development of these neurological disorders. Over-expression of PSA in the substantia nigra is associated with Parkinson disease (Sato *et al.*, 2016), implicating a role of PSA-NCAM in Parkinson's disease. Moreover, PSA has been found in the suprachiasmatic nucleus (SCN) which is the residence of the master circadian clock and is crucial for the generation and

entrainment of circadian rhythmicity in mammals (Glass *et al.*, 1994; Shen *et al.*, 1997; Shen *et al.*, 1999; Shen *et al.*, 2001; Fedorkova *et al.*, 2002). The circadian rhythm is regulated by the daily light-dark cycle and nonphotic inputs as locomotor activity, social interaction and sleep and it has been shown that PSA is involved in this process (Glass *et al.*, 2000; Prosser *et al.*, 2003; Glass *et al.*, 2003; Glombek and Rosenstein 2010). The mechanisms by which PSA regulates rhythmicity have remained largely unexplored. Since the circadian rhythm is controlled by circadian clocks like SCN through transcriptional-translational feedback loops which are mediated by clock-related genes (Ko and Takahashi 2006), it points out that PSA influences the gene expression of clock-related genes.

In summary, these combined observations suggest that PSA is important for proper learning, memory and social behavior as well as regulation of circadian rhythmicity.

#### **1.4 Interaction of PSA and/or NCAM with other molecules**

NCAM can homophilically interact in a cis- or trans-orientation with other NCAM molecules at the cell surface of the same or another cell, respectively. In addition, a number of heterophilic interactions of NCAM with other proteins have been reported (Brummendorf and Rathjen, 1995). Among these interaction partners are the cell adhesion molecule L1 (Horstkorte *et al.*, 1993),  $\alpha$ -amino-3-hydroxy-5-methyl-4-isoxazolepropionic acid (AMPA) and N-methyl-D-aspartate (NMDA) glutamate receptors (Vaithianathan *et al.*, 2004; Hammond *et al.*, 2006), glia-derived neurotrophic factor (GDNF) (Paracha *et al.*, 2003), fibroblast growth factor FGF (Francavilla *et al.*, 2007; Kochoyan *et al.*, 2008), FGF-receptor (Kiseljov *et al.*, 2005), and brain-derived neurotrophic factor (BDNF) (Muller *et al.*, 2000), as well as heparin and chondroitin sulphate proteoglycans (Cole *et al.*, 1986; Milev *et al.*, 1994; Storms and Ruthishauser, 1998) which all have been shown to interact with the extracellular domain of NCAM. Moreover, the interaction of these proteins with NCAM is often modulated or dependent on PSA (Brummendorf and Rathjen, 1995). Spectrin (Leshchyn'ska *et al.*, 2003), the BDNF receptor TrkB (Cassen *et al.*, 2010) and the inwardly rectifying K<sup>+</sup> channel Kir3.3 (Kleene *et al.*, 2010b), as well as the phosphatase RPTP $\alpha$  (Bodrikov *et al.*, 2005), focal adhesion kinase (FAK) and calmodulin (Kleene *et al.*, 2010a) are among the proteins which bind to the intracellular NCAM domain. The binding of NCAM to L1 has an effect on L1-mediated cell aggregation and adhesion (Horstkorte *et al.*, 1993), while binding of spectrin to NCAM and formation of the NCAM/spectrin complex is essential for synaptic signaling and required for the neuritogenic effects of NCAM and the activation of protein kinase C (PKC) (Leshchyn'ska *et al.*, 2003). The interaction of AMPA and NMDA receptors with PSA-

NCAM has been shown to play an important role in synapse formation during development (Vaithianathan *et al.*, 2004; Hammond *et al.*, 2006). The interaction of NCAM with TrkB has been shown to regulate phosphorylation of NCAM and NCAM-dependent neurite outgrowth by TrkB-mediated regulation of Kir3.3 (Cassen *et al.*, 2010; Kleene *et al.*, 2010b).

In contrast to NCAM, only a few PSA binding partners have been identified yet. Histone H1 (Mishra *et al.*, 2010), and BDNF (Muller *et al.*, 2000; Vutskits *et al.*, 2001) as well as the FGF-2 and FGF-receptor (Ono *et al.*, 2012), which both also bind to NCAM, were found to interact with PSA in the extracellular space, while a direct interaction between MARCKS and PSA in the plasma membrane has been reported (Theis *et al.*, 2013). Interestingly, application of BDNF and recombinant PSA-NCAM as well as colominic acid, which is a bacterial homolog of PSA, were shown to rescue impaired LTP in PSA-NCAM-deficient mice (Patterson *et al.*, 1996; Muller *et al.*, 2000). Abnormalities in BDNF-dependent induced signal pathways in NCAM-deficient mice may be due to reduced phosphorylation of the BDNF receptor TrkB (Helm *et al.*, 2015), which is a interaction partner of NCAM, suggesting that PSA-NCAM mediates BDNF-dependent signaling. This notion is supported by the finding that PSA-NCAM is involved in BDNF-dependent neuronal survival and differentiation of cortical neurons (Vutskits *et al.*, 2001; Kiseljov *et al.*, 2005). NCAM has an inhibiting effect in FGF-induced FGF-receptor-mediated signaling and cell proliferation in cultured mouse fibroblast cells (Francavilla *et al.*, 2007; Kochoyan *et al.*, 2008). Direct interaction of PSA with FGF-2 is required for FGF-mediated FGF-receptor signaling to trigger cell growth (Ono *et al.*, 2012). The extracellular interaction of PSA with histone H1, which is a nuclear protein that is also present outside of the cell (Parseghian and Luhrs, 2006), is of importance for nervous system development and regeneration after injury in adult mice (Mishra *et al.*, 2010). A recent study showed that the direct interaction of PSA with the effector domain of myristoylated alanine-rich C-kinase substrate (MARCKS) within the plane of the plasma membrane from opposite sites is involved in the regulation of neurite outgrowth in hippocampal neurons (Theis *et al.*, 2013).

### **1.5 PSA-NCAM- mediated downstream signalling**

Heterophilic and/or homophilic PSA-NCAM interactions are involved in regulation of signal transduction. The presence of PSA influences NCAM-dependent signal transduction through its biophysical characteristics, e.g. large hydration volume and electric force, and by modifying functional properties of NCAM as well as by modulating the interaction of NCAM with its binding partners.

### 1.5.1 Fyn and focal adhesion kinase (FAK) dependent signal transduction

Palmitoylation of NCAM is required for the recruitment of NCAM to lipid microdomains (so called lipid rafts) to activate the non-receptor tyrosine kinases fyn and FAK which interacts with NCAM (Beggs *et al.*, 1997; Bodrikov *et al.*, 2005; Ponimaskin *et al.*, 2008; Kleene *et al.*, 2010a). Fyn is located in lipid rafts and is inactivated through tyrosine phosphorylation. Upon stimulation of NCAM-dependent signaling by NCAM ligands, e.g. function-triggering NCAM antibodies, NCAM shifts to lipid rafts, activates RPTP $\alpha$ , which binds to NCAM in lipid rafts. This interaction leads to a subsequent dephosphorylation and activation of fyn by RPTP $\alpha$  and binding of fyn to NCAM (Beggs *et al.*, 1997; Niethammer *et al.*, 2002; Maness and Schachner, 2007). NCAM-stimulated activation of fyn and FAK triggers then activation of the G-proteins Ras and Raf and the downstream mitogen-activated protein (MAP) kinase and extracellular signal-regulated kinases (Erk) pathway cascade (He and Meiri, 2002; Kolkova *et al.*, 2010). NCAM-induced neurite outgrowth in cells expressing NCAM140 has been demonstrated to occur through activation of FAK, Ras, Raf and Erk (Maness and Schachner, 2007). The MAPK/Erk-associated pathway triggers neurite outgrowth by activation of the transcription factor cAMP response element-binding protein (CREB) (Schmidt *et al.*, 1999). NCAM-stimulation of neurite outgrowth is also associated with the proteolytic processing of NCAM and of phosphorylated FAK, and the subsequent calmodulin-dependent import of a transmembrane NCAM fragment and a phosphorylated N-terminal FAK fragment into the nucleus (Kleene *et al.*, 2010a). Calmodulin not only acts as a carrier molecule and plays an important role for the transport of these fragments on their way to the nucleus, but it is also required for the activation and cleavage of FAK (Kleene *et al.*, 2010a). Moreover, activation of fyn/FAK signaling affects neurite outgrowth in cortical and hippocampal neurons (Hubschmann *et al.*, 2005; Hinkle *et al.*, 2006). Of note, the activation of GDNF, which binds to NCAM, leads to NCAM-dependent fyn and FAK activation (Paracha *et al.*, 2003).

### 1.5.2 Fibroblast growth factor (FGF)-receptor mediated signal transduction

The binding of the FGF-receptor to the first and second fibronectin domain of NCAM induces NCAM-mediated enhancement of intracellular Ca<sup>2+</sup>-levels and FGF-receptor-triggered activation of phospholipase C (PLC) (Williams *et al.*, 1994; Walsh and Doherty, 1996). Stimulation with a synthetic NCAM-derived P2 peptide leads to binding of the FGF-receptor to PLC and activation of PLC (Kiryushko *et al.*, 2006). Activated PLC can then

cleave phosphatidylinositol-1,4,5-bisphosphate (PIP<sub>2</sub>) resulting in the generation of inositol-1,4,5-trisphosphate (IP<sub>3</sub>) and diacylglycerol (DAG) (Litosch *et al.*, 2016). DAG is subsequently cleaved by DAG lipases to liberate arachidonic acid (AA). Since inhibition of DAG lipase activity and thus blocking of AA generation reduced NCAM-induced neurite outgrowth, it was concluded that PLC-triggered AA generation is required for NCAM-induced neurite outgrowth (Williams *et al.*, 1994). Furthermore, IP<sub>3</sub> generated via consecutive activation of NCAM, FGF-receptor and PLC induces the release of Ca<sup>2+</sup> from intracellular stores (Berridge *et al.*, 1994; Klint and Chlaesson-Welsh, 1999).

### 1.5.3 Protein kinase C (PKC) and MARCKS-dependent signal transduction

MARCKS, which binds to PSA via its effector domain (Theis *et al.*, 2013), co-localizes with PIP<sub>2</sub> at the plasma membrane and associates with PIP<sub>2</sub> through electrostatic interactions. MARCKS sequesters PIP<sub>2</sub> and thereby regulates the level of free PIP<sub>2</sub> within the lipid bilayer (Rauch *et al.*, 2002). Moreover, MARCKS is a major substrate for PKC and contains PKC phosphorylation sites in its effector domain (**Figure 3**) (Gallant *et al.*, 2005). MARCKS associates with the plasma membrane via its N-terminal myristate and the insertion of the effector (ED) domain into the lipid head group region of the plasma membrane is mediated by five phenylalanine residues within the ED (Arbuzova *et al.*, 1998; Gambhir *et al.*, 2004). Furthermore, it has been shown that the ED domain of MARCKS binds to calmodulin (CaM) and that this association is regulated by the concentration of free cytoplasmic Ca<sup>2+</sup> (Arbuzova *et al.*, 2002). Moreover, the ED domain of MARCKS is involved in activation of phospholipase D (PLD) which produces phosphatidic acid and can activate phosphatidylinositol 3-kinase (PI3K) (Morash *et al.*, 2005). PI3K catalyzes the conversion of PIP<sub>2</sub> to PIP<sub>3</sub> and it serves as positive regulator of PLD and co-activator of PLC (Czech *et al.*, 2000; Morash *et al.*, 2005). Interestingly, PIP<sub>2</sub> is also an important regulator for the activity of PI3K.

Upon phosphorylation by PKC, MARCKS is released from the plasma membrane and calmodulin dissociates from MARCKS (Gallant *et al.*, 2005; Morash *et al.*, 2005; Verghese *et al.*, 1994), leading to increased cytoplasmic levels of free calmodulin (Morash *et al.*, 2005). Free calmodulin is able to interact with the nitric oxide synthase (NOS) and to activate NOS. NOS subsequently produces nitric oxide (NO) which is released from the cells (Su *et al.*, 1995). NO has been shown to influence the expression of PSA-NCAM (Bouzioukh *et al.*, 2001) through NO-mediated activation of soluble guanylyl cyclase (sGC) which triggers the NMDA/NO cyclic guanosine monophosphate (cGMP) pathway (Denninger and Maletta,

1999; Park *et al.*, 2004). NO is known to induce NO-dependent S-nitrosylation of proteins which is an important physiological trigger for the neuronal NOS signaling (Jaffrey *et al.*, 2001). Previous findings suggest an activation of the matrix metalloprotease 9 (MMP-9) by NO through protein modification, by sGC-mediated down-regulation of the endogenous MMP-9 inhibitor tissue metalloprotease-1 (TIMP-1) or through proteolytic regulation of MMP-1 and -13 which are known to activate MMP-9 (Ridnour *et al.*, 2007).

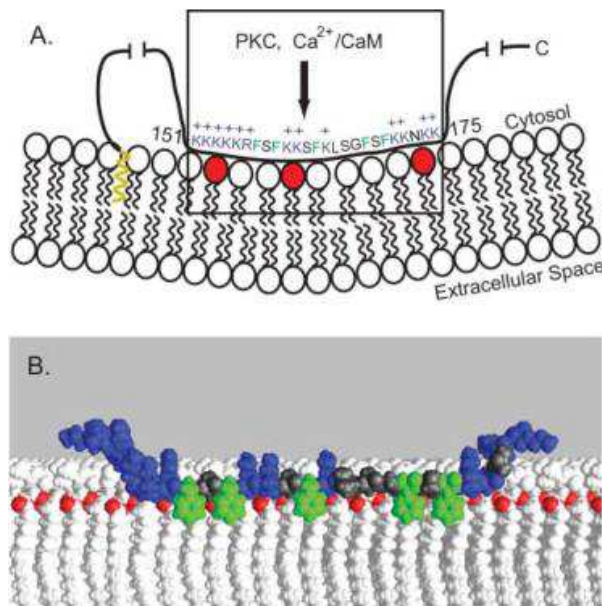


**Figure 3: Model of myristoylated alanine-rich C-kinase substrate (MARCKS) interacting with the plasma membrane.** (A) the myristoylated N-terminus of MARCKS dipping into the bilayer of the plasma membrane is displayed in yellow, and the MARCKS effector domain (ED) containing the calmodulin binding site and PKC phosphorylation site at residues 151-175 is indicated by the black box. The MARCKS-ED interacts electrostatically with acidic lipids like phosphatidylinositol-4,5-bisphosphate (PIP<sub>2</sub>) indicated in red. (B) Molecular model depicting the interaction of the MARCKS-ED with the plasma membrane. The five phenylalanine residues of the ED-domain, indicated in green, are penetrating into the lipid head group region of the membrane. Lipids are shown in white and PIP<sub>2</sub> is depicted in red. The basic N-terminal region of MARCKS is colored in blue (Gambhir *et al.*, 2004).

NCAM is a target for metalloproteases which play an important role in ectodomain shedding of NCAM (Hübschmann *et al.*, 2005; Hinkle *et al.*, 2006). More recent studies showed that NCAM is a substrate of MMP-2 (Dean and Overall, 2007) and indicated that the MMP-9- and MMP-2-dependent proteolytical cleavage of NCAM enhanced ischemic neuronal damage in mice (Shichi *et al.*, 2011). The production of MMP-2 is initiated by laminin-induced PLD activation and phosphatidic acid production (Reich *et al.*, 1995). Moreover, PI3K seems to be involved in the regulation of MMP-2 (Ispanovic and Haas, 2006).



## 2. RATIONALE AND AIM OF THE STUDY

---

The unusual glycan  $\alpha$ 2,8-linked PSA is important for the brain development in the early embryonic stage and is involved in neurogenesis and synaptic plasticity in the adult. Furthermore, PSA plays an important role in the regulation of the circadian rhythm. The membrane-associated glycoprotein NCAM is the main carrier of PSA in the mammalian brain and it mediates several important functions during nervous system development and is involved in synaptic plasticity and regeneration after injury in the adult nervous system. In a recent study, proteolytic cleavage of NCAM by a serine protease at the cell surface has been shown upon treatment of cultured cerebellar neurons or NCAM-expressing CHO cells with surrogate NCAM ligands. It has been further shown that the resulting transmembrane NCAM fragment is transported to the nucleus via the ER. Generation, intracellular trafficking and nuclear import of this PSA-lacking NCAM fragment depend on activation of the fyn/FAK pathway and on calmodulin.

Preliminary results from Prof. Schachner's group indicated the presence of PSA in the cell nucleus upon stimulation of cerebellar neurons with surrogate NCAM ligands. This observation suggests that PSA could enter the nucleus attached to the NCAM fragment and raised the question whether such a PSA-carrying NCAM fragment is generated and transported to the nucleus by similar or different pathways as described for the the generation and nuclear import of PSA-lacking NCAM fragment.

Thus, the aim of my thesis was to explore whether a PSA-NCAM fragment reaches the nucleus upon treatment with surrogate NCAM and PSA ligands and which physiological functions are induced by nuclear PSA-NCAM. To address these questions, a) the proteolytic processing of PSA-carrying NCAM and the proteases responsible for the cleavage were investigated; b) the signal transduction pathways leading to the cleavage of the full length PSA-carrying NCAM at the plasma membrane were characterized; c) the trafficking of the transmembrane PSA-NCAM fragment from the plasma membrane to the nucleus was analyzed; d) the physiological function of nuclear PSA in the circadian rhythm was examined and; e) the effect of the nuclear PSA-carrying NCAM fragment on differential gene expression was evaluated.

### 3. MATERIAL

---

#### 3.1 Animals

NCAM-deficient (-/-) mice (Cremer *et al.*, 1994) had been backcrossed onto the C57BL/6J background for more than eight generations. C57BL/6J mice, NCAM-deficient mice and their wildtype littermates of both sexes were used for all experiments. All animal experiments were approved by the local authorities of the State of Hamburg (animal permit number ORG 679) and conform to the guidelines set by the European Union. The animals were housed at 25°C on a 12 h light/ 12 h dark cycle (lights on either at 7.00 am or at 7.00 pm) with ad libitum access to food and water. All experiments were conducted in compliance with the ARRIVE guidelines for reports on animal research.

#### 3.2 Cell lines

Wildtype Chinese hamster ovary cell line (CHO) expressing NCAM-PSA and genetically modified cells which were expressing NCAM but were deficient for the PSA synthesizing polysialyltransferases ST8SiaII and ST8SiaIV and thus lacking PSA were a kind gift of Martina Mühlenhoff, Zentrum Biochemie, Institut für Zelluläre Chemie, Medizinische Hochschule, Hannover, Germany (Eckhardt *et al.*, 1995; Mühlenhoff *et al.*, 1996).

#### 3.3 Primers

Primers were provided by Metabion international AG (Steinkirchen, Germany).

**Table 1: Primers used for qPCR.** Primers were selected from the mouse qPrimerDepot bank (<https://primerdepot.nci.nih.gov/>). Gene name, sequence and gene bank number are indicated.

Transcript	Gene Name	Forward primer sequence (5'-3') Reverse primer sequence (5'-3')	Gene bank accession number
<i>Actin</i>		TCCTGTGGCATC CATGAAACT TTCTGCATCCTGTGTCAGCAATG	NM_007393
<i>CLOCK</i>	Cyclic Circadian Locomotor Output Cycles Kaput	TTGGACTAGGGCAACGATTC GAGTCTCCAACACCCACAGA	NM_007715
<i>GAPDH</i>	Glyceraldehyde 3- phosphate dehydrogenase	AGCCTCGTCCCGTAGACAAAA TGGCAATCTCCACTTTG	NM_008084.3

**Continuation of Table 1: Primers used for qPCR**

<i>Lrp2</i>	Low density lipoprotein receptor-related protein 2	GGC AGT GGG AAT TTT CGC TG CAGGAGCTAGGGATGCAGG	NM_001081088.1
<i>Nr2f6</i>	Nuclear Receptor Subfamily 2, Group F, Member 6	GAAGCACTTCTTGAGCCGAC AATCTCAGCTACACCTGCCG	NM_010150
<i>Per1</i>	Periodic 1	GAAACGGCAAGCGGATGGAG CTCTGGTGGCAGTCGAAGTT	NM_011065
<i>Snca</i>	Synuclein, alpha, transcript variant 2	CAG GCA TGT CTT CCA GGA TT GGGAATATAGCTGCTGCCAC	NM_009221.2
<i>Tubulin</i>		CGCACGACATCTAGGACTGA TGAGGCCTCCTCTCACAAGT	NM_021885

### 3.4 Antibodies

The primary antibodies used in this study are listed in **Table 2**. All HRP-coupled secondary antibodies and the Fc fragment of human IgG were purchased from Dianova (Hamburg, Germany) and used in a dilution of 1:10,000 – 1:50,000 in immunoblot and 1:2,000 in ELISA.

**Table 2: Primary antibodies used in the study.** Suppliers and names of antibodies as well as application and appropriate dilution of the antibodies are indicated. Antibodies were used for Immunoblot (IB), proximity ligation assay (PLA), immunoelectron microscopy (EM), translocation assay (TA), nuclear import assay (NI), immunoprecipitation (IP), ELISA (E) and for NCAM antibody treatment (T).

Antibody	Species	Target	Dilution	Provider
actin antibody (ACTN05)	mouse	monoclonal IgG antibody against actin	IB: 1:1,000	Abcam plc., Cambridge, UK
Calreticulin (C-17)	goat	polyclonal IgG antibody against calcium binding protein calreticulin	IB: 1:500	Santa Cruz Biotechnology, Heidelberg, Germany
CaM I (FL-149)	rabbit	polyclonal IgG antibody against full length calmodulin	IB: 1:1,000 TA: 8 µg/mL NI: 8 µg/mL	Santa Cruz Biotechnology
Cofilin	mouse	monoclonal IgG antibody against cofilin	IB: 1:1,000 PLA: 1:200 IP: 2 µg NI: 12 µg/mL	BD Bioscience, New Jersey, USA
GAPDH (FL-335)	rabbit	polyclonal IgG antibody against glyceraldehyde 3-phosphate dehydrogenase	IB: 1:100	Santa Cruz Biotechnology

**Continuation of Table 2: Primary antibodies used in the study.**

histone H1	rabbit	polyclonal IgG against histone H1	PLA: 1:200	Acris antibodies GmbH, Herford, Germany
histone H3 (C-16)	goat	polyclonal IgG against histone H3 (C-terminus)	IB: 1:500	Santa Cruz Biotechnology
IgG	rabbit	non-immune, ChromoPure	IP: 5.1 µg TA: 6 µg NI: 6 µg	Jackson ImmunoResearch Laboratories Inc., Newmarket, UK
MARCKS	rabbit	polyclonal IgG against myristoylated alanine-rich C-kinase substrate (MARCKS)	IB: 1:1,000	Lobaugh <i>et al.</i> , 1990 Kind gift from Prof. Perry J. Blackshear, Durham, USA
MMP2	goat	polyclonal IgG against MMP2	IB: 2.5 µg/mL	R&D Systems GmbH, Wiesbaden-Nordenstadt, Germany
MMP2	mouse	monoclonal IgG against MMP2	IB: 1:1,000	Santa Cruz Biotechnology
MMP9	goat	polyclonal IgG against MMP9	IB: 2.5 µg/mL	R&D Systems GmbH,
NCAM (C-20)	goat	polyclonal IgG against the extracellular domain of NCAM (C-terminus)	IB: 1:1,000 PLA: 1:200	Santa Cruz Biotechnology
NCAM 1β2	rabbit	polyclonal IgG against the extracellular domain of NCAM	IB: 1:1,000 PLA: 1:200 EM: 1:200	Niethammer <i>et al.</i> , 2002
NCAM chicken (egg yolk)	chicken	polyclonal IgY against the extracellular domain of NCAM	T: 400 µg/mL	Pineda, Berlin, Germany
NCAM chicken (serum)	chicken	polyclonal IgY against the extracellular domain of NCAM	T: 100 µg/mL	Pineda
NCAM guinea pig (serum)	guinea pig	polyclonal IgG against the extracellular domain of NCAM	T: 100 µg/mL	Pineda
NCAM P61	rat	monoclonal IgG against the intracellular domain of NCAM	IB: 1:50	Gennarini <i>et al.</i> , 1984

**Continuation of Table 2: Primary antibodies used in the study.**

pan hnRNP A (H-200)	rabbit	polyclonal IgG against heterogeneous nuclear ribonucleoprotein A	IB: 1:1,000	Santa Cruz Biotechnology
PC4	rabbit	polyclonal IgG antibody against PC4	IB: 1:1,000 PLA: 1:200 IP: 2 µg NI: 12 µg	Abcam plc.
p-MARCKS (Ser 152/156)	rabbit	polyclonal IgG against phosphorylated MARCKS	IB: 1:1,000	Cell Signaling Technology Inc., Danvers, USA
PSA (735)	mouse	monoclonal IgG antibody against PSA	IB: 1:1,000 PLA: 1:200 EM: 1:200 IP: 2,3 µg E: 1:400	Rita Gerardy-Schahn, Medizinische Hochschule-Hannover, Hannover, Germany
Rab7 (D95F2)	rabbit	monoclonal IgG against Rab7 protein (late endosome marker)	IB: 1:500	Cell Signaling Technology Inc.
transferrin (F-8)	mouse	monoclonal IgG against transferrin	IB: 1:500	Santa Cruz Biotechnology

### 3.5 Reagents

Purified recombinant human cofilin was a kind gift from James Bamburg (Biochemistry & Molecular Biology, Colorado State University, Fort Collins, CO, USA). Cloning, bacterial expression and purification of the recombinant untagged cofilin have been described (Dai *et al.*, 2004; Giuliano *et al.*, 1988). Glutathione S-transferase-tagged (GST-tagged) murine cofilin and untagged cofilin deriving from GST-tagged cofilin after removal of the GST-tag (Breitsprecher *et al.*, 2011) were a kind gift from Jan Faix (Department of Biophysical Chemistry, Medizinische Hochschule Hannover, Germany). Plasmids for the expression of polyhistidine-tagged (His-tagged) full-length PC4 and His-tagged PC4 mutants with deletion of amino acids 1-87 or 62-127 were a kind gift from Tapas K. Kundu (Transcription and Disease Laboratory, Molecular Biology & Genetics Unit, Jawaharlal Nehru Centre for Advanced Scientific Research, Bangalore, India). The other reagents used in this study are listed in **Table 3**.

**Table 3: Proteins, enzymes and other reagents used in the study.** Final concentrations of reagent used in this study are indicated.

Components	Description	Final concentration	Provider
APMA	4-aminophenylmercuric acetate activator of metalloproteases	1 mM	Sigma-Aldrich GmbH, Taufkirchen, Germany
BDNF	brain derived neurotrophic factor	100 ng/mL	Sigma-Aldrich GmbH
Biotin HPDP	N-[6-(biotinamido)hexyl]-3'-(2'-pyridyldithio) propionamide	5 mM	Santa Cruz Biotechnology
Colominic acid	colominic acid from Escherichia coli	1 mg/mL	Sigma-Aldrich GmbH
Control peptide	MARCKS control peptide (H-KKKKKRASAKKSAKLSGASAKKNKK-OH)	50 µg/mL	Schafer-N, Copenhagen, Denmark
EndoN	endoneuraminidase cleaving alpha-2, 8-linked polysialic acid	25 units/mL	Rita Gerardy-Schahn, Medizinische Hochschule, Hannover, Germany
FGF	fibroblast growth factor	100 ng/mL	Sigma-Aldrich GmbH
Human-Fc fragment	chromePure human IgG, Fc Fragment	40 µg/mL	Jackson ImmunoResearch
MARCKS ED peptide	myristoylated alanine-rich C-kinase substrate effector domain peptide (H-KKKKKRFSFKKSFKLSGFSFKKNKK-OH)	50 µg/mL	Schafer-N
Na-ascorbate	(+)-sodium L-ascorbate, reducing agent	0.5 M	Sigma-Aldrich GmbH
NCAM-Fc	NCAM/hIgG1-Fc	20 µg/mL	InVivo BioTech Service GmbH Henningsdorf, Germany
PLL	poly-L-lysine hydrobromide, MW 70,000-150,000	0.01%	Sigma-Aldrich GmbH
PNGase F	peptide-N-glycosidase F	500 units/µL	New England BioLabs, Frankfurt, Germany
Sulfo-NHS-LC-Biotin	EZ-link™ sulfo-NHS-LC-biotin	0.5 mg/mL	Thermo Scientific, Rockford, USA

### 3.6 Inhibitors

Inhibitors used for pretreatment of cells are listed in **Table 4**.

**Table 4: List of inhibitors used in this study.** Inhibitors with the applied final concentration.

Inhibitors	Description	Final concentration	Provider
Aprotinin	serine protease inhibitor	1 $\mu$ M	Merck Millipore, Darmstadt, Germany
CGS9343B	calmodulin inhibitor	10 $\mu$ M	Jacob Zijlstra, Novartis consumer health
FAK Inhibitor 14	focal adhesion kinase inhibitor 14	10 $\mu$ M	Sigma-Aldrich GmbH
FIPI	phospholipase D 1/2 inhibitor	40 nM	Santa Cruz Biotechnology
GM6001	broad spectrum inhibitor of matrix-metalloproteinases	100 nM	Merck Millipore (Calbiochem)
L-NAME hydrochloride	N-Nitro-L-arginine methyl ester hydrochloride inhibitor of NO synthase	1 mM	Sigma-Aldrich GmbH
LY294002	phosphoinositide 3-kinase inhibitor	4 $\mu$ M	Santa Cruz Biotechnology
MMP-2/9	matrix metalloproteinase 2 and 9 inhibitor	100 $\mu$ M	Merck Millipore
MMP-2	matrix metalloproteinase 2 inhibitor III	25 nM	Merck Millipore
MMP-9	matrix metalloproteinase 9 inhibitor	10 nM	Merck Millipore
PD173074	fibroblast growth factor-receptor inhibitor	100 nM	Tocris
PKC (19-36)	pseudosubstrate peptide inhibitor of protein kinase C	1.5 $\mu$ M	Tocris
U73122	phospholipase C inhibitor	10 $\mu$ M	Tocris

### 3.7 Buffers and solutions

All buffers and solutions which were used in this study are listed below, containing the name of chemicals and appropriate concentrations used in the assays. The chemicals were provided by Carl Roth GmbH & Co. KG, (Karlsruhe, Germany), Sigma-Aldrich (Taufkirchen, Germany), Serva (Heidelberg, Germany) and Roche Diagnostics GmbH

(Mannheim, Germany). Cell culture media and supplements were purchased by PAN Biotechnology (Aidenbach, Germany), Biochrome (Berlin, Germany), Sigma-Aldrich (Taufkirchen, Germany), GE Healthcare Life Science (Freiburg, Germany) and Thermo Scientific (Darmstadt, Germany). Buffers were supplemented with complete protease inhibitor, EDTA-free (Roche).

Blotting buffer (10×)	Tris	250 mM
	Glycine	1.9 M
Blotting buffer (1×)	10 × Blotting buffer	10 %
	Methanol	20 %
	A. dest	70 %
Cell lysis buffer (pH 7.5)	HEPES	10 mM
	KCl	10 mM
	EDTA	0.1 mM
	DTT	1 mM
	Triton X-100	0.5 %
Glasgow-minimal essential medium (GMEM) (with L-glutamine and NaHCO <sub>3</sub> )	Fetal bovine serum	10 %
	Penicillin/Streptomycin	2 %
	Master Mix	5 %
Ham's F12 medium (with L-Glutamine and NaHCO <sub>3</sub> )	Fetal bovine serum	10 %
	Penicillin/Streptomycin	2 %
HBSS (without Ca and Mg and NaHCO <sub>3</sub> )		
HEN buffer (pH 7.7)	HEPES	25 mM
	EDTA	0.1 mM
	Neocuproine	10 μM
	SDS	2 %
HENS buffer (pH 7.7)	HEPES	25 mM
	EDTA	0.1 mM
	Neocuproine	10 μM
	SDS	1 %



## MATERIAL

HOMO buffer (pH 7.4)	Tris/HCl	10 mM
	Sucrose	0.32 M
Hypotonic buffer (pH 7.8) (10×)	HEPES	100 mM
	KCl	20 mM
Isotonic buffer (7.8) (5×)	HEPES	50 mM
	KCl	20 mM
	Sucrose	0.25 mM
Master mix (CHO cells) 500 mL	Non essential amino acids (100×)	100 mL
	Sodium-pyruvate (100 mM)	100 mL
	Glutamate + aspartate (100×)	100 mL
	Nucleosides:	200 mL
	Adenosine, Guanosine, Cytidine, Uridine	0.35 mg/mL
Neutralization buffer (pH 7.7)	HEPES	20 mM
	NaCl	100 mM
	EDTA	1 mM
	Triton X-100	0.5 % (v/v)
Nuclear translocation buffer (pH7.4)	HEPES	25 mM
	KCl	12.5 mM
	MgCl <sub>2</sub>	2.5 mM
	CaCl <sub>2</sub>	1.5 mM
	ATP	0.1 mM
PBS (pH 7.4) (10×)	NaCl	137 mM
	KCl	2 mM
	Na <sub>2</sub> HPO <sub>4</sub>	8 mM
	KH <sub>2</sub> PO <sub>4</sub>	1.5 mM

## MATERIAL

Perfusion buffer (pH 7.3)	cacodylate buffer	0.1 M
	paraformaldehyde	4 %
	CaCl <sub>2</sub>	0.1 %
RIPA buffer	Tris	50 mM
	NaCl	180 mM
	NP40	1 % (v/v)
	Na <sub>4</sub> P <sub>2</sub> O <sub>7</sub>	1 mM
SDS sample buffer 4× (pH 6.8)	SDS	10 g
	Tris/HCl	1 mM
	Glycerin (100 %)	50 mL
	Bromphenolblue	50 mg
	DTT	200 mg
	dH <sub>2</sub> O	125 mL
SDS-PAGE running buffer (10×)	Glycine	1.9 M
	Tris	250 mM
	SDS	1 % (w/v)
TBS (pH 7.5) (10×)	Tris	100 mM
	NaCl	1.5 mM
TBS-T	TBS (1x)	
	Tween 20	0.05 % (v/v)
Translocation buffer	HEPES	10 mM
	Mg(CH <sub>3</sub> COO) <sub>2</sub>	40 mM
	DTT	1 mM
	CaCl <sub>2</sub>	2 mM
Wash buffer	Neutralization buffer	
	NaCl	600 mM

X-1 Medium	Neurobasal A	1 ×
	Penicillin/	50 U/mL
	Streptomycin	50 µg/mL
	Insulin	10 µg/mL
	Sodium-selenite	10 µg/mL
	Transferrin, holo	100 µg/mL
	L-Thyroxine	4 nM
	BSA	0.1 % (w/v)
	B27	1 % (w/v)
	Sodium-pyruvate	1 % (w/v)
	L-glutamine	1 % (w/v)

All consumables for the cell culture and materials which were used during the study were purchased by Greiner Bio-One International GmbH (Kremsmünster, Austria), Sarstedt AG & Co (Nümbrecht, Germany), Merck Millipore (Darmstadt, Germany) VWR International GmbH (Hannover, Germany) and Corning GmbH (Kaiserslautern, Germany).

## 4. METHODS

---

### 4.1 Primary cell culture / cell lines

Cerebellar granule neurons were prepared constantly at 8 am (lights on at 7 am) from early postnatal (6 to 8 days old) wildtype and NCAM-deficient littermate mice and cultured in serum-free X-1 medium as described (Chen *et al.*, 1999). Neurons were seeded at a density of  $1 \times 10^6$  cells/mL on PLL-coated 6-well and 12-well plates, or at  $2.5 \times 10^5$  cells/0.5 mL per well on Millicell EZ SLIDE 4-wells (Merck Millipore, Darmstadt, Germany) for immunohistochemistry for 30 h or different duration time, as indicated. CHO cells were grown in 175 cm<sup>2</sup> flasks with GMEM with master mix/Ham's F12 medium (1:1) containing 10% fetal bovine serum at a confluence of 80% and medium was changed against serum-free GMEM/Ham's F12 medium and cell were further incubated overnight. Cells were maintained at 37°C, 5% CO<sub>2</sub> and a constant humidity of 80%.

### 4.2 Cell surface biotinylation and cell treatment

For cell surface biotinylation experiments, cerebellar neurons were cultured for 30 h in 6-well plates and CHO cells were cultured overnight in serum free medium in 10 flasks per treatment. Neurons and CHO cells were then washed thrice with HBSS supplemented with 0.5 mM CaCl<sub>2</sub> and 2 mM MgCl<sub>2</sub> and incubated with 0.5 mg/mL EZ-link™ sulfo-NHS-LC-biotin in HBSS for 1 h at 4°C and gentle agitation. Cells were washed twice with 100 mM glycine in HBSS to quench the unreacted biotin and then with HBSS alone. Afterwards, neurons or CHO cells were mock-treated and chicken NCAM antibody, NCAM-Fc or Fc treated for 30 h and subjected to preparation of microsomes (CHO cells) as well as to subcellular fractionation (cerebellar neurons) as described in chapters 4.5 and 4.6.

Following, a general description of different pretreatments and function-triggering treatments of cerebellar neurons, which were not related to biotinylation experiments, is given. Different inhibitors, antibodies or proteins were applied directly to the cells into the medium (for dilutions see **Table 2**, **Table 3** and **Table 4**). Cerebellar neurons were subjected to pretreatment with endoneuraminidase (EndoN), PNGase, the general metalloprotease inhibitor GM6001, the serine protease inhibitor aprotinin and specific inhibitors which block the activity of matrix metalloprotease MMP-2 and MMP-9 as well as MMP-2/9 or with PBS as control for 1 h at 37°C. Specific inhibitors which block the activity of calmodulin, NOS,

FGF-receptor, FAK, PKC, PLC, PLD and PI3K or with PBS as control were also added to the neurons as pretreatment for 1 h at 37°C. Subsequently, cells were stimulated with function-triggering rabbit NCAM antibody (serum), chicken NCAM antibody (purified from egg yolk or serum, see 4.4), guinea pig NCAM antibody (purified IgG), NCAM-Fc or Fc, FGF-2, BDNF, histone H1, MARCKS-ED, control peptide (ctrl.) or mock-treated with PBS (unstimulated) for 30 min at 37°C. Neurons were then subjected to subcellular protein fractionation (see 4.6), isolation of PSA-carrying proteins (see chapter 4.7), nuclear import assay (see chapter 4.8), S-nitrosylation assay (see chapter 4.9), proximity ligation assay (see chapter 4.15), immunoelectron microscopy (see chapter 4.16) or RNA isolation (see chapter 4.17).

### 4.3 Preparation of mouse brain tissue sections and coronal brain slices

For the preparation of coronal brain slices and tissue fractionations of different brain regions 3 months old adult wildtype and NCAM-deficient males and females were used. The preparation of mouse brains was performed at different time periods during the 12 h light/12 h dark cycle (Zeitgeber time (ZT) 2, 6, 10, 14, 18, and 22 or ZT 2, 5, 8, 11, 14, 17, 20 and 23 relative to ZT 0 which is defined as lights on at 7.00 pm).

For subfractionation and RNA isolation, the adult male and female wildtype mice were sacrificed with a CO<sub>2</sub>/O<sub>2</sub> mixture. The brains were removed, put on ice and positioned upside down in an tissue slicer (Acrylic Brain Matrix for Adult Mouse, Coronal Slices, 40-75 g, (Item: RBMA-200C, World Precision Instruments, Sarasota, USA) and cut in 2 mm slices.

For coronal brain slices, two mice per time point were anesthetized with 85 mg/kg pentobarbital (Nembutal from Lundbeck, Valby, Denmark) and perfused intracardially with approx. 100 mL perfusion buffer containing 4% paraformaldehyde in 0.1 M cacodylate buffer, supplemented with 0.1% CaCl<sub>2</sub> (pH 7.3) at RT. Brains were dissected and further incubated for 4 h for *in situ* post-fixation in perfusion buffer at RT. The post-fixed brains were transferred into perfusion buffer containing 15% sucrose at 4°C. After overnight incubation at 4°C, brains were embedded in a one-way-embedding cup with Tissue Tek<sup>®</sup> (Sakura Finetek, Staufen, Germany) and frozen in 2-methyl-butane pre-cooled to -80°C. Brains were stored at -80°C until cryo-sectioning. Brains were cut into 10-25 µm thick sections using a cryostat (Leica CM3050, Leica instruments, Wetzlar, Germany), collected onto SuperFrost plus glass slides (Carl Roth) and stored at -20°C.

#### **4. 4 Polyethylene glycol precipitation of chicken NCAM antibody from egg yolk**

The IgY from egg yolk was purified by precipitation with polyethylene glycol (PEG 6000) (Sigma-Aldrich). All steps were performed at 4°C. The yolk was transferred into Falcon tubes and 2 volumes of PBS and 3.5% (w/v) PEG 6000 was added. The sample was mixed on a roller for 10 min and centrifuged for at  $13,000 \times g$  for 20 min. The supernatant was passed through a Whatman prepleated filter paper (Sigma-Aldrich) and PEG 6000 was added to achieve a PEG 6000 concentration of 8%. The supernatant was again subjected to centrifugation at  $13,000 \times g$  for 20 min after mixing on roller for 10 min. The supernatant was discarded and the pellet was dissolved in 10 mL PBS and the PEG 6000 concentration as adjusted to 10%. Then the probes were incubated for further 10 min on a roller. The solution was centrifuged at  $13,000 \times g$  for 20 min and the pellet was dissolved in 1 mL PBS and dialyzed using a Slide-A-Lyzer 10K dialysis cassette (Pierce) overnight in 0.1% PBS solution (2,000 times the volume of the sample) on a magnetic stirrer. At the next day, the saline solution was changed against fresh solution and the probe was further dialyzed for 3 h. The IgY extract was removed from the dialysis cassette and the protein concentration was measured at 280 nm (qQuant, Bio-Tek Instruments, Bad Friedrichshall, Germany) and analyzed by immunoblot.

#### **4. 5 Preparation of cytoplasmic fraction and microsome fractions**

The following procedure and the centrifugation steps were performed at 4°C unless stated otherwise. Neurons and CHO cells were biotinylated and chicken NCAM antibody treated as described in section 4.2. For the preparation of the cytoplasmic fraction for the nuclear import assay with neurons (chapter 4.8), non-biotinylated cells were used. The collected cell pellet was resuspended in about 600  $\mu\text{L}$   $1\times$  hypotonic buffer containing protease inhibitors (three times packed cell volume (PCV) and incubated for 20 min followed by centrifugation for 5 min at  $600 \times g$ . The cell pellet was resuspended in about 500  $\mu\text{L}$   $1\times$  isotonic buffer containing protease inhibitors (two times PCV) and homogenized using a Dounce homogenizer and passed through a 27-gauge needle. The probes were then centrifuged at  $1,000 \times g$  for 10 min and the  $1,000 \times g$  supernatants were transferred to a new tube and further centrifuged for 15 min at  $17,000 \times g$ . The  $17,000 \times g$  supernatants were centrifuged for 1 h at  $100,000 \times g$  in a Beckman Coulter Optima L-90K ultracentrifuge (Beckman Coulter GmbH, Krefeld, Germany) using a 70Ti rotor for the isolation of the cytoplasmic proteins (supernatant) and the microsomal proteins, containing endosomes. The cytoplasmic fraction of non-biotinylated

neurons was directly used for the nuclear import assay (chapter 4.8) and the cytoplasmic fraction of CHO cells was stored at  $-20^{\circ}\text{C}$  until further use. The pellets were resuspended in HOMO buffer and adjusted to further centrifugation for the isolation of endosomes and the endoplasmic reticulum (ER).

The isolation of fractions enriched in ER or endosomes was performed by ultracentrifugation with a density step gradient with iodixanol (OptiPrep™, Axis Shield, Dundee, Scotland). The microsomal suspension was loaded on top of a step gradient consisting of 30%, 20%, 15% and 10% iodixanol in HOMO buffer and centrifuged at  $100,000 \times g$  for 3 h in Beckman Coulter Optima L-90K ultracentrifuge (Beckman Coulter GmbH) using a swing out SW40Ti rotor. The interphases were collected, diluted 1:2 in HOMO buffer containing protease inhibitors and adjusted to further centrifugation at  $100,000 \times g$  for 30 min using a fixed angle rotor to pellet the endosomes and endoplasmic reticulum (ER). The pellets of the layers between 10/15 % iodixanol enriched in endosomes, 15/20% enriched in smooth ER and 20/30% enriched in rough ER were resuspended in 200  $\mu\text{L}$  RIPA buffer containing protease inhibitors or in about 200  $\mu\text{L}$  translocation buffer containing a protease inhibitor cocktail for translocation assay (chapter 4.8). When biotinylated protein were isolated the collected ER and endosome fractions were incubated with streptavidin-coupled Dynabeads MyOne™ Streptavidin (Invitrogen, Waltham, USA) overnight at  $4^{\circ}\text{C}$  on a head-over-head shaker. Biotinylated proteins bound to the beads were collected using a magnet and washed once with RIPA buffer containing protease inhibitors and twice with PBS containing protease inhibitors. The supernatants were stored at  $-20^{\circ}\text{C}$  and samples were subjected to gel electrophoresis and immunoblot analysis.

#### **4. 6 Subcellular protein fractionation**

For subcellular fractionation the “Subcellular Protein Fractionation Kit for Cells” or the “Subcellular Protein Fractionation Kit for Tissue” were used according to manufactures protocol (ThermoFisher Scientific). All incubation steps were performed at  $4^{\circ}\text{C}$  with gentle rotation unless stated otherwise. Cerebellar neurons which were pretreated and treated as described in chapter 4.2 were collected in the cytoplasmic extraction buffer containing a protease inhibitor cocktail using a cell scraper and incubated for 10 min at  $4^{\circ}\text{C}$ . Two mm tissue slices containing midbrain, cortex, hippocampus, suprachiasmatic nucleus, striatum or cerebellum were cut from adult wildtype and NCAM deficient mouse brains, cleaned from blood vessels and meninges, weighed and 50  $\mu\text{g}$  of the tissue was homogenized with 10

strokes in 500  $\mu$ L cytoplasmic extraction buffer containing a protease inhibitor cocktail. Tissue lysates were then transferred into a Pierce tissue strainer to remove residual not properly homogenized tissue pieces.

Cerebellar neuron lysates and tissue lysates then were centrifuged for 5 min at  $500 \times g$  and  $4^{\circ}\text{C}$ . Supernatants containing the cytoplasmic proteins were collected. Ice cold membrane extraction buffer containing a protease inhibitor cocktail was added to the pellets and probes were incubated for 10 min followed by 5 min centrifugation at  $3,000 \times g$  and  $4^{\circ}\text{C}$ . The supernatants containing the membrane proteins were collected and the pellets were resuspended in nuclear extraction buffer containing protease inhibitors, incubated for 30 min and centrifuged for 5 min at  $5,000 \times g$  and  $4^{\circ}\text{C}$ . The supernatants containing the soluble nuclear proteins were collected and the pellets were again resuspended in the nuclear extraction buffer with the addition of 100 mM  $\text{CaCl}_2$  and 100 units/ $\mu$ L micrococcal nuclease and incubated for 5 min at  $37^{\circ}\text{C}$  on ice. After centrifugation at  $16,000 \times g$  the supernatants containing the chromatin-bound proteins were collected and mixed together with the soluble nuclear protein fraction. Collected protein fractions of cerebellar neurons were subjected to further applications (see chapter 4.7) or to protein determination and protein precipitation (see chapter 4.10). Isolated proteins from tissue slices were directly subjected to SDS-gel electrophoresis and immunoblot analysis (see chapter 4.11).

#### **4. 7 Isolation of PSA-carrying proteins by immunoprecipitation (IP) and N-glycan digestion**

All incubation steps were performed with gentle rotation and as centrifugation steps performed at  $4^{\circ}\text{C}$  unless stated otherwise. For cell lysate preparation, cerebellar neurons were cultured and treated as described in chapter 4.2 and homogenized in 200  $\mu$ L ice-cold cell lysis buffer containing a protease inhibitor and a phosphatase inhibitor cocktail using a Dounce homogenizer. The lysates were centrifuged for 10 min at  $1,000 \times g$  and the supernatants were further cleared by centrifugation for 20 min at  $17,000 \times g$ . The supernatant contained the cleared cell homogenates. Cell homogenates and subcellular protein fractions (see chapter 4.6) were incubated with 20  $\mu$ L Agarose A/G beads (Santa Cruz Biotechnology) for 30 min. The beads were pelleted by centrifugation for 5 min at  $1,000 \times g$  and the supernatants were transferred to another tube and incubated with PSA antibody for 1 h followed by overnight incubation with 40  $\mu$ L Protein A/G PLUS-Agarose beads (Santa Cruz Biotechnology). The PSA-carrying proteins bound to the beads were collected by centrifugation for 5 min at  $1,000$



$\times g$  and probes were washed one time with RIPA buffer and two times with PBS (without  $\text{Ca}^{2+}$  and  $\text{Mg}^{2+}$ ). The isolated PSA-carrying proteins were either subjected to SDS-gel electrophoresis and immunoblot analysis (see chapter 4.11) or to N-glycan digestion.

For N-glycan digestion to remove all N-linked glycans and thus also PSA, the PSA immunoprecipitates were subjected to PNGase F treatment according to manufacturer's protocol (New England BioLabs) or to EndoN treatment. For PNGase F treatment the beads were resuspended in 20  $\mu\text{L}$  1 $\times$  glycoprotein denaturation buffer and boiled for 5 min at 95°C. Afterwards 4  $\mu\text{L}$  of 10 $\times$  G7 reaction buffer, 4  $\mu\text{L}$  of 10% NP40 and 1  $\mu\text{L}$  of PNGase F were added and the samples were incubated for 3 h at RT (New England BioLabs). The samples were incubated with 2 $\times$  sample buffer and boiled for 5 min at 95°C. The samples were centrifuged for 2 min at 1,000  $\times g$  and the supernatants were subjected to SDS-gel electrophoresis and immunoblot analysis (see chapter 4.11).

To remove specifically PSA, immunoprecipitates were subjected to EndoN treatment. For EndoN treatment beads were incubated with 1  $\mu\text{L}$  EndoN and PSA was digested for 1 h at 37°C. The beads were then resuspended in 2 $\times$  sample buffer, boiled for 5 min at 95°C and centrifuged at 1,000  $\times g$  for 5 min. The eluted proteins were afterwards subjected to gel electrophoresis and immunoblot analysis (see chapter 4.11).

#### **4.8 *In vitro* translocation and nuclear import assay**

The *in vitro* translocation assay to monitor the release of PSA from endosomes into the cytoplasm was performed using CHO cells. The fraction enriched with endosomes (100,000  $\times g$  pellet) obtained from biotinylated and NCAM antibody treated CHO cells (containing PSA-NCAM) and the cytoplasm (100,000  $\times g$  supernatant) of CHO cells (not expressing PSA) were prepared as described (chapter 4.3). 50  $\mu\text{L}$  of a fraction enriched with endosomes and containing PSA-NCAM was mixed with 150  $\mu\text{L}$  of a cytoplasmic fraction lacking PSA and the probes were incubated together for 1 h at 4°C in presence or absence of a calmodulin antibody, a calmodulin inhibitor or control rabbit antibody. After centrifugation for 1 h at 100,000  $\times g$ , the resulting endosomal protein pellet was resuspended in an equal volume of 2 $\times$  SDS sample buffer. The supernatants were incubated with streptavidin-coupled Dynabeads MyOne™ Streptavidin (Invitrogen) overnight at 4°C on a head-over-head shaker. Biotinylated proteins bound to the beads were collected using a magnet and washed once with RIPA buffer containing protease inhibitors and twice with PBS containing protease inhibitors.

Samples were diluted in 2× SDS sample buffer and then subjected to gel electrophoresis and immunoblot analysis (see section 4.11)

For the *in vitro* nuclear import assay, cerebellar neurons of NCAM-deficient mice were cultured and treated with NCAM antibody as described for cell treatment (see section 4.2). Treated neurons were resuspended in cell lysis buffer containing protease inhibitors, homogenized using a Dounce homogenizer and passed through a 27-gauge needle and centrifuged for 10 min at  $1,000 \times g$ . The resulting pellet containing nuclear proteins was resuspended in nuclear translocation buffer containing protease inhibitors for nuclear import assay. The nuclei were then added to the isolated cytoplasmic fractions of cerebellar neurons from wildtype mice after NCAM antibody treatment and incubated for 1 h at  $37^\circ\text{C}$  in the presence or absence of cofilin1, PC4 and control antibody or with nuclear translocation buffer as control. After incubation, the samples were centrifuged for 10 min at  $1,000 \times g$  and  $4^\circ\text{C}$  and the pellet was dissolved in 2× sample buffer. The supernatant was subjected to protein determination and precipitation (see chapter 4.10).

#### 4.9 S-nitrosylation assay

A three step method according to Jaffrey *et al.* (2001) was used for detection of S-nitrosylated proteins (**Figure 4**).

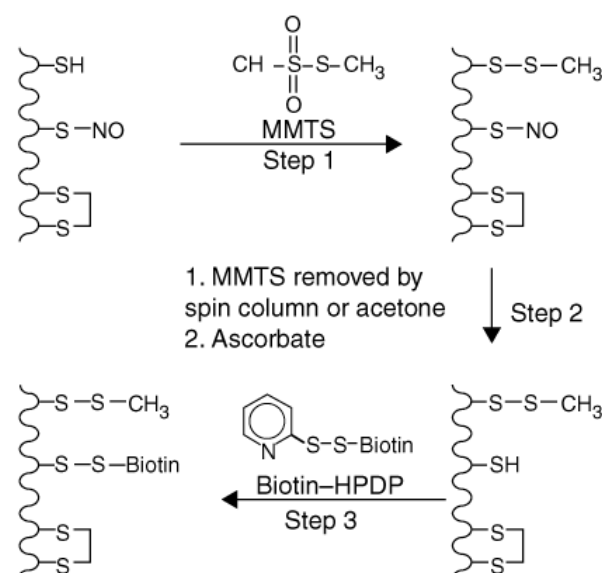


**Figure 4: Scheme for the isolation of S-nitrosylated proteins.** Step 1: Blocking of thiol groups, removal of methyl methanethiosulfonate (MMTS) by acetone precipitation. Step 2: Reduction of nitrosothiols with sodium ascorbate. Step 3: Reaction of the reduced thiols with the thiol-modifying reagent biotin (Jaffrey *et al.*, 2001).

Cerebellar neurons were cultured as described in chapter 4.2, followed by replacement of the medium by 0.5 mL HBSS without phenol red. Neurons were unstimulated or treated with guinea pig NCAM antibody treated for 10 min or 30 min followed by collection of the supernatants or the neurons in 1 mL HBSS of two wells per condition. Samples were incubated with 100  $\mu$ L 2 M thiol-specific methylthiolating agent (MMTS, Sigma-Aldrich) in HEN blocking solution containing 2% SDS for 20 min at 50°C. The MMTS was then removed by incubating the samples with 10 mL ice-cold acetone for 30 min at -20°C followed by centrifugation at 13,000  $\times$  g for 10 min at 4°C. The pellet was dissolved in 5 mL HENS buffer with the addition of 10  $\mu$ L 0.5 M sodium ascorbate and incubated with 1 mL of 5 mM biotin-HPDP in DMSO for 1 h at 25°C. The samples were then subjected again to acetone precipitation and the resulting pellet was resuspended in 0.5 mL of HENS buffer with the addition of 1 mL neutralization buffer and 80  $\mu$ L Dynabeads® My One™ streptavidin beads to isolate biotinylated proteins. After overnight incubation at 4°C, the beads were washed 5 times with washing buffer and the biotinylated proteins were eluted in 30  $\mu$ L non-reducing 2 $\times$  sample buffer (without DTT) and subjected to SDS-gel electrophoresis and immunoblot analysis.

#### **4. 10 Protein determination and precipitation**

The protein concentration was measured by bicinchoninic acid (BCA) Protein Assay Reagent Kit according to the manufacturer's protocol (ThermoFisher Scientific). The absorbance was measured at 562 nm using the  $\mu$ Quant™ microplate spectrophotometer (Bio-Tek Instruments). The protein concentration was calculated from a calibration curve of BSA standards. The method of methanol-chloroform precipitation for protein samples was used according to Wessel and Flügge (1984). Samples were subsequently mixed with 4 volumes of methanol and 1 volume of chloroform and 3 volumes of distilled H<sub>2</sub>O and then centrifuged for 1 min at 16,000  $\times$  g. The upper organic phase was removed and the lower phase and interphase containing the proteins were mixed with 3 volumes of methanol and centrifuged at 16,000  $\times$  g for 2 min. The supernatant was removed and after air drying of the pellet, proteins were suspended in 2 $\times$  sample buffer and boiled for 5 min at 95°C and subjected to SDS-PAGE and immunoblot analysis (see section 4.11).

#### **4. 11 Sodium dodecyl sulfate polyacrylamide gelelectrophoresis (SDS-PAGE) and immunoblot analysis**

Separation of proteins was performed by sodium dodecyl sulfate (SDS)-polyacrylamide gelelectrophoresis (SDS-PAGE) using 26-well 4-20 % Criterion™ Tris-HCl gels and 15-well 4–20% Mini-Protean TG™ Precast Protein Gels (Bio-Rad, München, Germany). The gels were run at constant voltage of 120 V for 10 min and of 200 V until complete separation using SDS running buffer in the Criterion™ vertical electrophoresis cell (Bio-Rad). ProSieve QuadColor protein marker (Lonza, Basel, Switzerland) was used for estimation of molecular masses. For immunoblot analysis proteins were transferred from the gels onto 0.45 µm Porablot NCP nitrocellulose membrane (Macherey-Nagel, Düren, Germany) using the Mini Trans-Blot® Cell or Criterion™ Blotter system (Bio-Rad). The transfer process was performed at 80 V and 4°C for about 3 h using blotting buffer containing methanol. Membranes were incubated in 4% skim milk powder in TBS buffer containing 0.05% Tween-20 (Amresco LLC, Solon, USA) (TBST) at RT for 1 h. After blocking, membranes were incubated overnight in appropriate primary antibody in 4 % skim milk powder in TBST buffer at 4°C with constant shaking followed by washing with TBST and by incubation with horseradish peroxidase (HRP)-conjugated secondary antibody in 4% skim milk powder in TBST at RT for 1 h with constant shaking. After 3 times washing for 5 min with TBST, immunopositive proteins were visualized by chemiluminescence using the Amersham™ ECL Select™ or ECL Prime™ western blotting detection reagent (GE Healthcare, Buckinghamshire, UK) and monitored using the ImageQuant™ LAS 4000mini (GE Healthcare). The intensities of the protein bands were quantified with ImageJ software.

#### **4. 12 Enzyme-linked immunosorbent assay (ELISA)**

Proteins were coated on 384-well microtiter plates with non-treated surface (Corning GmbH). The coating solution was prepared according to the molecular masses of the coated protein. For cofilin (~ 46 kDa) and PC4 (54 kDa) 25 µL per well with a concentration of 20 µg/mL were incubated overnight at 4°C. The non-absorbed proteins were removed by washing with 50 µL PBS (without Ca<sup>2+</sup> and Mg<sup>2+</sup>) per well for 30 sec and blocked with 50 µL 2% fatty acid free bovine serum albumin (BSA) in PBS for 1.5 h at RT. The wells were washed with PBS for 30 seconds and incubated with colominic acid in different concentrations for 1 h at RT. After washing for 2 times 10 s and 3 times 5 min with 50 µL PBST per well (without Ca<sup>2+</sup> and Mg<sup>2+</sup>, PBS containing 0.05% Tween-20), plates were

incubated with 25  $\mu\text{L}$  primary antibody recognizing PSA (1:400) per well for 1 h at RT. After washing 3 times for 5 min with 50  $\mu\text{L}$  PBST, wells were incubated with HRP-linked secondary anti-mouse antibody (1:2,000) for 1 h at RT. Wells were washed again for 2 times 10 s and 3 times 5 min and incubated with 1 mg/mL o-phenylenediamine dihydrochloride substrate (OPD; Thermo Fisher Scientific) for about 5 min to visualize the protein-carbohydrate interaction. The reaction was stopped by addition of 25  $\mu\text{L}$  2.4 M sulphuric acid. The colored product was measured using an ELISA reader ( $\mu\text{Quant}^{\text{TM}}$  microplate spectrophotometer (Bio-Tek Instruments) at 490 nm.

#### 4. 13 Measurement of nitric oxide levels

For determination of NO levels, the Nitrate/Nitrite Fluorometric Assay Kit (Cayman Chemical, Ann Arbor, USA) was used. In a first reaction step the nitrate ( $\text{NO}_3^-$ ) was reduced to nitrite ( $\text{NO}_2^-$ ) by nitrate reductase in presence of enzyme cofactor. Subsequently, the fluorescent aromatic diamine 2,3-diaminonaphthalene (DAN) reagent was added to the samples, which reacts with the nitrosonium cation ( $\text{NO}^+$ ) of NO. The addition of NaOH enhances the fluorescence signal. Cerebellar neurons were cultured as described in 12-well plates followed by replacement of culture medium by HBSS (without phenol red). Neurons were stimulated with guinea pig NCAM antibody, with FGF-2 and MARCKS-ED peptide, unstimulated or were treated with control peptide as controls for 15 sec, 30 sec, 1 min, 2 min and 5 min (see chapter 4.2). 100  $\mu\text{L}$  of cell supernatant from each sample were collected (three wells per conditions). Samples from NCAM antibody treated and mock-treated neurons were incubated with 20  $\mu\text{L}$  agarose A/G beads for 30 min at 4°C with rotation to remove the NCAM antibody which may interfere with the assay. After incubation, samples were centrifuged at  $1,000 \times g$  for 5 min. 20  $\mu\text{L}$  of the supernatants were adjusted to 80  $\mu\text{L}$  with assay buffer and mixed with 10  $\mu\text{L}$  enzyme cofactor mixture and 10  $\mu\text{L}$  nitrate reductase mixture and incubated for 1 h at RT in 96-well plates. Samples were then incubated with 10  $\mu\text{L}$  2,3-diaminonaphthalene (DAN) reagent for 10 min at RT and the reaction was stopped and the signal enhanced by addition of 20  $\mu\text{L}$  NaOH. Fluorescence of nitrite ( $\text{NO}_2^-$ ) was measured using an EnSpire multimode plate reader (PerkinElmer Cellular Technologies Germany GmbH, Hamburg, Germany) applying an excitation wavelength of 360 nm and an emission wavelength of 375 nm.

#### 4. 14 Proximity ligation assay

For the detection of close interactions between two proteins a proximity ligation assay (*in situ* PLA) was performed according to the manufacturers protocol (Sigma-Aldrich). The technique allows the detection of interacting proteins when binding partners are in close proximity (less than 40 nm apart).

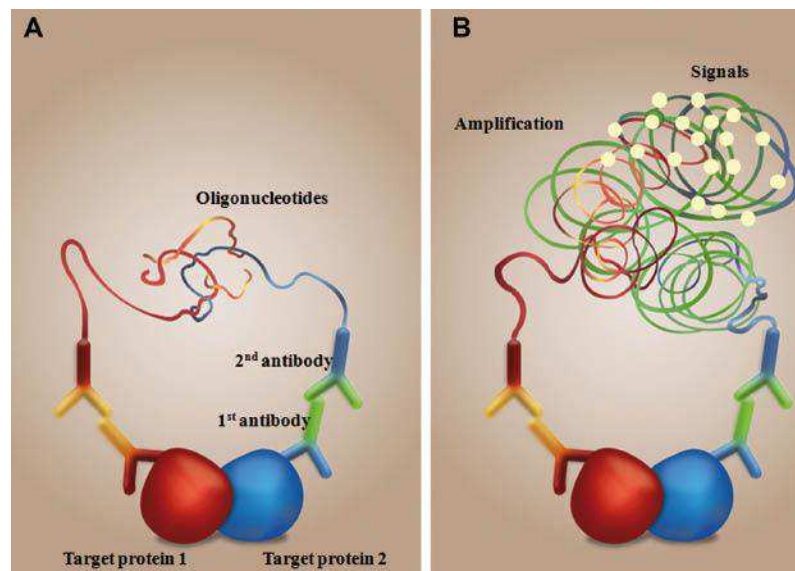


**Figure 5: Scheme of the proximity ligation assay (PLA).** (A) The target proteins are incubated with two antibodies (different species) against the respective specific target antigens. The species specific secondary antibodies are labeled with different connector oligonucleotides (PLA probes). (B) The circle-forming oligonucleotides of the two PLA probes hybridize to sequences homologues to each other if the target proteins are in close contact. A double stranded DNA is amplified by a polymerase to intensify the resulting fluorescence signal of the amplified PLA probes (Roh *et al.*, 2013).

Cerebellar neurons were cultured on Millicell EZ SLIDE 4-wells and treated with chicken NCAM antibody as described (chapter 4.2). Neurons were fixed for 30 min with 4% formaldehyde in PBS (without  $\text{Ca}^{2+}$  and  $\text{Mg}^{2+}$ ) at 37°C. Frozen cryo-sections and fixed cerebellar neurons were incubated with blocking solution (Duolink, Sigma-Aldrich) containing 250 U/mL Benzonase® nuclease (Qiagen, Hilden, Germany) for 20 min at RT followed by further incubation with blocking solution containing 1% Triton X-100. Specific primary mouse PSA antibody and rabbit histone H1, PC4 or cofilin antibody or goat NCAM antibody and rabbit histone H1 antibody (for dilution of antibodies see **Table 2**) were mixed and added to the tissue slices or cerebellar neurons and incubated for 2 days at 4°C. After washing with buffer A two times for 5 min, a pair of oligonucleotide labeled secondary antibodies in the dilution of 1:5 (Duolink anti-goat or anti-mouse PLA probe MINUS and Duolink anti-rabbit PLA probe PLUS) was added and incubated for 1 h at 37°C in a humidified chamber. The tissue slices and cerebellar neurons were again washed with Buffer

A two times for 5 min and subjected to the ligation solution containing ligase in a dilution of 1:40 for 30 min at 37°C in humidified chamber. The incubation step with the polymerase in a dilution of 1:80 was conducted after a short wash with Buffer A for 100 min at 37°C in a dark humidified chamber. After washing two times for 10 min and one time for 1 min with Buffer B, the samples were mounted with Duolink® In Situ Mounting Medium with DAPI or Roti-Mount FluorCare DAPI (Carl Roth). The images were monitored on the Olympus Fluoview FV1000 confocal laser-scanning microscope equipped with the Fluoview software package, in sequential mode with a 60x objective (Olympus, Hamburg, Germany). The quantification of the fluorescence spots was performed along the z-axis in three-dimensional images using the ImageJ software.

#### 4. 15 Immunoelectron microscopy

Cerebellar neurons were cultured on Millicell EZ SLIDE 4-wells, treated with chicken NCAM antibody as described (chapter 4.2) and fixed with 4% formaldehyde in 0.1 M sodium cacodylate buffer (pH 7.4) for at least 1 h at RT. Cells were then incubated with 2 % BSA (fatty acid free) in PBS for 1 h at RT followed by overnight incubation at 4°C with specific mouse PSA antibody or rabbit NCAM antibody (for dilutions **Table 2**). Immunogold labeling and imaging of the samples was performed by David Lutz (Zentrum für Molekulare Neurobiologie, Universitätsklinikum Hamburg-Eppendorf, Germany).

For post-embedding, cerebella were rapidly removed from brains of adult wildtype mice at different time points of the light/dark cycle and embedded in 3% agarose in PBS. Sagittal vibratome cross-sections of 100 µm thickness were collected on Millicell membrane carriers (Merck Millipore) which had been immersed in PBS. Biopsies from vermis and paravermis of the cerebellum were punched out and transferred onto gold-coated copper planchettes (1.5 mm × 0.2 mm) with a malleable membrane displaying isentropic properties (Leica, Wetzlar, Germany). The duration of the tissue processing prior to freezing was less than 10 min. High pressure freezing was performed on the EM PACT2 high pressure freezer (Leica) under 2050 bar for 50 ms. The planchettes carrying the biopsies were submerged in substitution cocktail containing 2% osmium tetroxide (Sigma-Aldrich) in 2-methyl-butane (Carl Roth) pre-cooled to -160°C. Isenthalpic freeze substitution was performed on a freeze substitution processor AFS (Leica) according to the following program: -160°C for 3 h, slope +3°C/h for 23.3 h, -90°C for 8 h, slope +3°C/h for 13.3 h, -50°C for 8 h, slope +3°C/h for 23.3 h, +20°C for 3 h. The specimens were washed several times with acetone (Carl Roth) at -90°C, at -50°C and

+20°C followed by incubation in a mixture of 3:1 acetone/Epon for 1 h under rotation at ambient temperature (23.5°C). Biopsies were then removed from the planchettes and incubated under rotation at ambient temperature in 1:1 acetone/Epon for 1 h, in 3:1 acetone/Epon for 1 h, and in Epon for two days. Epon-infiltrated samples were cured at 60°C for 2 days. Sections (60 nm thick) were collected on nickel grids (50 mesh) (Plano, Wetzlar, Germany) coated with Butvar (Plano).

Post-embedded tissue sections and fixed cerebellar neurons were incubated at ambient temperature for 1 h with donkey anti-mouse or anti-rabbit antibody conjugated to 6 or 10 nm colloidal gold or with goat anti-mouse antibody conjugated to 1.4 nm gold particles (both diluted 1:100) (Abcam). After washing in PBS (10 times for 5 min), incubation in 1% glutaraldehyde for 2 min and washing in water (5 times for 5 min), sections and neurons were incubated for 30 min in aqueous 1% uranyl acetate or in aqueous solution containing 1% osmium tetroxide and 1% uranyl acetate. After washing in water (5 times for 5 min), sections were incubated in Reynolds lead citrate solution for 2 min, washed in water for 8 times, and air-dried. Samples were washed in water (5 times for 5 min), dehydrated in 50%, 75%, 90% and 100% ethanol for 10 min each, infiltrated with mixtures of ethanol/Epon at a ratio of 3:1, 1:1 and 1:3 for 15 min each, incubated for 15 min in Epon, and cured at 60°C for 2 days. Epon embedded specimens were released from the carriers under liquid nitrogen and sections were collected on Butvar-coated copper slots (50 mesh) (Plano). Transmission electron microscopy was performed at 60 kV and 6,600 $\times$  or 15,000 $\times$  magnification using the Phillips C100 microscope (Phillips electron optics, Cambridge, UK). For determination of nuclear PSA levels in cerebellar tissue sections, gold grains in 10 nuclei of 5 sections (100  $\mu$ m apart from each other) from 2 males and 2 females were counted.

#### **4. 16 RNA isolation and microarray analysis**

QIAshredder (Qiagen) and RNeasy Plus Kit (Qiagen) were used according to the manufacturers' protocols for the isolation of RNA from cells and tissue. Cerebellar neurons used for microarray analysis were treated with NCAM antibody for 30 min as usual or additionally for 6 h (see section 4.2). Brain tissues slices and cells were lysed in 600  $\mu$ L RLT buffer containing  $\beta$ -mercaptoethanol, transferred into QIAshredder columns and centrifuged for 2 min at 16,000  $\times$  g. The lysates were transferred into gDNA Eliminator spin columns and centrifuged for 30 s at 8,000  $\times$  g to remove genomic DNA. The flow throughs were mixed with 600  $\mu$ L ethanol and spun through RNeasy spin columns for 15 s at 8,000  $\times$  g to bind the



RNA. The columns were washed with 700  $\mu\text{L}$  RW1 buffer by centrifugation for 15 s at  $8,000 \times g$ , with 500  $\mu\text{L}$  RPE buffer at  $8,000 \times g$  for 15 s and again with 500  $\mu\text{L}$  RPE at  $8,000 \times g$  for 2 min. The spin columns were transferred to a new 2 mL cup and centrifuged at  $16,000 \times g$  for 1 min to dry the column. The RNA was then eluted with 30  $\mu\text{L}$  RNase and DNase free water and the RNA content was measured using a Nanodrop 1000 spectrophotometer (ThermoFisher Scientific).

The processing of the cDNA and hybridization of the cDNA on Affymetrix GeneChip DNA microarray chips Mouse Genome 430 2.0 arrays and signal detection were performed by the Analytical and Informatics Services at the Rutgers University Cell and DNA Repository (RUCDR) in accordance with the manufacturer's protocol (Affymetrix, Santa Clara, CA, USA). For data and statistical analysis and data visualization, extraction of expression values from the CEL file, GC-RMA (robust multi-array average) and quantile normalization and pairwise differential expression analysis using a standard t-test with a Benjamini and Hochberg multiple testing correction were performed using the Geospiza Genesifter software package (PerkinElmer, Waltham, MA, USA). The exploratory list was generated by selecting genes with a t-test p-value of  $< 0.05$ . Normalized log values of signal intensities from each group were compared to those of the other groups and genes showing differences in signal intensities between groups were listed by average fold-change expression with SEM (calculated by taking the antilog of log values). Data elevation of the gene expression profile was performed by Dr. Ralf Kleene.

#### **4. 17 Quantitativ real-time polymerase chain reaction (qRT-PCR)**

##### *Reverse transcription*

The first strand reaction of the RNA was performed in the *SimpliAmp* Thermal Cycler (Life Technologies, Darmstadt, Germany). Total RNA from cultured cerebellar neurons and brain tissues was converted into cDNA using M-MLV reverse transcriptase (Sigma-Aldrich). The RNA was diluted with nuclease-free water to reach a concentration of 1-5  $\mu\text{g}$  RNA and mixed with 1  $\mu\text{L}$  oligo-dT-nucleotide (oligo (dT)) primer and 2  $\mu\text{L}$  of 5 mM deoxyribonucleotide (dNTP). The components were gently mixed, centrifuged and heated to  $70^\circ\text{C}$  for 10 min. After reaction, the tubes were placed on ice for 2 min and then mixed with 2  $\mu\text{L}$   $10\times$  M-MLV transcriptase buffer, 1  $\mu\text{L}$  M-MLV reverse transcriptase and nuclease free water to a total volume of 20  $\mu\text{L}$  and incubated at  $37^\circ\text{C}$  for 50 min. The reaction was stopped at  $90^\circ\text{C}$  for 10 min.

*qPCR*

The amplification of the template was performed in triplicates using the *Taq* Hot gold star DNA polymerase qPCR kit SYBR<sup>®</sup> Green I, ROX (Eurogentec, Cologne, Germany) in the 7900HT Fast Real-Time PCR System (Thermo Fisher Scientific). The primers used for the target genes and the reference genes are listed in **Table 1**.

**Table 5: Protocol for the amplification of the cDNA in quantitative qPCR.**

<b>Components</b>	<b>Volume (μL)</b>
SYBR green	0.6
dNTP mix (5 mM)	0.8
10× PCR buffer [200 mM Tris-HCl (pH 8.4), 500 mM KCl]	2
RNase-free H <sub>2</sub> O	8.1
<i>Taq</i> Hot gold star DNA polymerase (5 U/μL)	0.1
cDNA template (cDNA ) 1:10 diluted	5
Forward primer (10 pmol/μL)	1
Reverse Primer (10 pmol/μL)	1
MgCl <sub>2</sub>	1.4
<b>PCR reaction volume</b>	<b>20</b>

*PCR Program for the amplification of the cDNA:*

Time (sec)	Temperature (°C)
120	50
300	95
30	95
45	63
60	72
300	72
15	95
15	65
15	95

40  
cycles

The SDS 2.4 software was used for the data analysis and the mRNA levels of the target genes were calculated relative to the reference genes using the comparative cycle threshold (Ct) method ( $\Delta\Delta\text{Ct}$  method) for data analysis. The relative levels of mRNA of wildtype and NCAM deficient cerebellar neurons (mock-treated, NCAM antibody treated without and with EndoN pretreatment) as well as the mRNA levels of brain sections from wildtype and NCAM-deficient mice were calculated and the reciprocal mean value was plotted against the time in culture.

#### 4. 18 Statistical analysis

Statistical analysis of relative mRNA expression levels in cultured cerebellar neurons from wildtype and NCAM deficient mice were calculated from mean values of three independent experiments with three technical replicates and standard deviation (SD). Data were analyzed by two-way analysis of variance ANOVA with Bonferroni post-hoc test with alpha level set to 0.05. Significant differences of the gene expression level (Per-1, CLOCK, Nr2f6, Lrp2 and  $\alpha$ -synuclein) of NCAM antibody treated cerebellar neurons and NCAM antibody treated and EndoN pretreated or MMP-2 and aprotinin pretreated neurons against mRNA level of mock-treated and neurons are indicated as  $p > 0.05$  and considered as not significant, \*  $p < 0.05$  as significant, \*\*  $p < 0.01$  as very significant and \*\*\*  $p < 0.001$  as extremely significant different. The relative gene expression of isolated RNA of cerebellum and SCN tissue of adult mice were examined at different ZT and presented as mean values

(SD) from 3 independent experiments with 2 males and 2 females per group (n=12). Differences in expression levels relative to the levels at ZT2 are indicated (\*  $p < 0.05$ , \*\*  $p < 0.01$ , \*\*\*  $p < 0.001$ ; two-way ANOVA with Dunnett's multiple comparison test).

Statistical analysis of the red fluorescence spots examined by proximity ligation assay depicting the nuclear interaction of PSA with histone H1, PC4 or cofilin as well as of NCAM with histone H1 was performed by counting positive red spots. The positive red spots in 50 nuclei per image of randomly chosen areas were counted in duplicate of three independent experiments. Significance of difference was calculated by two-way ANOVA with Bonferroni post-hoc test. Differences are indicated for the interaction of PSA with histone H1, PC4 or cofilin as well as of NCAM with histone H1 between mock-treated cerebellar neurons relative to NCAM antibody and NCAM antibody treated and EndoN pretreated neurons as (\*\*\*)  $p < 0.001$ , considered as extreme significant) as well as for the interaction in NCAM antibody treated cerebellar neurons relative to mock-treated and NCAM antibody treated and EndoN pretreated neurons as (###  $p < 0.001$ , considered as extreme significant)

Nuclear PSA levels in cultured cerebellar neurons and brain tissue were visualized by immunoblot and quantified by densitometry using ImageJ software. The data for cerebellar neurons are presented as mean values of three or five independent experiments and standard deviation (SD). PSA levels of NCAM antibody, FGF-2 or MARCKS-ED peptide treated and pretreated neurons are shown relative to the PSA levels of mock-treated neurons NCAM antibody (set to 100%). Differences between groups are indicated as (\*  $p < 0.05$ , \*\*  $p < 0.01$ , \*\*\*  $p < 0.001$ ; two-way ANOVA with Dunnett's multiple comparison test). The data for the brain tissue is presented as mean values of two independent experiments with three males and three females each and standard deviation (SD) and data were analyzed by one-way ANOVA followed by Dunnett's multiple comparison test. Significance of difference was calculated for nuclear PSA levels between groups relative to the ZT2 group (set to 100%). Significance of  $p > 0.05$  was considered as not significant (-), \*  $p < 0.05$  was considered as significant, \*\*  $p < 0.01$  as very significant and \*\*\*  $p < 0.001$  as extremely significant different.

## 5. RESULTS

---

### 5. 1 Nuclear import of a PSA-carrying proteolytic NCAM fragment in cultured cerebellar neurons

Previously, it had been shown that a proteolytic fragment of NCAM is generated and transported into the nucleus of cultured cerebellar neurons upon application of function-triggering antibodies which served as surrogate ligands for NCAM (Kleene *et al.*, 2010a). Furthermore, preliminary results indicate that PSA-carrying NCAM is present in the cell nucleus after treatment with surrogate NCAM ligands. To confirm that indeed a PSA-carrying NCAM fragment is generated and transported into the nucleus upon NCAM stimulation, cerebellar neurons of wildtype and NCAM-deficient mice were treated with NCAM antibody and subjected to subcellular fractionation and isolation of nuclear proteins. An immune-positive band was detected with a PSA-specific antibody in the nuclear fraction of neurons from wildtype mice, but not in the nuclear fraction of neurons from NCAM-deficient mice (**Figure 6 A**), showing that PSA-carrying NCAM is present in the nucleus. Furthermore, a higher PSA level was seen in the nuclear fraction of neurons from wildtype mice upon NCAM antibody treatment compared to the level in untreated wildtype neurons, indicating enhanced nuclear PSA-NCAM levels after NCAM antibody treatment.

To analyze the generation of the PSA-NCAM fragment at the plasma membrane and its transport into the nucleus, cerebellar neurons were subjected to cell surface biotinylation and NCAM antibody treatment to ensure that the PSA-NCAM protein found in the nucleus derived from full-length PSA-NCAM present at the plasma membrane. Biotinylated PSA-NCAM was detected in cytoplasmic, membrane and nuclear fractions as shown in immunoblot analysis with PSA-specific antibody. An increased level of biotinylated PSA-NCAM was observed in nuclear fractions of NCAM antibody treated neurons relative to the level of PSA-NCAM in nuclear fractions of mock-treated neurons. After treatment of cerebellar neurons with NCAM antibody, a reduced level of biotinylated PSA-NCAM was found in the membrane fraction of neurons compared to the PSA-NCAM level in membrane fraction of mock-treated neurons. The level of nuclear PSA-NCAM was not altered in cytoplasmic fractions of cerebellar neurons upon treatment with NCAM antibody relative to PSA-NCAM level in mock-treated neurons. In summary, a higher level of nuclear biotinylated PSA-NCAM and a lower level of biotinylated membrane-bound PSA-NCAM

was observed after application of NCAM antibody (**Figure 6 B**), indicating that nuclear PSA derives from the plasma membrane.

To verify that the nuclear fractions were pure and did not contain contaminations from other compartments, the purity of the fractions was determined using antibodies against the cytoplasmic marker proteins actin and GAPDH as well as against the endoplasmic reticulum marker protein calreticulin or the nuclear marker proteins hnRNPA and histone H3. The nuclear marker proteins hnRNPA and histone H3 were only found in the nuclear fractions, which are devoid of the cytoplasmic and ER markers. This result demonstrates that the nuclear fraction does not contain contaminations from other compartments.

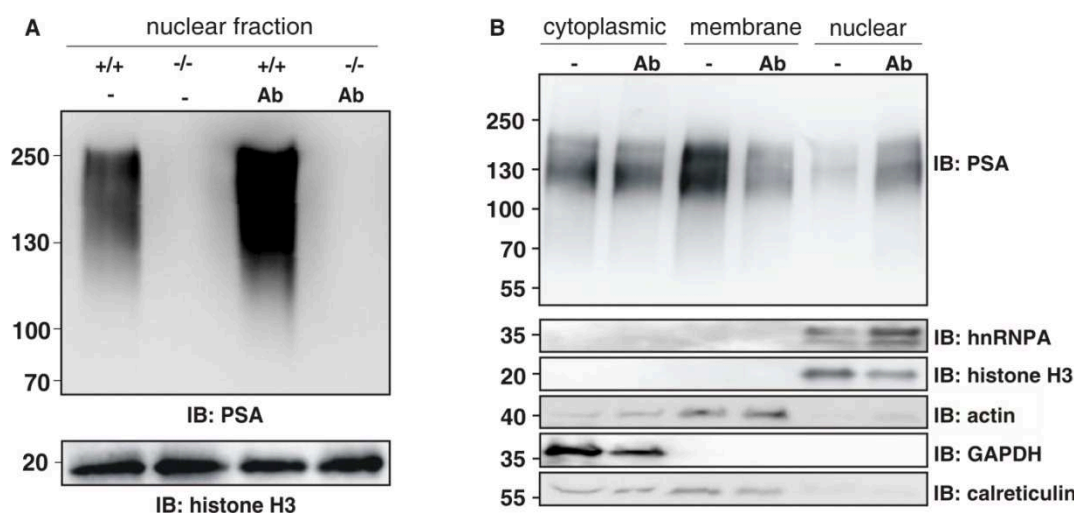


**Figure 6: Nuclear import of a PSA-carrying proteolytic NCAM fragment.** (A) Cerebellar neurons from wildtype and NCAM-deficient mice were mock-treated (-) or treated with rabbit NCAM antibody (Ab) and subjected to cellular subfractionation. Nuclear fractions were subjected to immunoblot analysis (IB) with PSA-specific antibody or with an antibody against the nuclear marker histone H3 to control for loading (immunoblot was performed by Thomas Theis). (B) Wildtype cerebellar neurons were subjected to cell surface biotinylation and were then mock-treated (-) and treated with function-triggering chicken NCAM antibody (Ab) and subjected to subcellular fractionation and isolation of biotinylated proteins. Immunoblots of biotinylated proteins were tested with PSA-specific antibody (upper panel) and the cytoplasmic, membrane and nuclear fractions were analyzed with antibodies against the nuclear marker proteins hnRNPA and histone H3, against the cytoplasmic marker proteins actin and GAPDH or against the endoplasmic reticulum marker protein calreticulin (lower panels) (Westphal *et al.*, 2016).

To substantiate whether PSA enters the nucleus attached either to full-length transmembrane NCAM or to a NCAM fragment, nuclear fractions of wildtype cerebellar neurons treated with NCAM-Fc or Fc as control were subjected to immunoprecipitation with PSA-specific antibody, followed by treatment with either PNGase F which removes N-linked glycans or with EndoN which digests PSA. The treatment with NCAM-Fc as a surrogate NCAM ligand was tested before and showed similar results compared to NCAM antibody

treatment (result not shown). The immunoprecipitates from neurons which were treated with NCAM-Fc showed a strong immunoreactive band of around 50 kDa with specific antibodies against the extracellular domain (ECD) or the intracellular domain (ICD) of NCAM (**Figure 7 A, B**). For Fc-treated cells only a basal nuclear level of NCAM was detectable with NCAM-ICD and -ECD antibodies. Furthermore, no 50 kDa fragments were observed with NCAM-ICD and -ECD antibodies in PSA immunoprecipitates of NCAM-Fc- and Fc-treated neurons without PSA digestion. However, a markedly higher amount of a PSA-carrying NCAM fragment was detectable in nuclear fractions of neurons after application of NCAM-Fc in comparison to Fc application (**Figure 7 C**). These results reinforced the notion that a PSA-carrying NCAM fragment enters the nucleus in form of a transmembrane fragment.

Immunoprecipitates from membrane fractions were also treated with PNGase F and EndoN to further confirm that the 50 kDa PSA-carrying NCAM fragment derives from the plasma membrane. No immunoreactive band corresponding to the 50 kDa NCAM fragment was detectable in the membrane fractions, but both NCAM antibodies detected NCAM forms of approximately 120 and 180 kDa after removal of their N-glycans (**Figure 7 D**). Moreover, a lower level of deglycosylated NCAM was seen in the membrane fraction of neurons upon NCAM-Fc treatment and glycan digestion compared to membrane fractions of Fc-treated neurons, indicating a reduced membrane-bound NCAM level after NCAM-Fc application. These results indicate that full length PSA-NCAM is proteolytically cleaved upon stimulation and imported into the nucleus.

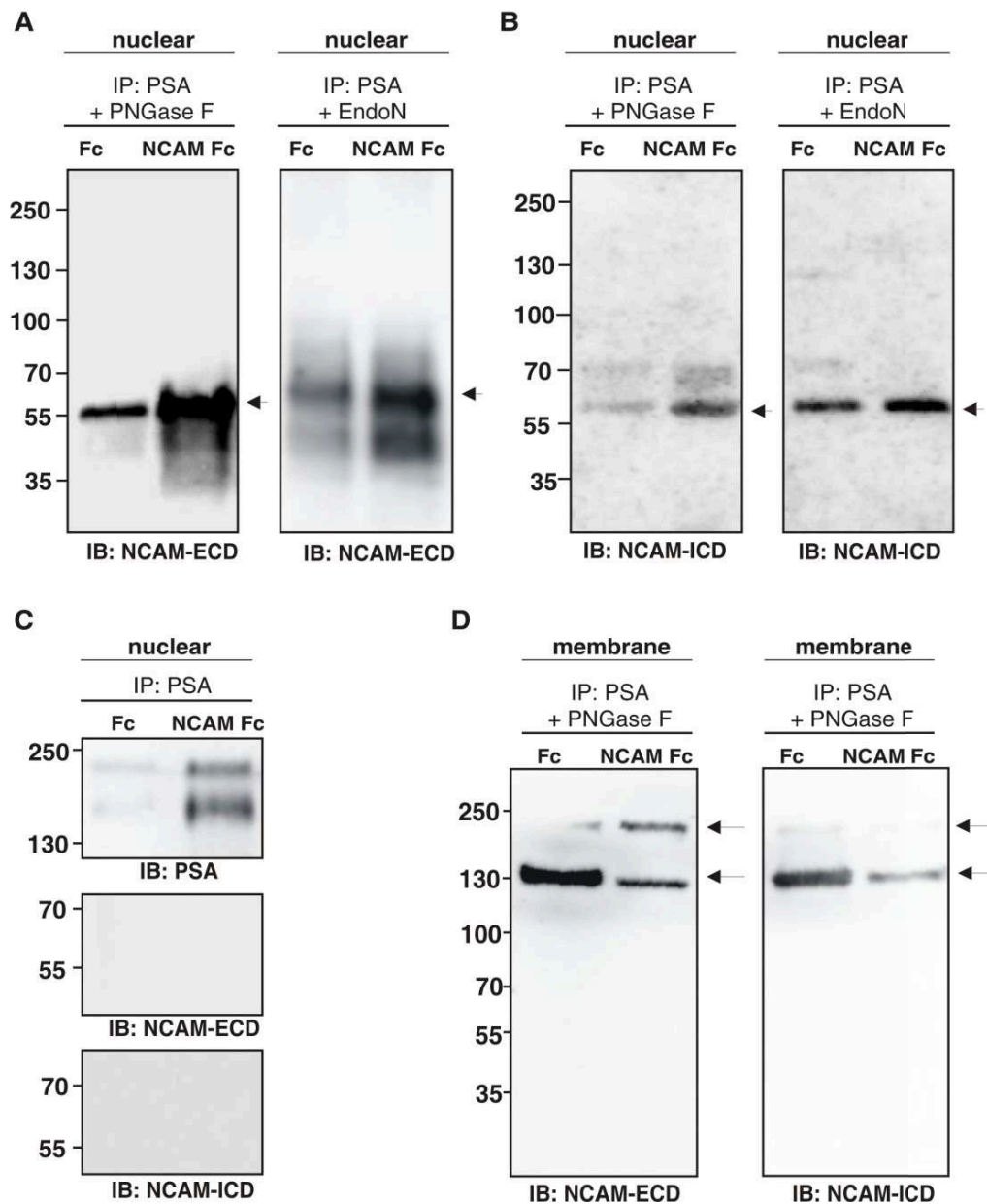


**Figure 7: Nuclear import of a 50 kDa PSA-carrying NCAM fragment after proteolytic cleavage of full length transmembrane PSA-NCAM.** (A-D) Nuclear and membrane fractions were isolated from cerebellar neurons after treatment with Fc or NCAM-Fc and then subjected to immunoprecipitation (IP) with PSA-specific antibody and treatment of the PSA immunoprecipitates with PNGase F or EndoN (A, B, D) or with buffer control (C). Nuclear fractions of PNGase F- or EndoN-treated PSA immunoprecipitates were tested with antibodies against the extracellular NCAM domain (NCAM-ECD) (A) or intracellular NCAM domain (NCAM-ICD) (B). Arrows indicate the major NCAM fragment. (C) Immunoblots of PSA immunoprecipitates without PNGase F or EndoN treatment were tested with antibodies against NCAM-ECD, NCAM-ICD and PSA. (D) PSA immunoprecipitates of membrane fractions were tested with antibodies against the extracellular NCAM domain (NCAM-ECD) or intracellular NCAM domain (NCAM-ICD). Arrows indicate the deglycosylated full-length NCAM bands of approximately 120 and 180 kDa. (A-D) Representative immunoblots from three independent experiments are shown (Westphal *et al.*, 2016).



## 5.2 PSA co-localizes with histone H1 in nuclei of wildtype cerebellar neurons

So far, I provided evidence for the presence of a PSA-carrying NCAM fragment in the nucleus of wildtype neurons which raises the question if PSA is in close contact with the DNA or interacting with nuclear proteins. Since PSA was shown to bind to the DNA-associated protein histone H1 in the extracellular matrix (Mishra *et al.*, 2010) it was interesting to test whether PSA also associates with histone H1 in the nucleus. Using proximity ligation assay with cultured cerebellar neurons and specific antibodies against PSA and histone H1, a co-localization of PSA and histone H1 could be detected as shown by the red fluorescent spots in the nucleus. A significantly enhanced number of red fluorescent spots was observed in nuclei of NCAM antibody treated wildtype neurons in comparison to nuclei of unstimulated wildtype neurons, showing a remarkably lower close interaction of PSA and H1 (**Figure 8 A**). A few extranuclear fluorescence spots in unstimulated wildtype neurons were visible, but no fluorescence signal was observed in NCAM antibody-treated and EndoN-pretreated wildtype neurons neither in the nucleus nor in the cytosol (**Figure 8 A**). Furthermore, no fluorescent spots were found in NCAM-deficient neurons (**Figure 8 B**). These results also excluded an unspecific interaction of the PSA antibody with nuclear proteins or DNA. Together, the findings indicate a direct interaction between PSA and histone H1 in neuronal nuclei.

In an unrelated study of our lab using a nuclear fraction from mouse brain for affinity chromatography, histone H1 was identified by mass spectrometry to bind to immobilized recombinant intracellular NCAM domain (unpublished observation). Based on this data, proximity ligation assay was performed to investigate whether histone H1 co-localizes not only with PSA but also with the intracellular domain of NCAM in the nucleus. Cerebellar neurons were unstimulated or treated with NCAM antibody and subjected to proximity ligation assay with specific antibodies against the intracellular domain of NCAM and histone H1. Higher fluorescence signal was determined in nuclei of NCAM antibody treated wildtype neurons in contrast to nuclei of unstimulated wildtype neurons. Furthermore, the fluorescent spots were seen outside of nuclei in unstimulated neurons (**Figure 9 A**). Next, the interaction of NCAM with histone H1 was examined in the nucleus of EndoN pretreated and NCAM antibody treated cerebellar neurons by proximity ligation assay with specific NCAM and histone H1 antibodies to test whether the nuclear NCAM fragment carries PSA or is devoid of PSA.

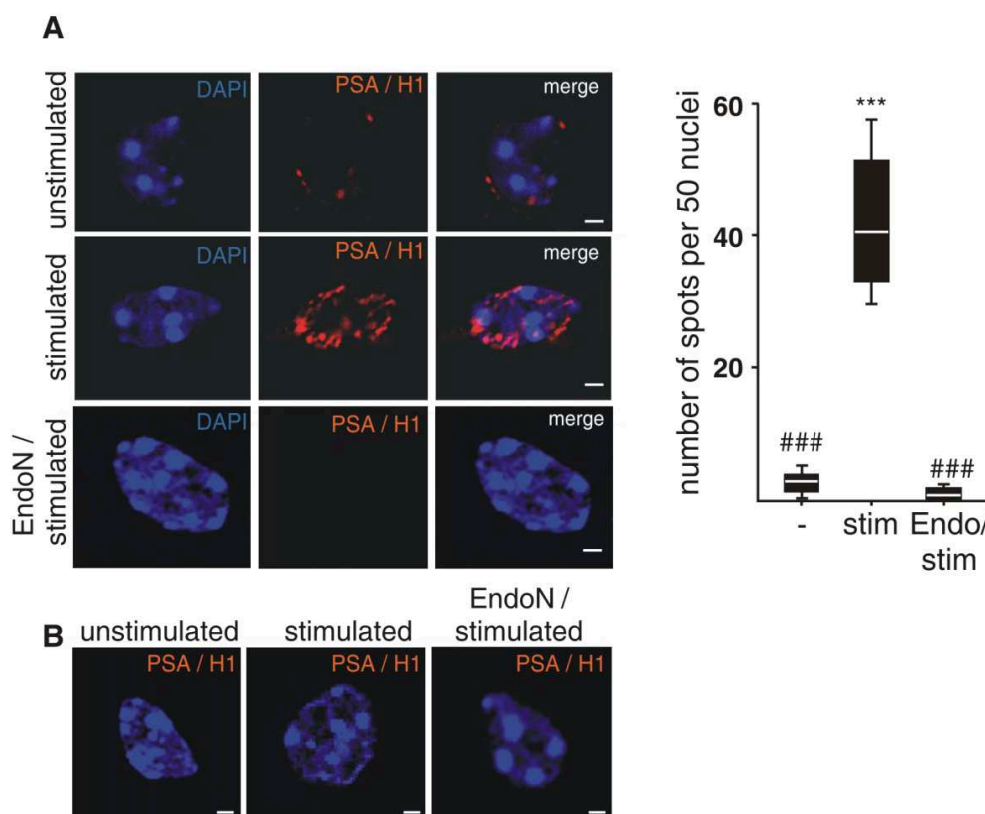


**Figure 8: PSA co-localizes with histone H1 in nuclei of cultured cerebellar neurons.** (A, B) Cerebellar neurons from wildtype (A) or NCAM-deficient (B) mice were unstimulated (-) or treated with function-triggering chicken NCAM antibody after pretreatment without (stimulated) or with EndoN (EndoN/stimulated) and subjected to proximity ligation assay with a PSA-specific mouse antibody and a rabbit antibody against histone H1 (PSA/H1). Nuclei were stained with DAPI (blue). Spots of intense fluorescent signals (red) indicate close PSA/histone H1 interactions. Representative confocal fluorescent images of unstimulated, stimulated and EndoN-pretreated stimulated neurons are shown. Scale bars: 1  $\mu$ m. A boxplot is shown for the level of nuclear PSA-histone H1 interactions, determined by counting the numbers of red spots in 50 nuclei of two images in randomly chosen areas per condition from three independent experiments. Differences for unstimulated (-), stimulated (stim) and EndoN-pretreated stimulated (Endo/stim) neurons relative to unstimulated (\*\*\*) or stimulated (###  $p < 0.001$ ) neurons are indicated (two-way ANOVA with Bonferroni post-hoc test) (Westphal *et al.*, 2016).

The number of fluorescent spots was significantly higher in nuclei of wildtype neurons after EndoN pretreatment and NCAM antibody application in comparison to nuclei of unstimulated wildtype neurons, but less than in nuclei of NCAM antibody-treated wildtype neurons that were not treated with EndoN before NCAM stimulation. This result showed that the NCAM antibody-triggered nuclear import of the PSA-lacking fragment was only slightly affected by the pretreatment with EndoN. No co-localization of NCAM and histone H1 was detected in neurons of NCAM-deficient mice (Figure 9 B).

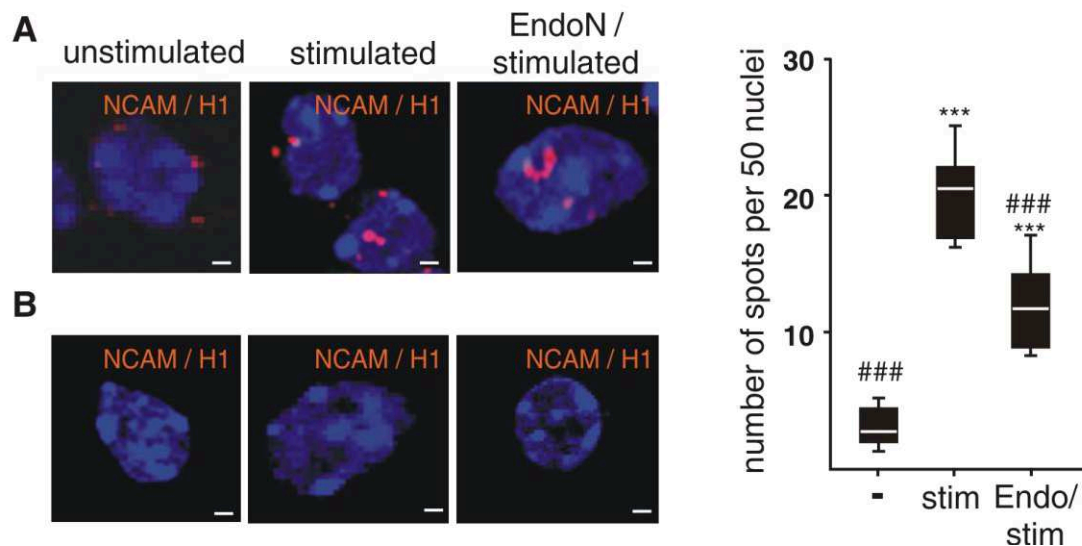


**Figure 9: Interaction of histone H1 with a nuclear NCAM fragment in cultured cerebellar neurons.** (A, B) Cerebellar neurons from wildtype (A) or NCAM-deficient (B) mice were unstimulated (-) as a control or treated with function-triggering chicken NCAM antibody after pretreatment without (stimulated) or with EndoN (EndoN/stimulated) and were subjected to proximity ligation assay with a goat antibody against the extracellular NCAM domain and a rabbit antibody which recognizes histone H1. Nuclei were stained with DAPI (blue). Spots of intense fluorescent signals (red) indicate close interactions between NCAM and histone H1 (NCAM/H1). Representative confocal fluorescent images of unstimulated, stimulated and EndoN-pretreated stimulated neurons are shown. Scale bars: 1  $\mu$ m. The boxplot represents the nuclear level of NCAM-histone H1 interactions determined by counting the numbers of red spots in 50 nuclei of two images in randomly chosen areas per condition from three independent experiments. Differences for unstimulated (-), stimulated (stim) and EndoN-pretreated stimulated (Endo/stim) neurons relative to unstimulated (\*\*\*)  $p < 0.001$  or stimulated (###)  $p < 0.001$  neurons are indicated (two-way ANOVA with Bonferroni post-hoc test) (Westphal *et al.*, 2016).

### 5.3 Detection of nuclear PSA by immunoelectron microscopy

To substantiate the nuclear localization of PSA, immunoelectron microscopy of unstimulated or NCAM antibody treated wildtype cerebellar neurons without and with EndoN pretreatment was performed with PSA-specific antibody and a secondary antibody coupled to gold particles. The nuclei of NCAM antibody-treated neurons showed high numbers of gold clusters in comparison to hardly detectable gold clusters in nuclei of unstimulated cells and in nuclei after pretreatment of cells with EndoN that removes PSA (Figure 10). With this additional method the nuclear localization of PSA-carrying NCAM could be confirmed.

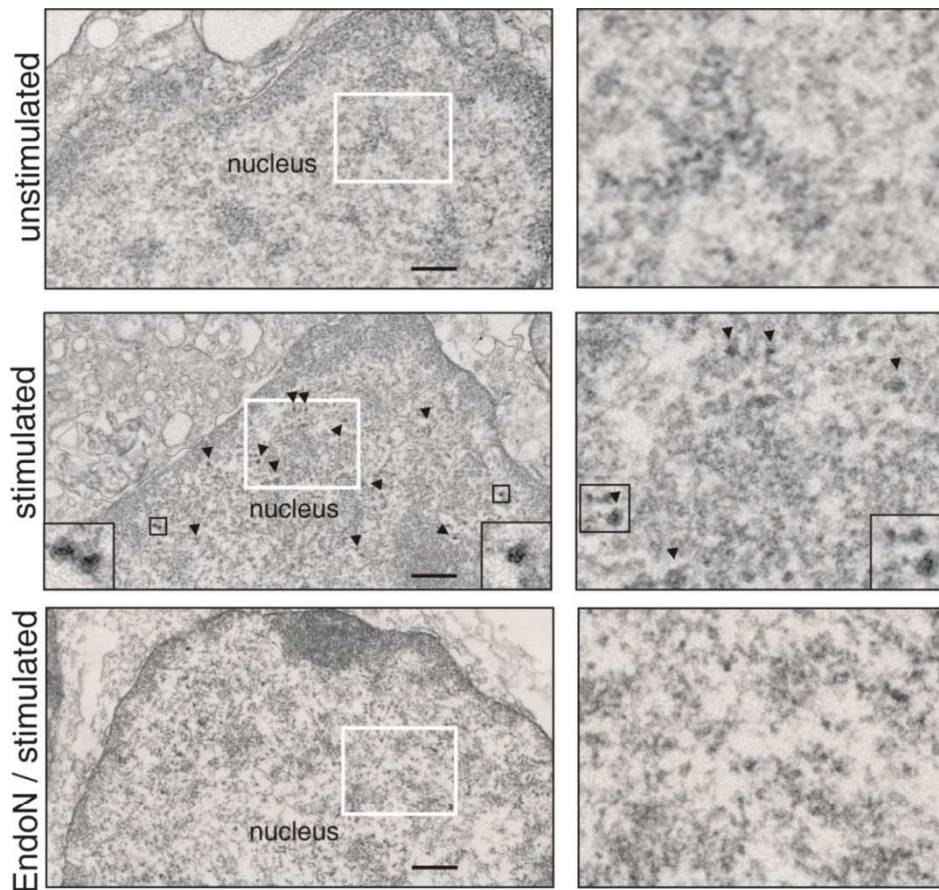


**Figure 10: Nuclear localization of PSA in cultured cerebellar neurons.** Wildtype cerebellar neurons were unstimulated or treated with function-triggering chicken NCAM antibody after pretreatment without (stimulated) or with EndoN (EndoN/stimulated) and subjected to immunoelectron microscopy. Nuclear PSA was detected with PSA-specific antibody and a secondary antibody coupled to gold particles. Representative images of nuclei of unstimulated, stimulated and EndoN-pretreated and stimulated neurons are shown (left panels) and white boxes indicate areas shown at higher magnification (right panels). Enhanced PSA levels are detected in clusters of gold particles which are indicated by arrows and shown at 10 $\times$  magnifications (black boxes). Scale bars: 500 nm. Immunoelectron images were taken by David Lutz, Institute for Structural Neurobiology, ZMNH (Westphal *et al.*, 2016).

#### 5.4 The nuclear PSA-carrying NCAM fragment is generated by matrix-metalloproteases MMP-2 and MMP-9 upon treatment with NCAM antibody

Since the previous results indicated that not full-length PSA-NCAM but a proteolytic PSA-NCAM fragment is present in the nucleus, I analyzed by which mechanism the full-length NCAM is cleaved at the plasma membrane. In earlier studies it was observed that transmembrane NCAM is cleaved by a serine protease upon NCAM antibody treatment and that a PSA-lacking fragment is translocated into the nucleus of wildtype cerebellar neurons (Kleene *et al.*, 2010a). Furthermore, the authors showed that the NCAM antibody-induced cleavage of transmembrane NCAM was blocked by the serine protease-specific inhibitor aprotinin. To determine whether the proteolytic processing of the PSA-carrying NCAM occurs also by a serine protease, wildtype cerebellar neurons were unstimulated or treated

with NCAM antibody in the presence and absence of aprotinin, nuclei were isolated and nuclear proteins were subjected to immunoblot analysis with a PSA-specific antibody. Interestingly, the nuclear PSA level was similarly enhanced in wildtype neurons which were treated with NCAM antibody in the presence and absence of aprotinin compared to the PSA level in nuclear fractions of unstimulated neurons (**Figure 11 A, C**). This result indicated that serine proteases are not involved in the generation of the PSA-NCAM fragment found in the nucleus.

Since *in vitro* and *in vivo* studies have indicated the proteolysis of NCAM by the matrix metalloproteases MMP-2 and MMP-9 (Dean and Overall, 2007; Shichi *et al.*, 2011), the influence of these MMPs in the generation of the nuclear PSA-carrying NCAM fragment was tested. Wildtype cerebellar neurons were cultured and pretreated with the broad range metalloprotease inhibitor GM6001 and with inhibitors specific for MMP-2, MMP-9 or MMP2 and MMP9 followed by treatment without and with NCAM antibody. The level of nuclear PSA was lower in neurons treated with NCAM antibody in the presence of GM6001, MMP-2, MMP-9 and MMP2/9 inhibitors than in neurons treated with NCAM antibody in the absence of inhibitors (**Figure 11 B, C**). In addition, nuclear PSA levels in neurons treated with GM6001, MMP9 and MMP2/9 inhibitor and NCAM antibody were comparable to those in unstimulated neurons, while the levels in neurons treated with MMP2 inhibitor and NCAM antibody were lower when compared to unstimulated neurons (**Figure 11 B, C**). In addition, immunoprecipitation using PSA-specific antibody and nuclear fractions of cerebellar neurons after treatment of neurons with NCAM-Fc in the presence of MMP-2- and MMP-9-specific inhibitors or Fc treatment was performed (**Figure 11 D**). The immunoprecipitates were subjected to deglycosylation with PNGase F to remove N-glycans including PSA. An apparent 50 kDa band was detectable with the NCAM-ECD antibody in nuclei of NCAM-Fc-treated neurons. In contrast, only basal levels of immunoreactive NCAM was observed in immunoprecipitates of neurons treated with Fc and neurons treated with NCAM-Fc in the presence of the MMP-9 inhibitor. The 50 kDa fragment was only barely detectable in immunoprecipitates of neurons treated with NCAM-Fc in the presence of MMP-2 inhibitor (**Figure 11 D**). This result showed that MMP-2 and also MMP-9 are involved in the generation and in nuclear import of a PSA-carrying NCAM fragment.



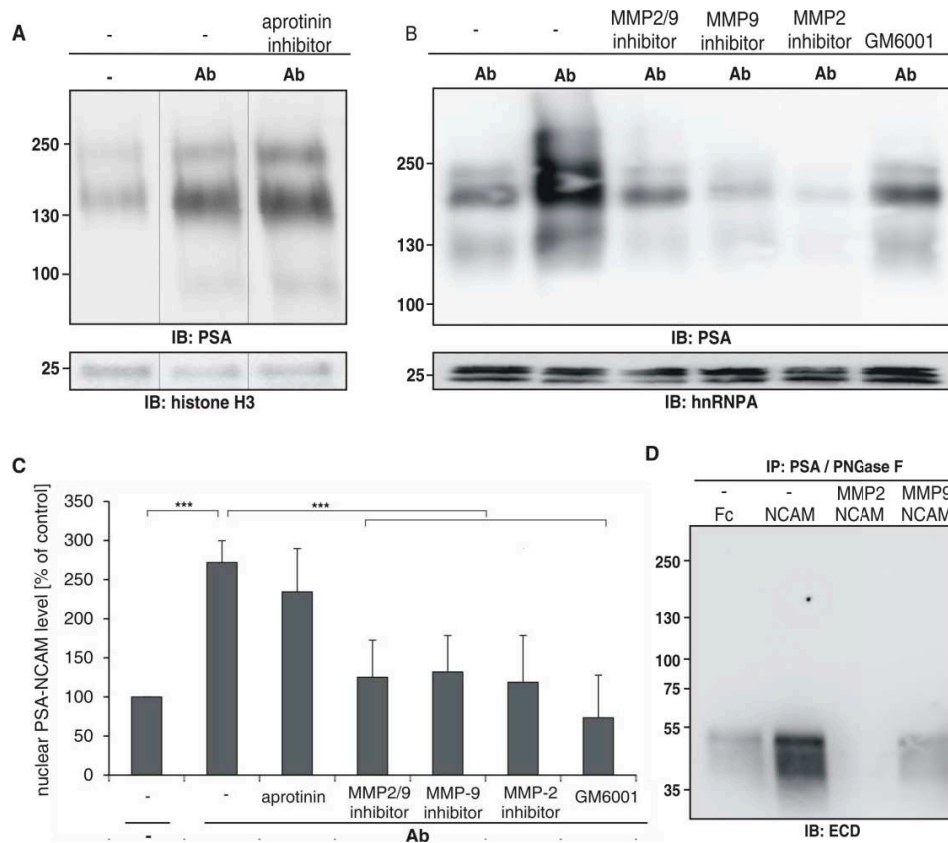


**Figure 11: Generation of the PSA-carrying nuclear NCAM fragment by matrix metalloproteases MMP-2 and MMP-9.** (A-C) Wildtype cerebellar neurons were mock-treated (-) or treated with chicken NCAM antibody (Ab) after pretreatment with reagents which block serine proteases (aprotinin) or metalloproteases (GM6001) and specifically inhibit MMP2, MMP9 or both MMP2 and MMP9 (MMP-2, MMP-9, MMP2/9). (A, B) Nuclear fractions were isolated and subjected to immunoblot analysis with PSA-specific antibody and antibodies against the nuclear marker proteins histone H3 (A) or hnRNPA (B). Representative immunoblots out of three independent experiments are shown. (C) Representative immunoblots from three independent experiments were quantified by densitometry. Nuclear PSA-NCAM level in unstimulated cells were set as 100 % (control). Mean values  $\pm$  s.d. from 3 independent experiments are shown. Differences between levels of nuclear PSA after stimulation with NCAM antibody and treatment with specific inhibitors (Ab), without treatment (-) relative to cells only stimulated with NCAM antibody are indicated (\* $p$ <0.05, \*\*\* $p$ <0.001; two-way ANOVA with Dunnett's multiple comparison test). (D) Nuclear fractions were isolated from cerebellar neurons after treatment with inhibitors and NCAM-Fc or Fc and were subjected to immunoprecipitation (IP) with PSA-specific antibody and followed by treatment with PNGase F. Immunoblots of PNGase F-treated PSA immunoprecipitates were tested with an antibody against the extracellular NCAM domain (ECD). A representative immunoblot out of three independent experiments is shown.

### 5.5 The PSA-carrying NCAM fragment is transported from the plasma membrane to the nucleus via late endosomes

After showing that the nuclear PSA-NCAM fragment derives from cleavage of full-length PSA-NCAM at the plasma membrane by matrix metalloproteases I addressed the question how this PSA-NCAM fragment is transported from the plasma membrane into the nucleus. Previous studies from our group showed that a PSA-lacking NCAM fragment is transported from the plasma membrane via the endoplasmic reticulum (ER) into the nucleus (Kleene *et al.*, 2010a). Hence, I investigated if the transport of the PSA-carrying NCAM

fragment also follows this pathway. To monitor the transport of the PSA-carrying NCAM fragment, PSA-NCAM expressing CHO cells were subjected to cell surface biotinylation followed by mock treatment or by treatment with function-triggering NCAM antibody. The biotinylated proteins of membrane, cytoplasmic and nuclear fractions were analyzed by immunoblotting with a PSA-specific antibody (**Figure 12 A**). The level of biotinylated PSA-carrying NCAM in plasma membrane-enriched fractions was reduced after NCAM antibody treatment relative to the level in fractions from unstimulated cells. After application of NCAM antibody, a higher level of biotinylated PSA-NCAM was observed in cytoplasmic and nuclear fractions of NCAM antibody-treated cells in comparison to the level in unstimulated cells. This result suggests a reallocation of PSA-NCAM from the plasma membrane to the nucleus through the cytoplasm after application of NCAM antibody to the cells. To unravel whether PSA-NCAM is present in subcellular organelles, CHO cells expressing PSA-NCAM were biotinylated and treated with NCAM antibody and subjected to ultracentrifugation to isolate fractions enriched in endosomes and ER (**Figure 12 B**). Biotinylated proteins were isolated from the endosomal and ER fractions and subjected to immunoblot analysis with a PSA-specific antibody and specific antibodies against the late endosome marker protein rab7 and the ER marker protein calreticulin. A high level of immune-positive PSA was detectable in a subcellular fraction enriched in the late endosome marker protein rab7. No PSA-NCAM was observed in the fraction which contained high levels of the ER marker protein calreticulin. This result provides evidence that the PSA-carrying NCAM fragment is translocated to the endosomes after internalization from the plasma membrane.

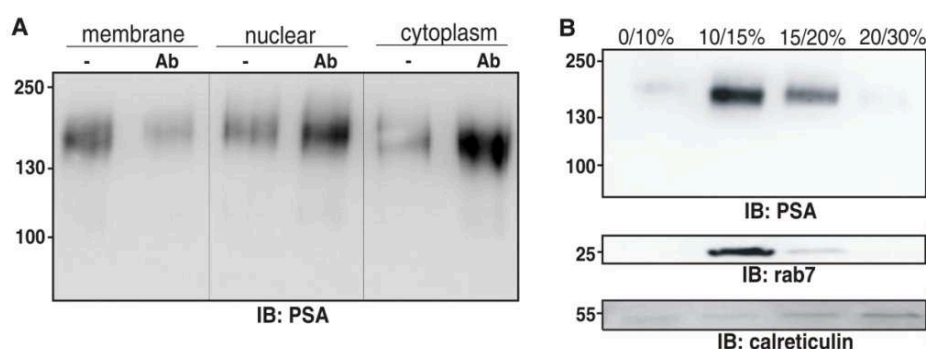


**Figure 12: The PSA carrying NCAM fragment is translocated from the plasma membrane to the nucleus via late endosomes.** (A, B) PSA expressing CHO cells were maintained in culture and subjected to cell surface biotinylation. Cells were mock-treated (-) or treated with a chicken NCAM antibody (Ab) and were then subjected to subcellular fractionation to isolate membrane, nuclear and cytoplasmic proteins (A) or collected for ultracentrifugation with an iodixanol step gradient for isolation of microsomes (B). Immunoblots of biotinylated proteins in subcellular fractions and gradient fractions were tested with a PSA-specific antibody. The gradient fractions were also probed with antibodies against the late endosomal marker protein rab7 and against the endoplasmic reticulum marker protein calreticulin (lower panels) (B). (A, B) Immunoblots are representatives from three independent experiments. Lanes not adjacent to each other but from the same blot are indicated by vertical lines.

Wildtype cerebellar neurons were mock-treated or treated with NCAM antibody and subjected to immunoelectron microscopy with a PSA-specific antibody and a secondary antibody coupled to gold particles. Gold clusters indicating PSA-NCAM were observed in endosomes of NCAM antibody treated neurons, but not in endosomes of unstimulated cells (**Figure 13 A, B**). Accumulations of gold clusters indicating PSA-NCAM were detectable at the plasma membrane of unstimulated neurons but not at plasma membrane of NCAM antibody-treated neurons. These results confirmed that PSA-NCAM is located in endosomes upon treatment of cerebellar neurons with NCAM antibody.

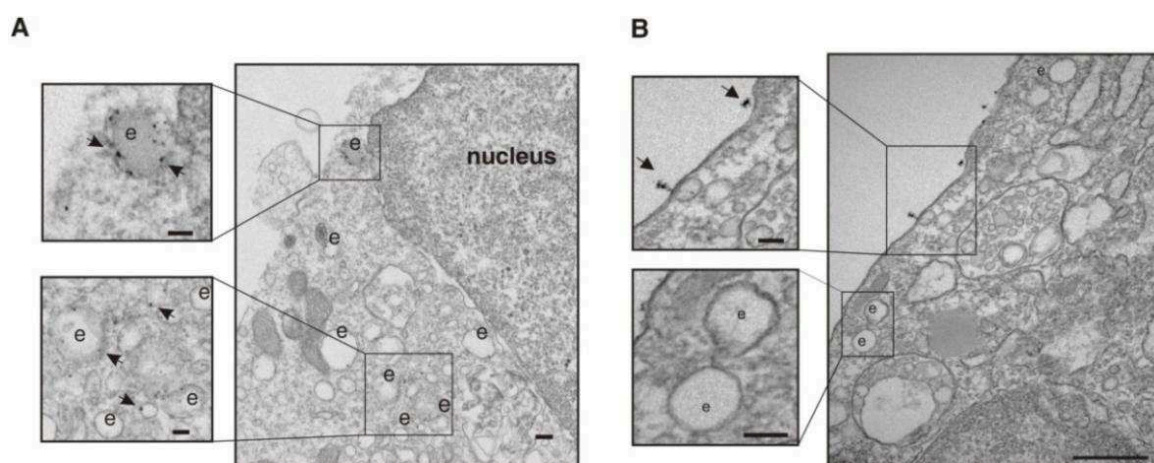


**Figure 13: Localization of PSA in endosomes of cultured cerebellar neurons.** (A, B) Wildtype cerebellar neurons were treated with function-triggering chicken NCAM antibody (A) or mock-treated (B) and subjected to immunoelectron microscopy. PSA-NCAM was detected in endosomes with a PSA-specific antibody and a secondary antibody coupled to gold particles. Representative images of a part of a neuron with endosomes (e) and nucleus after NCAM antibody treatment (A) and part of an untreated neuron with endosomes (e) (B) are shown (right panels). Black boxes indicate sections at higher magnification showing endosomes (left panels). Enhanced PSA-NCAM levels are detected in clusters of gold particles which are indicated by arrows and shown at 10× magnifications (black boxes). Scale bars: 500 nm. Immunoelectron images were taken by David Lutz, Institute for Structural Neurobiology, ZMNH.

### 5.6 The PSA-carrying NCAM fragment is released from endosomes into the cytoplasm in a calmodulin-dependent manner

The PSA-lacking NCAM fragment was shown to be transported from the plasma membrane to the ER and then to be subsequently released from the ER into the cytoplasm and to be further recruited into the nucleus in a calmodulin-dependent manner (Kleene *et al.*, 2010a). Although the PSA-carrying NCAM fragment is transported from the plasma membrane to late endosomes, it is feasible that calmodulin is also involved in the transport and/or nuclear import of the PSA-carrying NCAM fragment. To explore this hypothesis an *in vitro* translocation assay with a function-blocking calmodulin antibody and the calmodulin inhibitor CGS9343B was performed. This experiment was conducted exploiting CHO cells



either expressing PSA-NCAM or expressing NCAM, but lacking polysialyltransferases and therefore lacking PSA. The PSA-NCAM-containing cells were biotinylated, treated with NCAM antibody and subjected to ultracentrifugation for isolation of an endosomal fraction. The isolated endosomes were then incubated with a cytoplasmic fraction from PSA-lacking but NCAM-expressing CHO cells in the presence or absence of function-blocking calmodulin antibody or inhibitor to monitor the release of PSA-NCAM from endosomes into the cytoplasm. A high level of biotinylated PSA-NCAM was detected in the cleared supernatant that had been incubated with endosomes from NCAM antibody treated cells (**Figure 14 A**). Markedly reduced levels of PSA-NCAM protein were found in the cleared supernatants that were incubated with endosomes from cells treated with NCAM antibody and calmodulin antibody or calmodulin inhibitor. Furthermore, levels of biotinylated PSA-NCAM in the endosomal pellets were higher after incubation with the PSA-lacking cytosolic fraction in the presence of calmodulin antibody and calmodulin inhibitor in comparison to the levels in the endosomal pellet after incubation with the cytosolic fraction in the absence of antibody and inhibitor. In conclusion, the results show that the release of PSA-NCAM from endosomes into the cytoplasm is blocked in the presence of a function-blocking calmodulin antibody or of a calmodulin inhibitor. Immunoblot analysis with an antibody against the endosomal cargo marker transferrin showed the intactness of the endosomes after incubation and centrifugation (**Figure 14 A**). As an additional control, a non-immune IgG control antibody was used. The release of PSA-NCAM from the endosomes was only slightly affected by the non-immune antibody (**Figure 14 B**). These findings substantiate the notion that PSA-NCAM is translocated from the endosomes to the cytoplasm in a calmodulin-dependent manner.

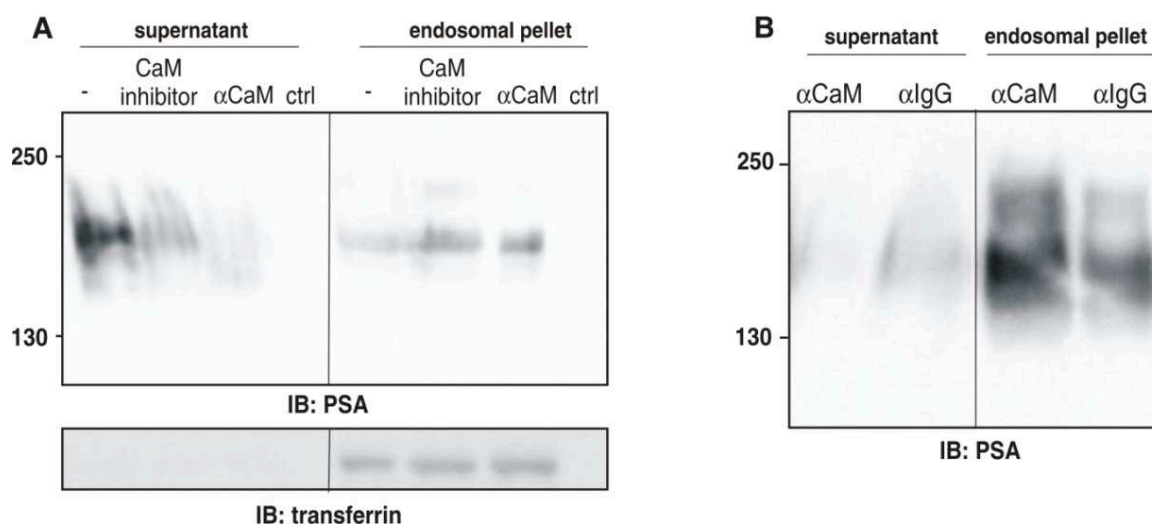


**Figure 14: The PSA-NCAM fragment is translocated from endosomes into the cytoplasm in a calmodulin dependent manner.** (A, B) PSA-NCAM expressing CHO cells were subjected to cell surface biotinylation and treated with a function triggering NCAM chicken antibody followed by isolation of an endosomal fraction. The endosomes were incubated in translocation buffer without (ctrl) or with a cytoplasmic fraction from PSA-lacking but NCAM-expressing CHO cells. The incubation was performed in the absence or presence of function-blocking calmodulin antibody ( $\alpha$ CaM) (A, B), calmodulin inhibitor (A) and of a non-immune IgG control ( $\alpha$ IgG) (B). After ultracentrifugation, biotinylated proteins were isolated from the supernatants containing the cytoplasm (supernatant) and from the endosomal pellets and were subjected to immunoblot analysis. PSA-NCAM fragment was detected with PSA-specific antibody (A, B). To show that endosomes were intact blots were probed with antibodies against the endosomal cargo marker transferrin (A). Immunoblots are representatives out of two independent experiments. Lanes which are not adjacent to each other but from the same blot are indicated by vertical lines.

Next, the transport of the PSA-NCAM fragment from the cytoplasm into the nucleus was analyzed by an *in vitro* import assay. Cerebellar neurons of wildtype mice were treated with NCAM antibody and the cytoplasm was isolated and incubated with a nuclear fraction from NCAM-deficient mice in the presence and absence of function-blocking calmodulin antibody, calmodulin inhibitor and non-immune control IgG. The supernatants and the nuclear pellets were subjected to immunoblot analysis with a PSA-specific antibody. Similar PSA-NCAM levels were found in the supernatants and nuclear pellets after incubation in the absence or presence of a function-blocking calmodulin antibody (Figure 15 A). Moreover, the PSA-NCAM levels were similar in the nuclear pellets after incubation in the absence or presence of non-immune IgG and calmodulin antibody or inhibitor (Figure 15 B). Thus, the transport of the PSA-carrying NCAM fragment from the cytoplasm into the nucleus is not mediated by calmodulin.

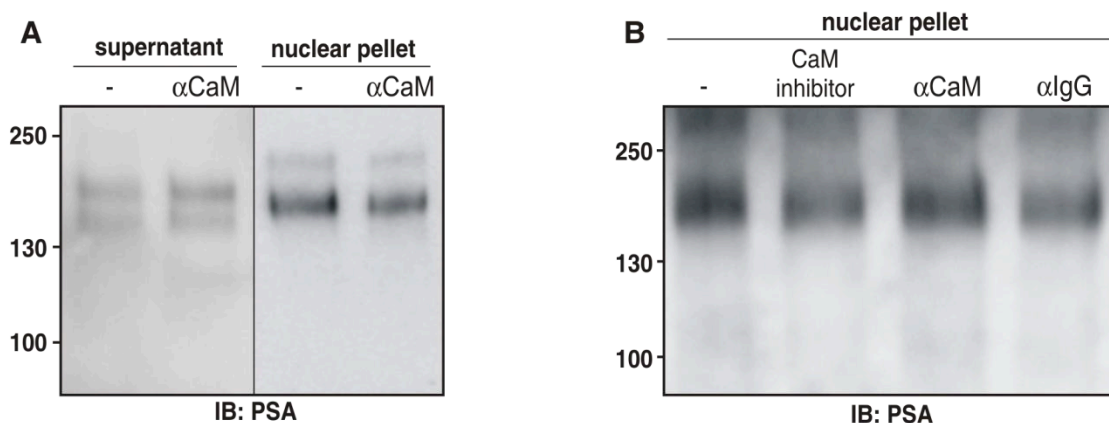


**Figure 15: The nuclear import of the PSA-NCAM fragment does not depend on calmodulin.** (A, B). Cerebellar neurons from wildtype mice were treated with function-triggering chicken NCAM antibody and cerebellar neurons from NCAM-deficient mice were left untreated. Nuclei from NCAM-deficient neurons and cytoplasm from stimulated wildtype neurons were isolated and incubated in nuclear translocation buffer in the absence (-) or the presence of calmodulin antibody ( $\alpha$ CaM) (A, B), calmodulin inhibitor (CaM inhibitor), and rabbit IgG control ( $\alpha$ IgG) (B) at 37°C for 1 h. After centrifugation, cytoplasmic proteins (supernatant) (A) and nuclear pellets were isolated and subjected to immunoblot analysis (A, B). Immunoblots are representatives from two independent experiments. Lanes not adjacent to each other but from the same blot are indicated by a vertical line.

### 5.7 Binding of PSA-NCAM to PC4 and cofilin in nuclei of dissociated cerebellar neurons and cerebellar tissue

In a previous study from our group two novel potential binding partners of PSA were identified (unpublished data). Nuclear, membrane-associated and cytoskeletal proteins were isolated from adult wildtype mice and subjected to immunoaffinity chromatography with PSA mimicking anti-idiotypic scFv antibody (Mishra *et al.*, 2010; Theis *et al.*, 2013) followed by SDS-PAGE purification. Two proteins with the mass of around 14 and 18 kDa were observed after silver staining of the gel. ESI-MS/MS mass spectrometry revealed MS/MS spectra of 1258.0 and 1336.6 Da precursor masses (detected as doubly charged ion at  $m/z=630.8$  and 669.3) that matched the tryptic peptides EQISDIDDAVR (1260.6 Da) and YALYDATYETK (1337.6 Da) of mouse positive cofactor 4 (PC4) and cofilin, respectively. The transcriptional coactivator PC4 is also known as activated RNA polymerase II distal enhancer sequence specific binding protein, SUB1 yeast homolog and p14 and is a non-histone chromatin associated protein which plays a complex role in gene expression (Conesa and Acker, 2010). The second identified protein was the non-muscle isoform of cofilin, which interacts with actin and is involved in the regulation of cytoskeletal dynamics. Cofilin has also been found in the nucleus and it has been shown to play a role in elongation of transcription by polymerase II (Obrdlik and Percipalle, 2011).

To verify a direct interaction of PSA with PC4 and cofilin an ELISA was performed using colominic acid, which is the bacterial homolog of PSA, as the ligand. A direct and concentration-dependent binding of colominic acid to coated His-tagged full length PC4, but not to His-tagged N- and C-terminal parts of PC4 was observed (**Figure 16 A**). This result indicated that the whole molecule of PC4 is important for the specific binding to PSA. Furthermore, a concentration-dependent and saturable interaction of colominic acid with GST-tagged and untagged mouse and human cofilin was observed (**Figure 16 B**), showing the direct binding of cofilin to PSA. In addition, higher amounts of PC4 and cofilin could be co-immunoprecipitated with the PSA antibody from nuclei of NCAM-antibody-treated cerebellar neurons than from nuclei of unstimulated neurons (**Figure 16 C**). These results together indicate that PSA directly binds to PC4 and cofilin and that cofilin and PC4 interact with PSA in the nucleus.

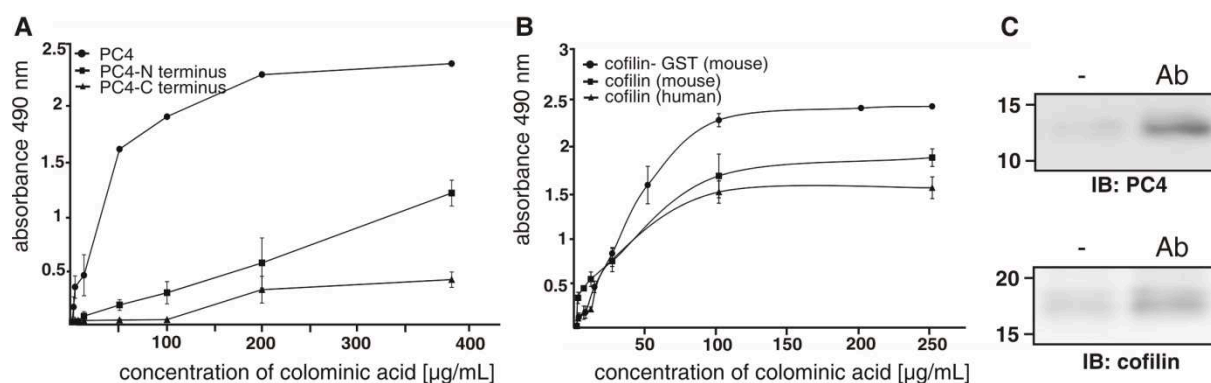


**Figure 16: Colominic acid interacts with PC4 and cofilin.** (A, B) For ELISA, proteins were coated overnight at 4°C on microtiter plates in a concentration of 20  $\mu\text{g/mL}$  for PC4 and 10  $\mu\text{g/mL}$  for N- terminal and C-terminal parts of PC4 (A) and 20  $\mu\text{g/mL}$  for GST-tagged cofilin and 10  $\mu\text{g/mL}$  for untagged human cofilin and mouse cofilin (B). The plates were incubated with colominic acid at indicated concentrations for 1 h at room temperature. Wells were then incubated with PSA-specific antibody and HRP-linked secondary antibody and were incubated with the peroxidase substrate OPD (1 mg/mL) and absorbance at 490 was measured. A representative result of one experiment out of three independent experiments is shown and PBS control was subtracted from each value. (C) Nuclear extracts from wildtype cerebellar neurons mock-treated (-) or treated with function-triggering chicken NCAM antibody (Ab) were subjected to immunoprecipitation with PSA antibody followed by Western blot analysis of the immunoprecipitates with cofilin or PC4 antibody.

To provide further evidence for the indication that cofilin and PC4 bind to PSA in the nucleus, proximity ligation assay was used. Wildtype cerebellar neurons were mock-treated or treated with NCAM antibody after pretreatment with and without EndoN and subjected to proximity ligation assay with PSA-specific mouse antibody and cofilin-specific or PC4-specific rabbit antibody. Prominent fluorescence signals were seen in nuclei of NCAM antibody-treated wildtype neurons probed with PSA antibody and cofilin or PC4 antibody compared to nuclei of unstimulated wildtype neurons which showed only weak extranuclear

fluorescence signals (**Figure 17 A, 18 A**). Hardly detectable fluorescence signals were observed in NCAM antibody-treated and EndoN-pretreated wildtype neurons (**Figure 17 A, 18 A**). This result indicates that PSA-NCAM interacts with cofilin and PC4 in the nuclei of neurons after NCAM antibody treatment. Furthermore, no interaction was detectable in NCAM-deficient neurons irrespective of the treatment (**Figure 17 B**).

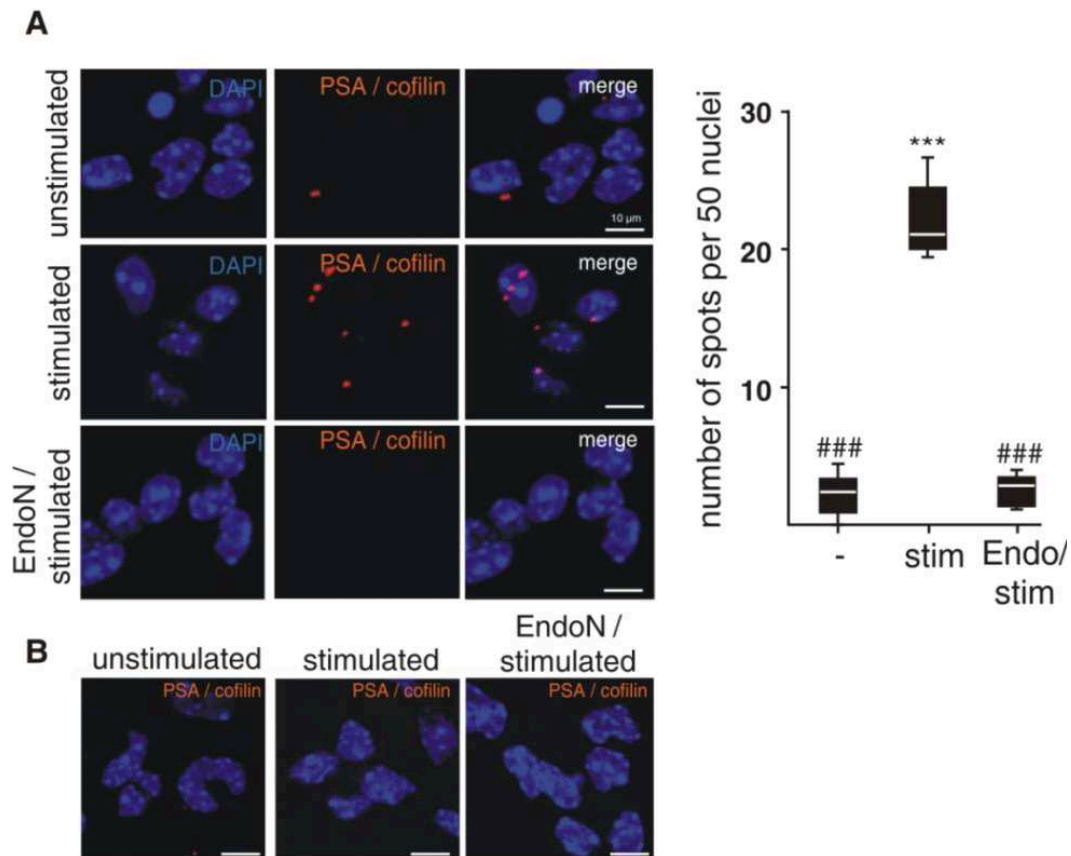


**Figure 17: PSA co-localizes with cofilin in nuclei of cultured cerebellar neurons.** (A, B) Cerebellar neurons from wildtype (A) or NCAM-deficient (B) mice were mock-treated (unstimulated) or treated with function-triggering chicken NCAM antibody after pretreatment without (stimulated) or with EndoN (EndoN/stimulated) and subjected to proximity ligation assay with PSA-specific mouse antibody and a rabbit antibody against the binding partner cofilin (PSA/cofilin). Nuclei were stained with DAPI (blue). Spots of intense fluorescent signals (red) indicate close PSA/cofilin interactions. Representative confocal fluorescent images of unstimulated, stimulated and EndoN-pretreated stimulated neurons are shown. Scale bars: 10  $\mu$ m. A boxplot is shown for the nuclear cofilin-PSA interaction level, determined by counting the numbers of red spots in 50 nuclei of two randomly chosen areas per condition from three independent experiments. Differences for unstimulated (-), stimulated (stim) and EndoN-pretreated stimulated (Endo/stim) neurons relative to unstimulated (\*\*\*) or stimulated (###) p<0.001) neurons are indicated (two-way ANOVA with Bonferroni post-hoc test).

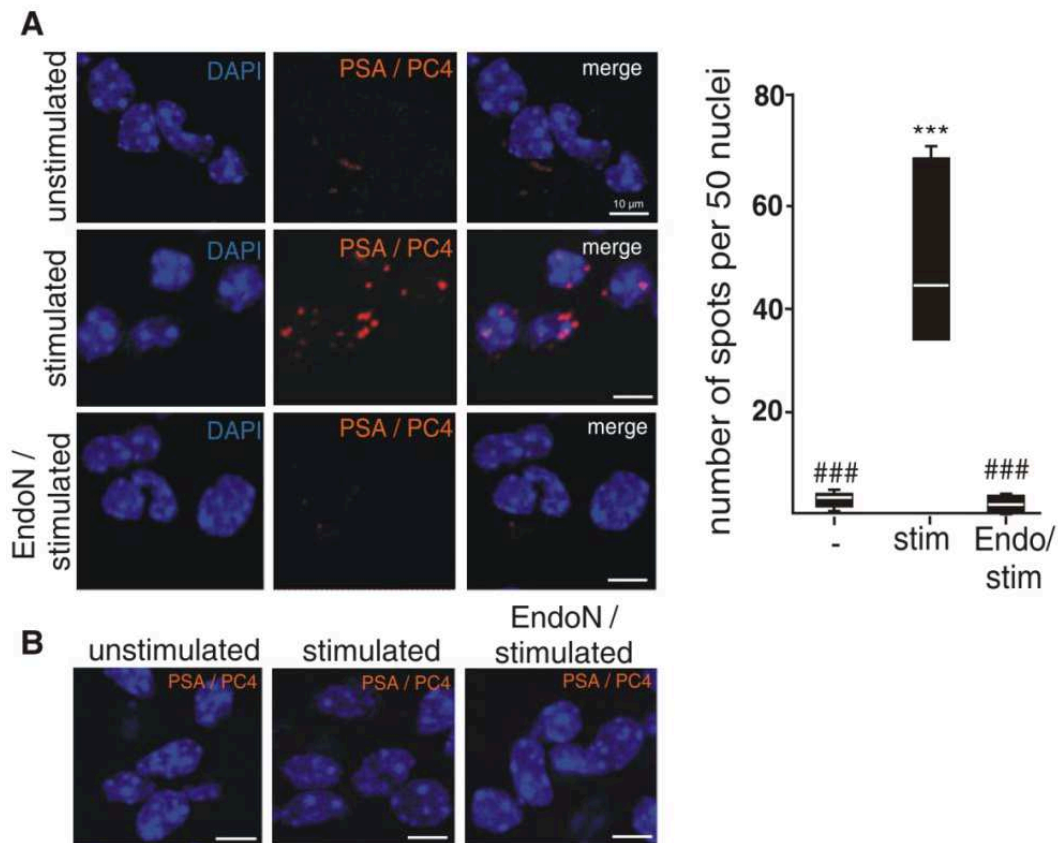


**Figure 18: PSA co-localizes with PC4 in nuclei of cultured cerebellar neurons.** (A, B) Cerebellar neurons from wildtype (A) or NCAM-deficient (B) mice were mock-treated (unstimulated) or treated with function-triggering chicken NCAM antibody after pretreatment without (stimulated) or with EndoN (EndoN/stimulated) and subjected to proximity ligation assay with PSA-specific mouse antibody and a rabbit antibody against the PSA binding partner PC4 (PSA/PC4). Nuclei were stained with DAPI (blue). Spots of intense fluorescent signals (red) indicate close PSA/PC4 interactions. Representative confocal fluorescent images of unstimulated, stimulated and EndoN-pretreated stimulated neurons are shown. Scale bars: 10  $\mu$ m. A boxplot is shown for the nuclear interaction level of PSA and PC4, determined by counting the numbers red spots in 50 nuclei of two randomly chosen areas per condition from three independent experiments. Differences for unstimulated (-), stimulated (stim) and EndoN-pretreated stimulated (Endo/stim) neurons relative to unstimulated (\*\*\*) or stimulated (###  $p < 0.001$ ) neurons are indicated (two-way ANOVA with Bonferroni post-hoc test).

To examine whether the interaction of PSA with PC4 and cofilin also takes place *in vivo*, proximity ligation assay was applied to cerebellar slices of wildtype and NCAM-deficient mice. Many fluorescence spots were visible in nuclei in wildtype tissue, indicating a close interaction of PSA-NCAM with PC4 and cofilin (**Figure 19 A, B**). Moreover, no fluorescent dots were observed in tissue from NCAM-deficient mice, which is devoid of NCAM-PSA.



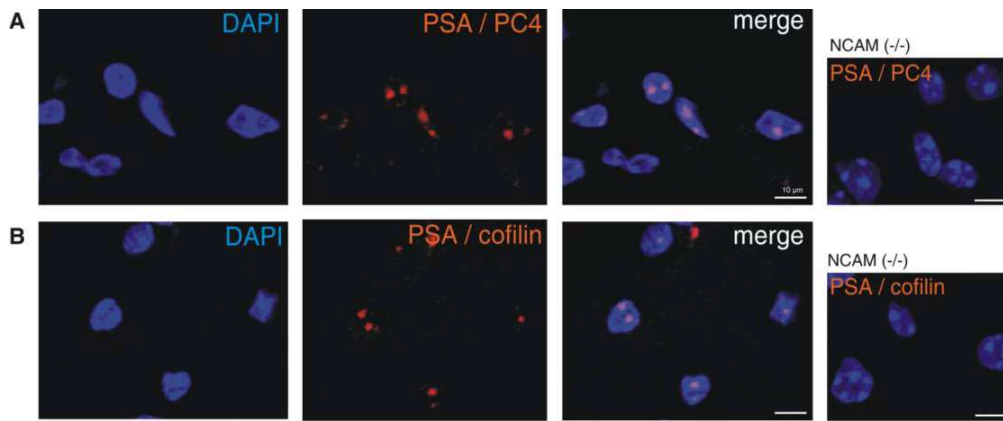


**Figure 19:** *In vivo* co-localization of PC4 and cofilin with PSA in nuclei of cerebellar tissue. (A, B) Cerebellar slices from 3 months old wildtype and NCAM-deficient mice (small images on right side) were subjected to proximity ligation assay with antibodies against PSA and PC4 (A) or PSA and cofilin (B). Representative confocal images of neuronal nuclei in the cerebellum from wildtype and NCAM-deficient mice are shown. Nuclei were stained with DAPI (blue). Spots of intense fluorescent signals (red) indicate close interactions between PSA and PC4 or cofilin. Scale bars: 10  $\mu$ m.

### 5.7.1 PC4 and cofilin contribute to the translocation of the PSA-carrying NCAM fragment from the cytoplasm into the nucleus

Cofilin is not only located in the cytoplasm but is also transported via the nuclear receptor importin  $\beta$  to the nucleus (Obrdlik and Percipalle, 2011). Since there was no evidence for a calmodulin-dependent import of PSA-NCAM into the nucleus, the idea that cofilin could be involved in the translocation of PSA-NCAM from the cytoplasm to the nucleus was tested by the *in vitro* import assay. In parallel, PC4 was also tested for its contribution in the nuclear import of the PSA-NCAM fragment. To this aim, wildtype cerebellar neurons were treated with NCAM antibody and the cytoplasm was isolated and incubated with nuclei from NCAM-deficient mice in the presence and absence of PC4 and cofilin antibodies or non-immune control IgG. After centrifugation at  $1,000 \times g$ , the supernatant and nuclear pellets were analyzed by immunoblot with PSA-specific antibody. A strong PSA-NCAM band was detected in the supernatant after incubation in the presence of PC4 and cofilin antibody. This PSA-NCAM band was hardly detectable in the supernatant after incubation in presence of non-immune control IgG or in the absence of antibodies (Figure 20). However, high PSA-NCAM levels were found in the nuclear pellets in the absence of antibodies or in the presence of non-immune control IgG when compared to the PSA-NCAM levels in nuclear pellets in the presence of the PC4 or cofilin antibody. Hence, the transfer of PSA-NCAM from the cytoplasm of NCAM antibody-treated neurons into the nucleus of NCAM-deficient neurons was blocked by application of cofilin and PC4

antibodies, suggesting that PC4 and cofilin are involved in the nuclear import of the PSA-carrying NCAM fragment.

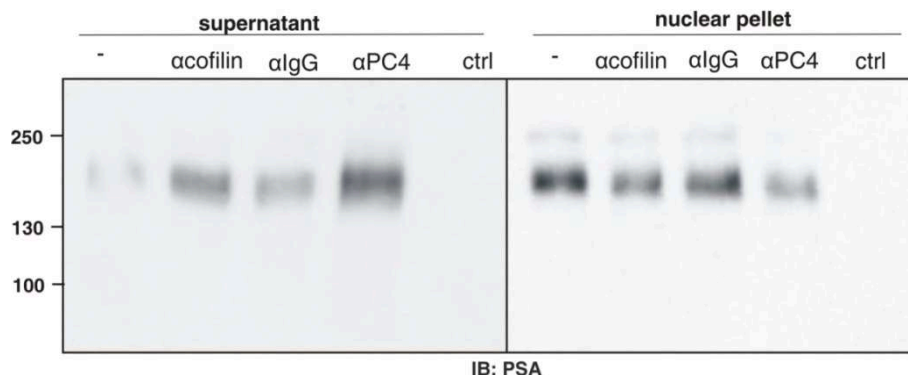


**Figure 20: Nuclear import of the PSA-NCAM fragment is influenced by cofilin and PC4.** Cerebellar neurons from wildtype mice were treated with function-triggering chicken NCAM antibody and cerebellar neurons from NCAM-deficient mice were left untreated. Nuclei from antibody treated wildtype neurons and cytoplasm from unstimulated NCAM-deficient neurons were isolated by centrifugation and incubated in nuclear translocation buffer in the absence (-) or presence of cofilin antibody ( $\alpha$ cofilin), PC4 antibody ( $\alpha$ PC4) and non-immune control IgG ( $\alpha$ IgG). As control (ctrl) nuclei of NCAM-deficient mice were treated with translocation buffer alone. After centrifugation, supernatants and nuclear pellets were subjected to immunoblot analysis with PSA-specific antibody. Immunoblots are representatives out of two independent experiments.

### 5.9 NCAM antibody, FGF-2 and the MARCKS-derived ED peptide trigger phosphorylation of MARCKS and induce the generation and nuclear import of the PSA-NCAM fragment

So far, the nuclear import of a PSA-carrying NCAM fragment was triggered in wildtype cerebellar neurons after application of NCAM antibodies or NCAM-Fc as surrogates for NCAM ligands. Additionally, it has been shown in previous studies that PSA binds to FGF-2, histone H1 and BDNF (Kanato *et al.*, 2008; Mishra *et al.*, 2010; Ono *et al.*, 2012). Therefore it was interesting to investigate if the interaction of PSA-NCAM with this physiological interaction partners might also trigger the generation and nuclear import of the PSA-NCAM fragment. Since PSA and the effector domain (ED) of MARCKS interact with each other in the plane of the plasma membrane from opposite sides, it was also interesting to examine if this interaction is involved in the generation and nuclear import of the PSA-NCAM fragment and whether disturbance of this interaction by a synthetic peptide containing the effector domain of MARCKS (MARCKS-ED) (Theis *et al.*, 2013) affects the generation and nuclear import of the PSA-NCAM fragment.

Thus, wildtype cerebellar neurons were mock-treated and treated with chicken and guinea pig NCAM antibodies, FGF-2, BDNF, histone H1 or MARCKS-ED and control peptides and



subjected to subcellular fractionation. Nuclear fractions were analyzed by immunoblotting with PSA-specific antibody. Higher levels of PSA-NCAM were seen in the nuclear fractions from neurons treated with chicken and guinea pig NCAM antibody and FGF-2 than in nuclear fractions of unstimulated neurons and in nuclear fractions of neurons after treatment with BDNF and histone H1 (**Figure 21 A**). After treatment of neurons with the MARCKS-ED peptide, enhanced levels of PSA-NCAM were detected in nuclear fractions of neurons relative to nuclear PSA-NCAM observed in unstimulated neurons and neurons treated with control peptide, implying that the disruption of the interaction between PSA and MARCKS by the MARCKS-ED peptide treatment triggers the generation or import of the PSA-carrying NCAM fragment (**Figure 21 B**).

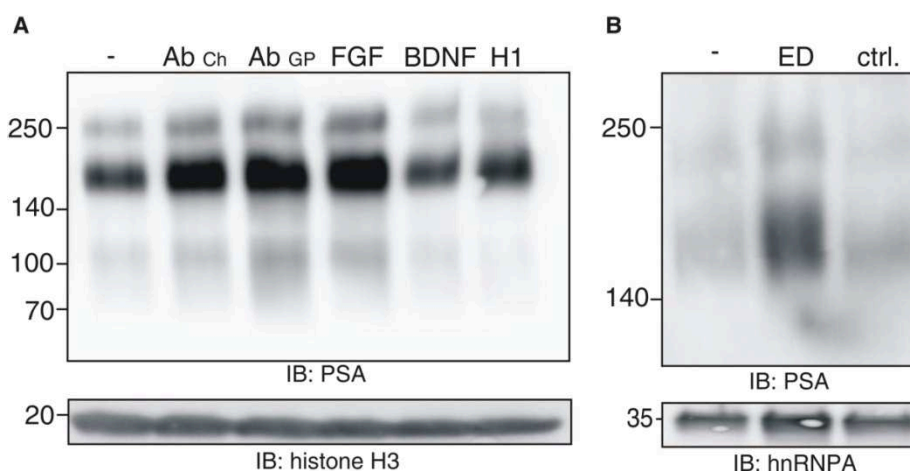


**Figure 21: Generation and nuclear import of the PSA-carrying NCAM fragment is triggered by FGF but not by histone H1 and BDNF and is enhanced after disruption of the PSA-MARCKS interaction by application of the MARCK-ED peptide.** (A, B) Cerebellar neurons of wildtype mice were treated without (-) or with function-triggering chicken (Ab Ch) or guinea pig (Ab GP) NCAM antibody, FGF-2, BDNF histone H1 (A), MARCKS-ED peptide (ED) or control peptide (ctrl.) (B). Nuclear fractions were isolated and subjected to immunoblot analysis with PSA-specific antibody and antibodies against the nuclear marker protein histone H3 (A) or hnRNPA (B). Representative blots out of two independent experiments are shown.

Recent studies showed that MARCKS is released from the inner leaflet of the plasma membrane and calmodulin dissociates from MARCKS after phosphorylation of MARCKS (Gallant *et al.*, 2005) by PKC (Morash *et al.*, 2005; Vergheze *et al.*, 1994). Moreover, the calmodulin/ $Ca^{2+}$  complex is disrupted when MARCKS is phosphorylated which leads to increased cytoplasmic levels of free calmodulin and  $Ca^{2+}$  (Morash *et al.*, 2005) and the level of phosphorylated MARCKS can provide information about the amount of free calmodulin in the cell. Thus, it deemed interesting to investigate if phosphorylation of MARCKS by PKC and dissociation of MARCKS from the plasma membrane are required for the generation or nuclear import of the PSA-NCAM fragment. The level of phosphorylated MARCKS relative to the level of total MARCKS is increased in wildtype cerebellar neurons treated with NCAM

antibody, FGF-2 and the MARCKS-ED peptide in contrast to cells without treatment and with control peptide treatment (**Figure 22**). These results indicate that MARCKS is phosphorylated after stimulation of PSA-NCAM dependent signaling. Moreover these findings suggest that MARCKS phosphorylation could lead to dissociation of calmodulin from MARCKS and that free calmodulin could induce signaling pathways which might be involved in the generation or nuclear import of the PSA-NCAM fragment.

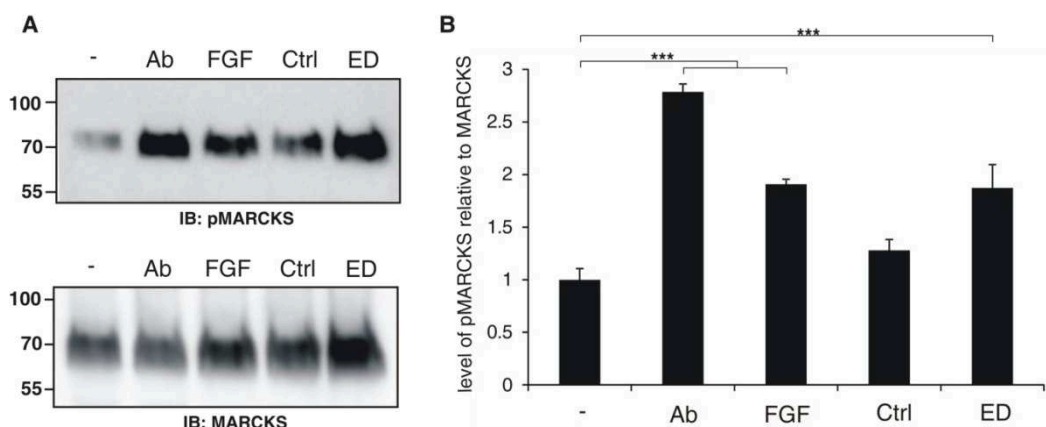


**Figure 22: Phosphorylation of MARCKS is stimulated by NCAM antibody, FGF-2 or MARCKS-ED peptide treatment.** (A, B) Cerebellar neurons from wildtype mice were mock-treated (-) or treated with chicken NCAM antibody (Ab), FGF-2, MARCKS-ED peptide (ED) or control peptide (Ctrl). Cell lysates were subjected to immunoblot analysis with antibody against phosphorylated MARCKS (pMARCKS) and total MARCKS. Representative immunoblots out of three independent experiments (A) are shown. (B) Levels of phosphorylated and total MARCKS were quantified by densitometry. Mean values  $\pm$  s.d. from 3 independent experiments are shown for the levels of phosphorylated MARCKS relative to levels of total MARCKS. Differences between groups are indicated (\*\*\*)  $p < 0.001$ ; two-way ANOVA with Dunnett's multiple comparison test).

### 5.10 The generation of the PSA-carrying NCAM fragment is induced by different pathways which require activation of the FGF-receptor

In the previous experiments I could show that the generation and nuclear import of PSA-carrying NCAM can be triggered by FGF-2, which is an activator of the FGF-receptor. It is known that activation of the FGF-receptor induces PLC activation which leads to the activation of PKC (Goetz and Mohammadi, 2013). Upon PKC-mediated phosphorylation of MARCKS which contains PKC phosphorylation sites in its effector domain (Gallant *et al.*, 2005) calmodulin dissociates from MARCKS. Free calmodulin interacts with the nitric oxide synthase (NOS) and this interaction leads to the activation of NOS (Su *et al.*, 1995). Furthermore, recent studies demonstrated that PIP<sub>2</sub> is associated with MARCKS at the plasma membrane and that phosphorylation of MARCKS leads to the dissociation of MARCKS and PIP<sub>2</sub> which is hydrolyzed to DAG and IP<sub>3</sub> by PLC. IP<sub>3</sub> is converted to PIP<sub>3</sub> which is a

product of PI3K (Czech *et al.*, 2000). Moreover free PIP<sub>2</sub> can recruit PI3K to the membrane and regulates the activity of PI3K (Ziembra *et al.*, 2016). PI3K serves as positive regulator of PLD and co-activator of PLC and was shown to regulate and activate MMP-2 (Ispanovic and Haas, 2006; Reich *et al.*, 1995).

### **5.10.1 The FGF-2- and NCAM antibody-induced generation and nuclear import of the PSA-carrying NCAM fragment depends on calmodulin-induced NO synthesis and NO-mediated activation MMP-9**

To test the idea that MARCKS-mediated and calmodulin-dependent signaling pathways contribute to the generation or nuclear import of the PSA-NCAM fragment, wildtype cerebellar neurons were pretreated with specific inhibitors of the FGF-receptor, calmodulin, NOS, PKC, PLC, focal adhesion kinase (FAK), PLD and PI3K followed by treatment with function-triggering NCAM antibody. Nuclear fractions were isolated and subjected to immunoblot analysis with PSA-specific antibody. The level of the PSA-NCAM fragment was remarkably reduced in nuclear fractions from neurons treated with NCAM antibody in the presence of calmodulin, NOS and FGF-receptor inhibitors compared to the levels in nuclear fractions from neurons treated with NCAM antibody in the absence of inhibitors or in the presence of the FAK inhibitor (**Figure 23 A, D**). This result indicates that a calmodulin and NOS are required for the generation and nuclear import of the PSA-carrying NCAM fragment, while FAK is not involved in the generation of the PSA-carrying NCAM fragment. Furthermore, a lower level of the PSA-NCAM fragment was observed in nuclear fractions of neurons treated with NCAM antibody in the presence of PKC and PLC inhibitors relative to nuclear fractions of neurons treated only with the NCAM antibody, indicating that PKC and PLC are involved in the signaling cascade leading to the generation of the PSA-NCAM fragment (**Figure 23 B, D**). Since PLC and PI3K are involved in the regulation of PLD, I tested whether the inhibition of PI3K and PLD could block the generation and nuclear import of PSA-NCAM. Cerebellar neurons were treated with NCAM antibody and pretreated with inhibitors specific for PI3K and PLC or were mock-treated as control. Reduced levels of the PSA-NCAM fragment were seen in nuclear fractions of unstimulated and NCAM antibody treated neurons in the presence of PI3K inhibitor in contrast to NCAM antibody-treated neurons in absence or presence of a PLD inhibitor (**Figure 23 C, D**). This result suggests that PLD is not involved in the signaling cascade leading to the generation or nuclear import of PSA-NCAM fragment upon treatment with NCAM antibody.

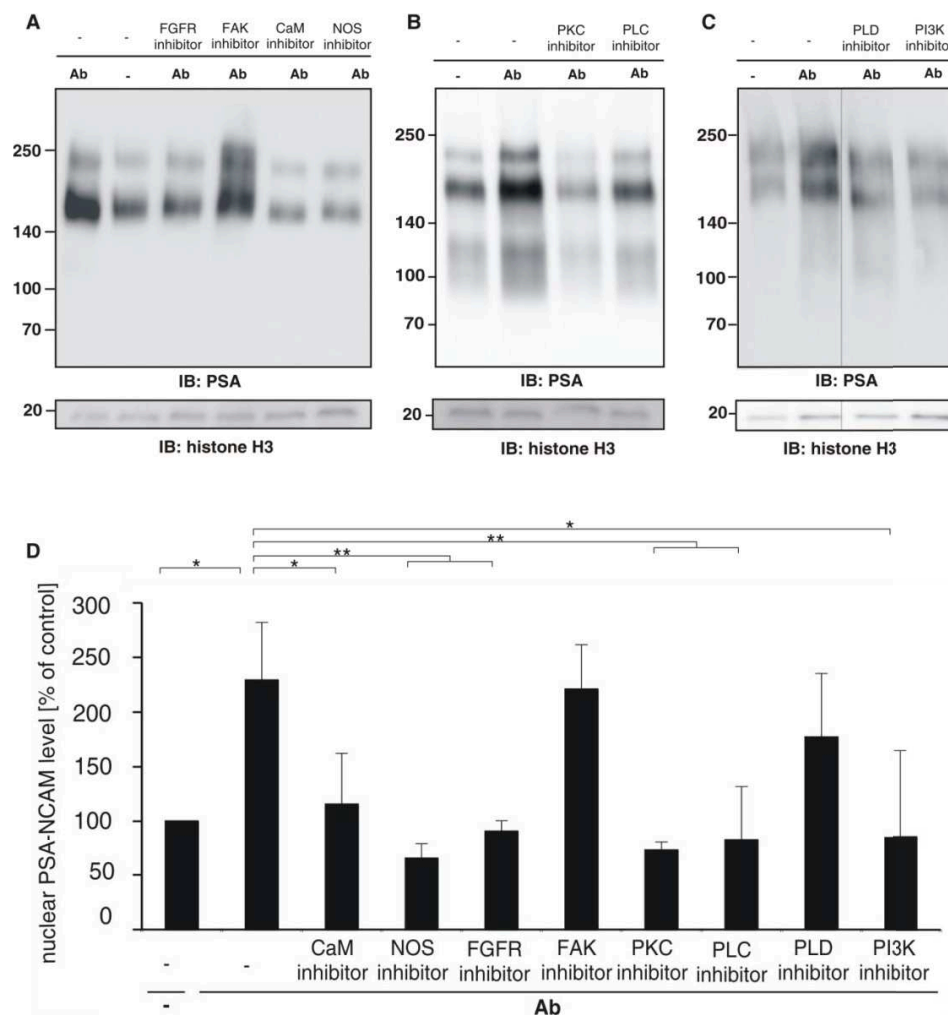


**Figure 23: NCAM antibody stimulated generation and nuclear import of the PSA-carrying NCAM fragment depends on calmodulin induced NO-synthesis and FGF-receptor activation.** (A-C) Cerebellar neurons derived from wildtype mice were pretreated with inhibitors against FGFR, FAK, calmodulin (CaM), NOS (A), PKC and PLC (B), PLD and PI3K (C) and treated with NCAM antibody (Ab) or mock-treated (-). Nuclear fractions were isolated and subjected to immunoblot analysis with antibody against PSA or the nuclear marker protein histone H3 (A-C). Representative immunoblots out of three independent experiments are shown. (D). PSA levels were quantified by densitometry. Mean values  $\pm$  s.d. of experiments ( $n=3$ ) are shown for levels of nuclear PSA-NCAM fragments after treatment with specific inhibitors (inhibitor) and stimulation with NCAM antibody (Ab) as well as unstimulated (-) relative to cells stimulated only with NCAM antibody (Ab). Differences between groups are indicated (\*\* $p < 0.001$ ; two-way ANOVA with Dunnett's multiple comparison test).

Similar levels of the PSA-NCAM fragment were found in nuclear fractions of neurons which were mock-treated and treated with FGF-2 in the presence of FGF-receptor, NOS, calmodulin, PLC and PKC inhibitor and which were lower than PSA-NCAM fragment levels in nuclei of neurons treated with FGF-2 in the absence of inhibitors or in the presence of the FAK inhibitor (Figure 24). The combined results support the hypothesis that NCAM antibody as well as FGF-2 treatment lead to activation of the FGF-receptor and subsequently to a calmodulin/NOS interaction and activation of NOS.

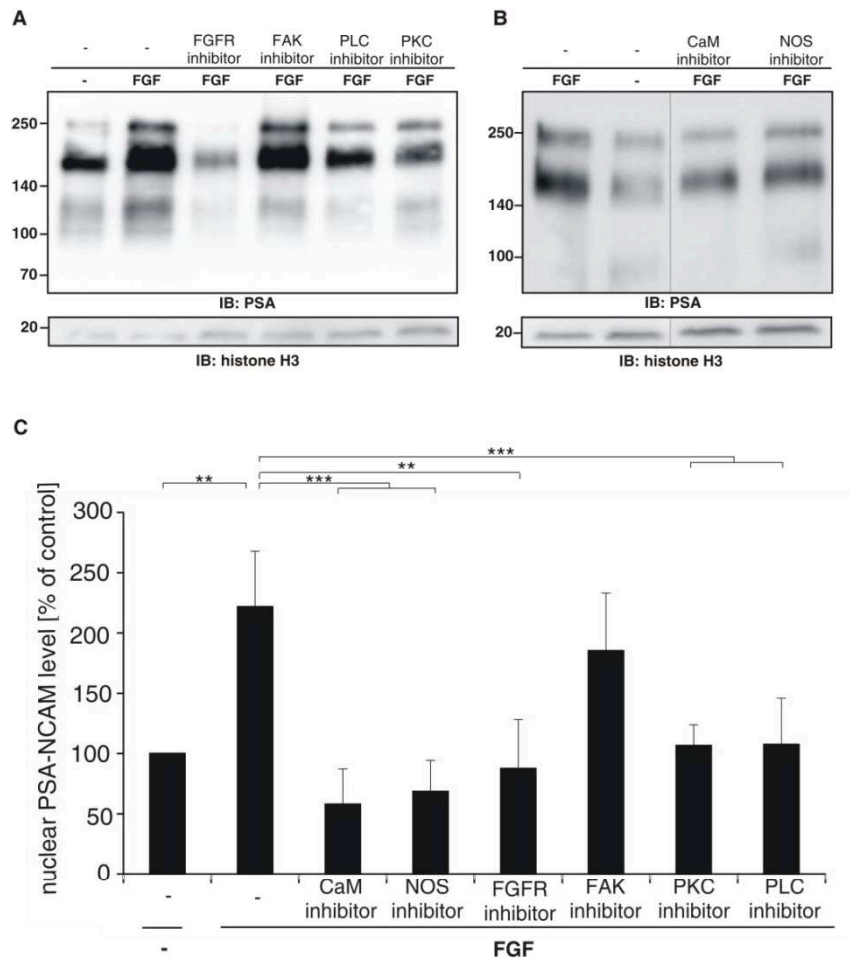


**Figure 24: FGF induced generation and nuclear import of the PSA-carrying NCAM fragment depends on calmodulin induced NO-synthesis and FGF-2 receptor activation.** (A-C) Cerebellar neurons derived from wildtype mice were pretreated with inhibitors against FGFR, FAK, PLC and PKC (A), calmodulin (CaM) and NOS (B) and treated with FGF-2 or mock-treated. Nuclear fractions were isolated and subjected to immunoblot analysis with an antibody against PSA and the nuclear marker protein histone H3 (A, B). Representative immunoblots from three independent experiments are shown (A, B) and were quantified by densitometry. (C) Mean values  $\pm$  s.d. of experiments (n=3) are shown for the levels of nuclear PSA-NCAM fragments after treatment with specific inhibitors (inhibitor) and stimulation with FGF as well as unstimulated (-) relative to only FGF-2 stimulated cells (FGF). Differences between groups are indicated (\*\*p<0.001; two-way ANOVA with Dunnett's multiple comparison test).

Based on the fact that the NCAM antibody and FGF-2 induced generation of the PSA-NCAM fragment in neurons depend on a calmodulin/NOS interaction, it was examined whether a calmodulin-triggered NOS activation leads to a higher intracellular nitric oxide (NO) production and an efflux of NO (Su *et al.*, 1995). Thus, the extracellular NO levels were measured in supernatants of untreated and NCAM antibody- and FGF-2-treated cerebellar neurons. The extracellular NO levels increased within 15 sec after NCAM antibody and FGF-2 treatment and thereafter declined slowly and reached the NO level of unstimulated cells after 5 minutes (Figure 25 A, B).

It is known that NO can influence the activity of proteins by posttranslational modification via nitrosylation of cysteine thiol residues. MMP-9 is activated by NO-induced S-nitrosylation of cysteine thiols in its prodomain (Gu *et al.*, 2002; Ridnour *et al.*, 2007). Since MMP-9 is involved in the generation of the PSA-carrying NCAM fragment the level of S-nitrosylated MMP-9 in lysates and culture supernatants of wildtype cerebellar neurons was analyzed after treatment of cells with NCAM antibody. As control cells were mock-treated. Samples were subjected to reduction of the cysteines to nitrosothiols followed by attachment of biotin residue to the nitrosothiols by generating biotinylated proteins. Biotinylated S-nitrosylated proteins were analyzed by immunoblot with MMP-9- and MMP-2-specific antibodies. In supernatants of NCAM antibody-treated neurons an immunoreactive band of around 90 kDa was detected with a MMP-9-specific antibody (**Figure 26 A**), indicating S-nitrosylated MMP-9.

In immunoblots probed with MMP-2 antibody, no S-nitrosylated MMP-2 was found in supernatants of mock-treated and NCAM antibody treated neurons (**Figure 26 B**), hence MMP-2 was not S-nitrosylated by NO upon NCAM antibody treatment. These results suggest that NCAM antibody treatment triggers a calmodulin/NOS mediated NO efflux, which induces the activation of MMP-9 by S-nitrosylation.

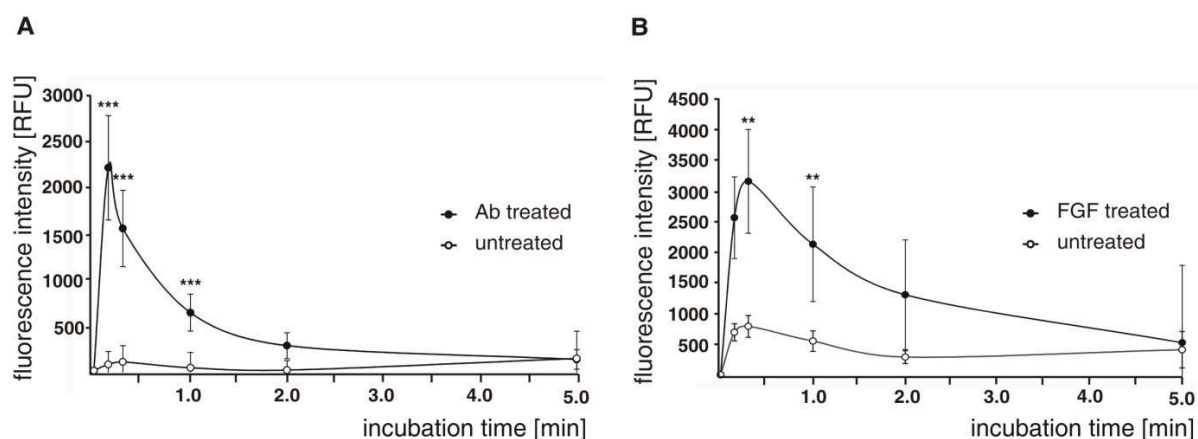


**Figure 25: Efflux of nitric oxide (NO) from cultured cerebellar neurons after treatment with function triggering NCAM antibody and FGF-2.** (A, B) Wildtype cerebellar neurons were cultured and the medium was exchanged against HBSS without phenol red. Cells were not treated (untreated) or treated with guinea pig NCAM antibody (Ab treated) (A) or FGF-2 (B) for 0 sec, 15 sec, 30 sec, 1 min, 2 min and 5 min followed by collection of the cell culture supernatant. Samples of antibody-treated cells and untreated control cells were incubated with agarose A/G beads to remove the antibody. All samples were subjected to a nitrate/nitrite fluorometric assay and the fluorescence intensity [RFU] was measured. Mean values  $\pm$  s.d. from 3 technical replicates of 3 experiments are shown. Differences between groups are indicated (\*\*  $p < 0.01$ , \*\*\*  $p < 0.001$ ; two-way ANOVA with Dunnett's multiple comparison test).



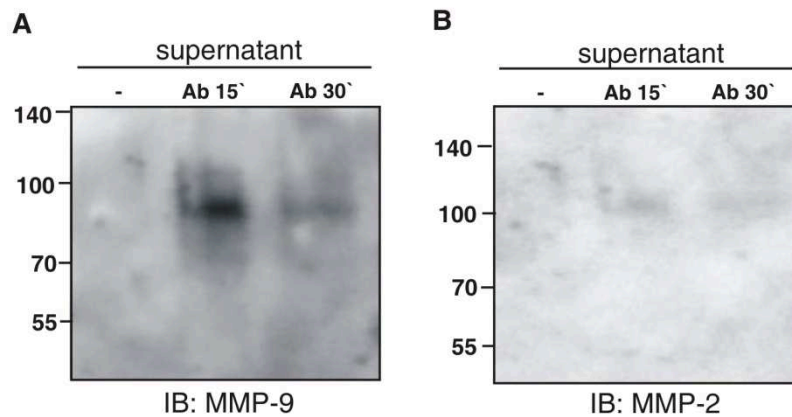


**Figure 26: S-nitrosylation of MMP-9 is triggered after treatment of cultured cerebellar neurons with function triggering NCAM antibody.** (A, B) Wildtype cerebellar neurons were treated with NCAM antibody for 15 min and 30 min and mock-treated. The supernatants were collected and subjected to a S-nitrosylation assay allowing to exchange the S-nitrosyl residues by biotin-residues. Biotinylated proteins of the supernatants were subjected to pull down and immunoblot analysis with antibodies against MMP-9 (A) and MMP-2 (B).

### 5.10.2 MARCKS-ED peptide-induced generation and nuclear import of the PSA-carrying NCAM fragment requires FGF-receptor-mediated PKC-, PLC-, PLD-, and PI3K-dependent activation of MMP-2

Next, I determined whether the MARCKS-ED peptide mediated generation and nuclear import of the PSA-NCAM fragment involves the activation of MMPs. Wildtype cerebellar neurons were pretreated with specific inhibitors of MMP-2 and MMP-9 and treated with MARCKS-ED peptide or mock-treated. Nuclear fractions were isolated and subjected to immunoblot analysis with PSA-specific antibody. The level of the nuclear PSA-NCAM fragment was lower in unstimulated neurons and in neurons treated with the MARCKS-ED peptide in the presence of MMP-2 inhibitor relative to the levels in neurons treated with MARCKS-ED peptide in absence or presence of the MMP-9 inhibitor (**Figure 27 A, B**). This result showed that MMP-2 is involved in the generation in nuclear import of the PSA-NCAM fragment after MARCKS-ED treatment.

I measured the extracellular NO level in supernatants of cerebellar neurons treated with control peptide and MARCKS-ED peptide. No significant difference in NO levels in supernatants of neurons treated with control peptide or MARCKS-ED peptide was observed (**Figure 27 C**). These results indicate that no NO was released and/or produced upon MARCKS-ED peptide treatment and that the MMP-2 activation is triggered by the MARCKS-ED peptide via a NO-independent pathway. Furthermore, the results show that MMP-9 is not involved in the MARCKS-ED peptide-induced generation and nuclear import of the PSA-NCAM fragment.

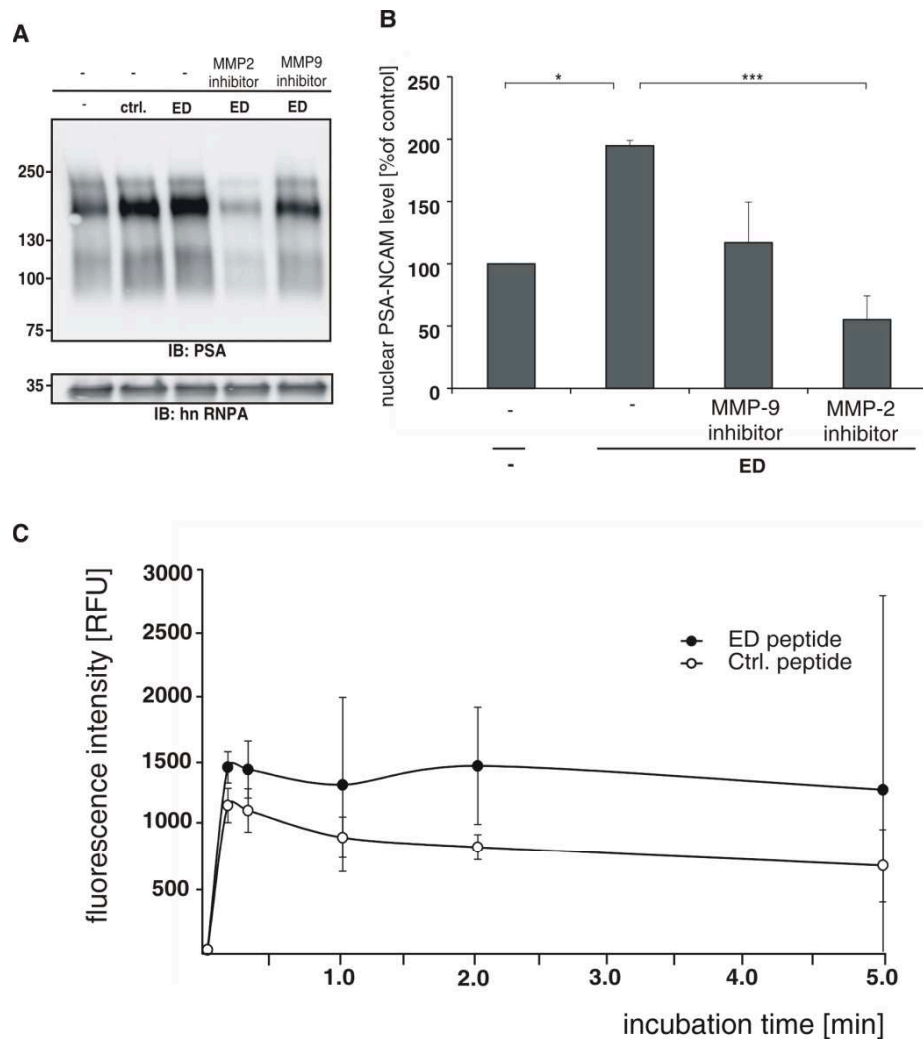


**Figure 27: MARCKS-ED peptide induced generation of the PSA-carrying NCAM fragment by MMP-2 is independent of NOS activation.** (A-C) Wildtype cerebellar neurons were mock-treated (-) or treated with MARCKS-ED peptide (ED) after pretreatment with inhibitors which specifically inhibit MMP-2 or MMP-9 (A, B). Nuclear fractions were isolated and subjected to immunoblot analysis with PSA-specific antibody and an antibody against the nuclear marker protein hnRNPA (A). A representative immunoblot out of three independent experiments is shown. PSA-levels were quantified by densitometry (B). Mean values  $\pm$  s.d. from 3 independent experiments are shown for the level of nuclear PSA-NCAM fragments after treatment without or with specific inhibitors followed by MARCKS-ED peptide treatment relative to unstimulated cells (set to 100 %). Differences between groups are indicated (\*\* $p < 0.01$ , \*\*\* $p < 0.001$ ; two-way ANOVA with Dunnett's multiple comparison test). (C) Wildtype cerebellar neurons were cultured and the medium was exchanged against HBSS without phenol red and cells were not treated (untreated) or treated with MARCKS-ED peptide for 0 sec, 15 sec, 30 sec, 1 min, 2 min and 5 min followed by collection of the cell supernatant. Samples were subjected to nitrate/nitrite fluorometric assay and fluorescence intensity [RFU] was measured. Mean values  $\pm$  s.d. from 3 technical replicates of 3 experiments are shown.

Although the generation of the PSA-NCAM fragment by MARCKS-ED peptide treatment did not depend on NO generation and depends only on MMP-2 activation but not on MMP-9 activation, it deemed interesting to determine if nevertheless FGF-receptor, calmodulin and PKC are activated after MARCKS-ED peptide treatment. Wildtype cerebellar neurons were mock-treated or pretreated with inhibitors of the FGF-receptor, calmodulin, NOS and PKC, followed by treatment with MARCKS-ED peptide. Nuclear fractions were



isolated and subjected to immunoblot analysis with PSA-specific antibody. The level of the PSA-NCAM fragments was enhanced in nuclear fractions of neurons treated with MARCKS-ED peptide in the presence of NOS and calmodulin inhibitor in comparison to the level in nuclear fractions from unstimulated neurons and in neurons treated with MARCKS-ED peptide in the presence of FGF-receptor and PKC inhibitor (**Figure 28 A, C**). Calmodulin and NOS activation are not required to trigger the generation and nuclear import of PSA-NCAM upon MARCKS-ED peptide treatment, but activation of the FGF-receptor and of PKC are needed for the nuclear import of PSA-NCAM.

My experiments showed that endogenous MARCKS is phosphorylated upon MARCKS-ED peptide treatment and that besides the FGF-receptor inhibitor only the PKC inhibitor had an effect on the MARCKS-ED peptide-induced generation and nuclear import of the PSA-NCAM fragment. Since PLC is involved in the regulation of PLD and activated PLD produces phosphatidic acid and can activate PI3K (Czech *et al.*, 2000; Morash *et al.*, 2005) and activated PI3K is together with PLD involved in the regulation of MMP-2 (Reich *et al.*, 1995; Ispanovic and Haas, 2006), I examined whether PLC, PLD and PI3K are involved in the signaling pathway which leads to the generation and nuclear import of the PSA-NCAM fragment.

Wildtype cerebellar neurons were mock-treated and treated with MARCKS-ED peptide in the presence and absence of inhibitors for PLD, PLC and PI3K and subjected to subcellular fractionation. Nuclear fractions were analyzed by immunoblot with PSA-specific antibody. The immunoreactive signal indicated significantly less PSA-NCAM fragment in the nuclear fractions of neurons pretreated with PLC, PLD and PI3K inhibitors followed by treatment with MARCKS-ED peptide compared to nuclear fractions of neurons treated with MARCKS-ED peptide alone (**Figure 28 B, C**), suggesting that in this signaling pathway PLD, PLC and PI3K are involved

Together, these results support the notion that the MARCKS-ED peptide-induced generation of the PSA-NCAM fragment is triggered by a signaling pathway which is different to the NCAM antibody- and FGF-2-triggered signal transduction.

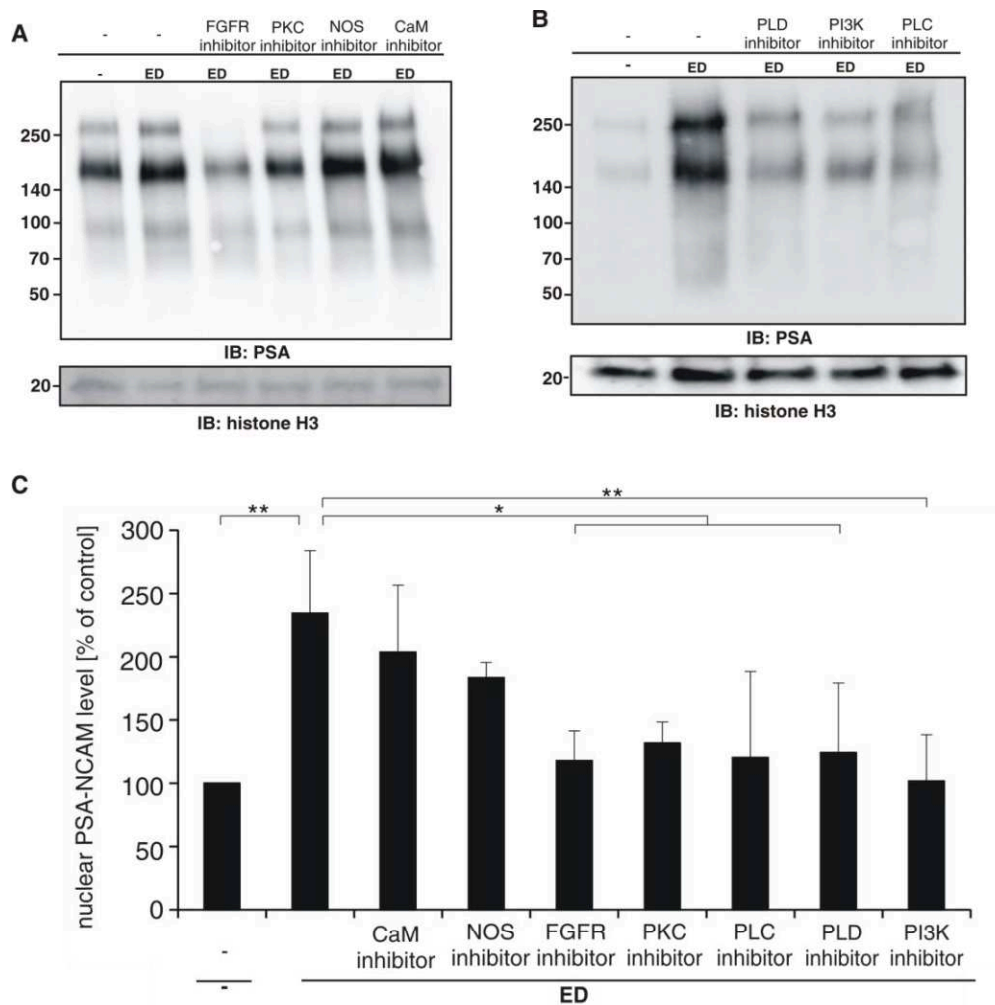


**Figure 28: MARCKS-ED peptide induced generation and nuclear import of the PSA-carrying NCAM fragment depends on PI3K, PLC and PLD and is not regulated by calmodulin and NOS.** (A-C) Wildtype cerebellar neurons were pretreated with inhibitors for the FGF-receptor (FGFR), PKC, NOS, calmodulin (CaM) (A, C), PLD, PI3K and PLC (B, C) and treated with MARCKS-ED peptide (ED) or mock-treated (-). Nuclear fractions were isolated and subjected to immunoblot analysis with PSA specific antibody and an antibody against the nuclear marker protein histone H3. Representative immunoblots out of three independent experiments are shown (A, B). PSA-NCAM levels were quantified by densitometry (C). Mean values  $\pm$  s.d. of 3 independent experiments are shown for the level of nuclear PSA-NCAM after treatment without or with specific inhibitors and stimulation with MARCKS-ED peptide relative to unstimulated cells. Differences between groups are indicated ( $p < 0.05$ ;  $***p < 0.001$ ; two-way ANOVA with Dunnett's multiple comparison test).

## **5.11 Nuclear PSA-NCAM is involved in the circadian rhythm *in vitro* and *in vivo***

Next, I was interested to discover the functional role of the PSA-carrying NCAM fragment in the nucleus.

### **5.11.1 Nuclear import of the PSA-NCAM fragment affects mRNA expression of the clock-related genes CLOCK and Per-1 in cerebellar neurons**

PSA has been shown to be involved in regulating nonphotic inputs like locomotor activity, social interaction and sleep which beside the daily light-dark cycle control the circadian rhythm (Glass *et al.*, 2003; Golombek *et al.*, 2010). To investigate the functional consequence of the nuclear PSA-carrying NCAM fragment, the influence of nuclear PSA-NCAM on the circadian biorhythm was examined. Since the circadian rhythm and regulation of the expression of clock-related genes persist in cultured cerebellar granule cells (Kaeffer and Pardini, 2005), cerebellar neurons were used to investigate the role of nuclear PSA-NCAM levels in the circadian rhythm. Therefore, neurons were cultured for different time periods and subsequently exposed to chicken NCAM antibody or mock treatment. Nuclear fractions were isolated and analyzed by immunoblot with PSA-specific antibody. Reduced levels of the PSA-NCAM fragment were detectable in nuclear fractions of unstimulated neurons cultured for 30 h and 36 h relative to levels in nuclear fractions of neurons cultured for 24 h, 42 h and 48 h (**Figure 29**). After 30 h and 42 h in culture, an enhanced level of the PSA-NCAM fragment was observed in nuclear fractions of neurons treated with NCAM antibody relative to the PSA-NCAM level nuclear fractions of unstimulated neurons. This result suggests that the nuclear level of the PSA-carrying NCAM fragment varies upon NCAM antibody treatment at different culture time periods

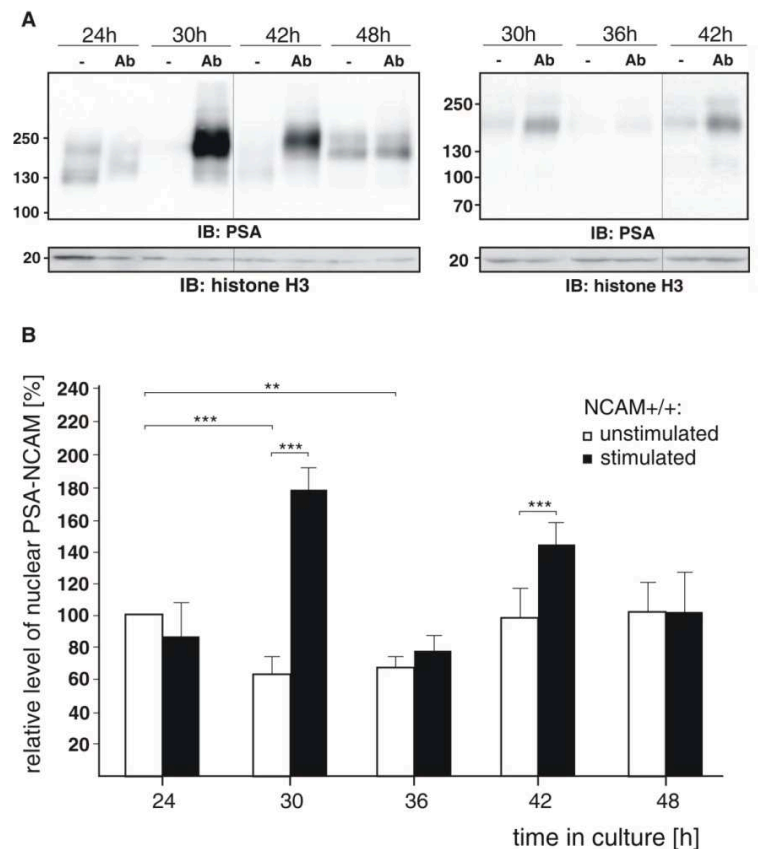


**Figure 29: Nuclear levels of the PSA-carrying NCAM fragment are altered with the inherent circadian rhythm of cultured cerebellar neurons.** (A, B) Wildtype cerebellar neurons were maintained in culture for different time periods (as indicated) and treated with chicken NCAM antibody (Ab) or mock-treated (-). Nuclear fractions were isolated and subjected to immunoblot analysis with PSA-specific antibody and an antibody against the nuclear marker histone H3. Representative immunoblots are shown out of five independent experiments. Lanes not adjacent to each other but from the same blot are indicated by vertical lines (A). Bands were quantified by densitometry (B) and mean values  $\pm$  s.d. from 5 independent experiments are shown for the PSA-NCAM fragment levels relative to the PSA-NCAM fragment level of unstimulated cells after 24 h in culture (set to 100%). Differences between groups are indicated (\*\*  $p < 0.01$ , \*\*\*  $p < 0.001$ ; two-way ANOVA with Dunnett's multiple comparison test) (Westphal *et al.*, 2016).

To elucidate whether the nuclear PSA-NCAM fragment has an influence on expression of clock-related genes qPCR was performed. The clock-related genes circadian locomotor output cycles kaput (CLOCK) and period-1 (Per-1) were chosen for analysis since they are known as important regulators in transcriptional-translational feedback loops controlling the circadian rhythm. Wildtype and NCAM-deficient cerebellar neurons were cultured for different time periods and then mock-treated or treated with NCAM antibody. mRNA was isolated and used for qPCR with CLOCK- and Per-1-specific primers. In unstimulated cerebellar neurons, CLOCK mRNA showed an oscillation with a phase of 12 h with highest CLOCK mRNA levels found in neurons cultured for 30 h (Figure 30 A). The CLOCK mRNA levels after application of NCAM antibody were decreased in neurons cultured for 30 h in contrast to neurons cultured for 24 h, 36 h, 42 h and 48 h. The Per-1 mRNA levels displayed an oscillation with a phase of 6 h in mock-treated cerebellar neurons and maximal Per-1 mRNA

expression levels were detectable in neurons cultured for 30 h and 42 h in comparison to neurons cultured for 24 h, 36 h and 48 h (**Figure 30 B**). Upon NCAM antibody treatment the Per-1 mRNA levels declined in neurons cultured for 30 h and 42 h compared to unstimulated neurons. In contrast, Per-1 mRNA levels were increased after NCAM antibody treatment in neurons cultured for 36 h relative to unstimulated neurons, while mRNA levels were not altered after NCAM antibody treatment in neurons cultured for 24 h and 48 h. No difference in expression level between unstimulated and NCAM antibody treated neurons cultured for 24 h and 48 h was observed for both genes.

To examine whether a correlation between the nuclear PSA-NCAM fragment level and the mRNA expression of CLOCK and Per-1 exists, a correlation analysis using a scatterplot was performed. A moderate negative correlation ( $r^2=0.7938$ ) between nuclear PSA-NCAM fragment levels and CLOCK mRNA levels but only a weak negative correlation ( $r^2=0.3105$ ) between nuclear PSA-NCAM fragment levels and Per-1 mRNA levels was observed in NCAM antibody-treated cerebellar neurons. These results showed that enhanced nuclear PSA-NCAM fragment levels lead to a reduced expression of the clock-related genes CLOCK and Per-1.

Furthermore, cerebellar neurons were pretreated with EndoN to digest PSA prior to mock treatment and treatment with NCAM antibody to analyze if the NCAM protein core alone affects the expression of the clock-related genes. Neurons pretreated with EndoN and treated with NCAM antibody displayed similar gene expression profiles as unstimulated neurons with and without EndoN pretreatment (**Figure 30**). Hence, the mRNA expression levels of CLOCK and Per-1 in cultured cerebellar neurons were altered by PSA and not influenced by the presence of the NCAM protein core.

In addition, very little oscillation of CLOCK and Per-1 mRNA levels could be detected in neurons from NCAM-deficient mice, indicating that clock-related gene expression and thus circadian rhythmicity is impaired in these animals. Furthermore, in NCAM-deficient neurons the application of NCAM antibody did not have any effect on Per-1 and CLOCK mRNA expression levels, showing that the presence of the PSA-NCAM fragment in the nucleus was responsible for alterations in CLOCK and Per-1 mRNA levels.

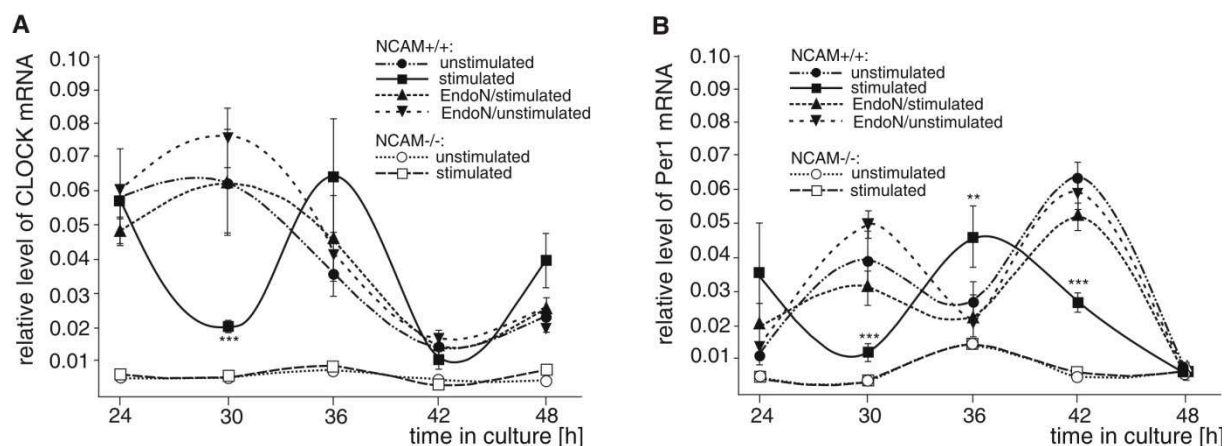


**Figure 30: Nuclear import of PSA affects the expression levels of CLOCK and Per-1 mRNA in cultured cerebellar neurons.** (A, B) Wildtype (NCAM<sup>+/+</sup>) and NCAM-deficient (NCAM<sup>-/-</sup>) cerebellar neurons were maintained in culture for different time periods (as indicated) and were mock-treated (unstimulated) or treated with chicken NCAM antibody (stimulated). In parallel, wildtype neurons were pretreated with EndoN and mock-treated (EndoN/unstimulated) or treated with NCAM antibody (EndoN/stimulated). mRNA was isolated and subjected to qPCR. Mean values  $\pm$  s.d. from 3 independent experiments are shown for the levels of CLOCK (A) and Per-1 (B) mRNA relative to reference genes (actin, tubulin and glyceraldehyde 3-phosphate dehydrogenase). Differences between groups are indicated (\*\*  $p < 0.01$ , \*\*\*  $p < 0.001$ ; two-way ANOVA with Bonferroni post-hoc test) (Westphal *et al.*, 2016).

### 5.11.2 Nuclear PSA-NCAM fragment levels in the cerebellum and suprachiasmatic nucleus are associated with reduced expression of clock-related genes

Since my previous results show that nuclear PSA-NCAM levels vary at different time periods and plays a role in the regulation of CLOCK and Per1 in cerebellar neurons I analyzed the importance of PSA in gene regulation *in vivo* in the cerebellum. Cerebella of 3 months-old female and male wildtype mice were collected at different Zeitgeber time (ZT) points of the 12 h light/12 h dark cycle and subjected to subcellular fractionation, immunoblotting of nuclear fractions with PSA-specific antibody and quantification of nuclear PSA-NCAM levels by densitometry. To ensure that the fractions were pure, cytoplasmic, membrane, nuclear and cytoskeletal fractions were also analyzed with marker proteins. An immunoreactive band of PSA-NCAM was detected in membrane and nuclear fractions but not in cytoplasmic and cytoskeletal fractions (**Figure 31 A**). Nuclear fractions were enriched in the nuclear marker proteins hnRNPA and histone H3 but not in actin, indicating the purity of the nuclear fractions. A high level of PSA-NCAM was found in nuclear fractions of cerebella collected at the middle and the end of the dark phase at ZT17 and ZT23, respectively, relative to lower PSA-NCAM levels detected in nuclear fractions of cerebella collected during the light phase until the beginning of the dark phase at ZT14 (**Figure 31 B** and **Figure 32 A**).

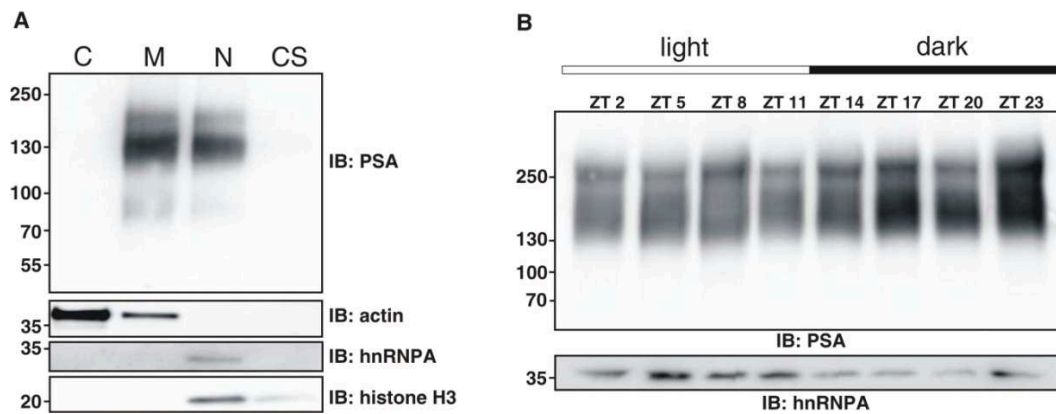


**Figure 31: PSA is present in nuclei isolated from cerebellar tissue.** (A, B) Cytoplasmic (C), membrane (M), nuclear (N) and cytoskeletal (CS) fractions from cerebella of 3 months old wildtype mice were isolated by subcellular fractionation and subjected to immunoblot analysis with PSA-specific antibody or with antibodies against actin and the nuclear marker proteins histone H3 and hnRNPA (A). Nuclear fractions were isolated from cerebella of 3 months-old wildtype mice at different ZT points of the 12 h light/12 h dark cycle (ZT0: lights on) by subcellular fractionation and subjected to immunoblot analysis with PSA-specific antibody or with an antibody against the nuclear marker hnRNPA to control for loading (B) (Westphal *et al.*, 2016).

The nuclear PSA-NCAM fragment level was also examined in nuclear fractions isolated from the SCN, cerebral cortex, striatum, hippocampus and midbrain of wildtype mice at different ZT points of the 12 h light/12 h dark. Interestingly, the oscillation of the PSA-NCAM level in nuclear fractions of the striatum (**Figure 33 B**) was similar to the oscillation found in the cerebellum (**Figure 32 A**). Nuclear fractions of the SCN showed a high PSA-NCAM fragment level at the beginning of the light phase at ZT2 and ZT5 and at the middle of the dark phase at ZT17 compared to a low PSA-NCAM level in nuclear fractions collected at the middle of the light phase at ZT8 and the end of the dark phase at ZT23 (**Figure 32 B**). Nuclear fractions of the cerebral cortex displayed a low PSA-NCAM level at the middle of the light phase until the end of the light phase at ZT5-ZT11 relative to a high level of nuclear PSA-NCAM at the beginning of the light phase at ZT2 and during the complete dark phase at ZT14-ZT23 (**Figure 33 A**). The nuclear PSA-NCAM fragment level was lower in nuclear fractions of the hippocampi at ZT5 and ZT11 at the middle and end of the light phase and at the beginning and middle of the dark phase at ZT14 and ZT20 compared to higher levels of PSA-NCAM found at the other ZT times (**Figure 33 C**). In the midbrain the level of nuclear PSA-NCAM was high in the middle of the light phase at ZT8 and middle of the dark phase at ZT20 with less difference between the ZT times, as compared to other brain regions (**Figure 33 D**). Thus, the nuclear PSA-NCAM fragment level varied in different brain regions depending on the 12 h light/12 h dark cycle.

Since I could observe that nuclear PSA-NCAM fragment levels and the expression of the clock-related genes CLOCK and Per-1 correlate in cerebellar neurons and since the nuclear

PSA-NCAM fragment levels vary in different brain regions during the circadian rhythm, I was interested to investigate whether the gene expression profile of CLOCK and Per-1 is also altered in different brain tissues during the light/dark cycle and if the expression levels of CLOCK and Per-1 correlate with the nuclear PSA-NCAM levels. Hence, the mRNA levels of CLOCK and Per-1 in the cerebellum and the SCN were analyzed at different time points of the light/dark cycle. RNA was isolated from cerebellum and SCN of adult wildtype and NCAM-deficient mice at different ZT times of the 12 h light/ 12 h dark cycle every 4 hours and subjected to qPCR. The CLOCK mRNA levels in the cerebellum were low at the beginning of the light phase, increased until the end of light phase and persisted until the end of the dark phase (**Figure 32 C**). A significantly enhanced expression level of Per-1 mRNA was observed at the end of light period and Per-1 mRNA levels remained low at the beginning of light phase and during the dark phase (**Figure 32 C**). Correlation analysis by scatter plots revealed a moderate negative correlation between the nuclear PSA-NCAM fragment levels and Per-1 mRNA expression levels ( $r^2=0.6057$ ), whereas no correlation between the nuclear PSA-NCAM level and CLOCK mRNA expression ( $r^2=0.0276$ ) was found, indicating a correlation between low nuclear PSA-NCAM fragment levels and high mRNA levels of Per-1 in the cerebellum (**Figure 32 A, C**). In the SCN, elevated levels of CLOCK mRNA in the early light phase and in the middle of the dark period were found (**Figure 32 D**). Thus, the high CLOCK mRNA levels correlated with the high nuclear PSA-NCAM levels seen at this time points of the circadian rhythm in the SCN (**Figure 32 B**). Per-1 mRNA levels in SCN showed only one peak at the end of the dark period, while the mRNA levels were low during the light period until the end of the dark phase (**Figure 32 D**). The correlation analysis indicated a moderate negative correlation between nuclear PSA-NCAM fragment levels and CLOCK mRNA levels in SCN tissue ( $r^2=0.4175$ ), whereas no correlation was seen for nuclear PSA-NCAM levels and Per-1 mRNA expression levels ( $r^2=0.1532$ ) (**Figure 32 B, D**). In NCAM-deficient mice, no significant oscillation of CLOCK mRNA was seen in the cerebellum and only a weak oscillation could be observed in SCN tissue. However, the mRNA expression levels of Per-1 in the cerebella of NCAM-deficient mice were higher compared to those of wildtype mice and showed in addition a different expression pattern. In the SCN of NCAM-deficient mice a prominent rhythmic expression pattern for Per-1 mRNA was observed (**Figure 32 E, F**). The combined results demonstrate a differential influence of nuclear PSA-NCAM on the expression profile of CLOCK and Per-1 during the light/dark cycle in different brain areas *in vivo*.



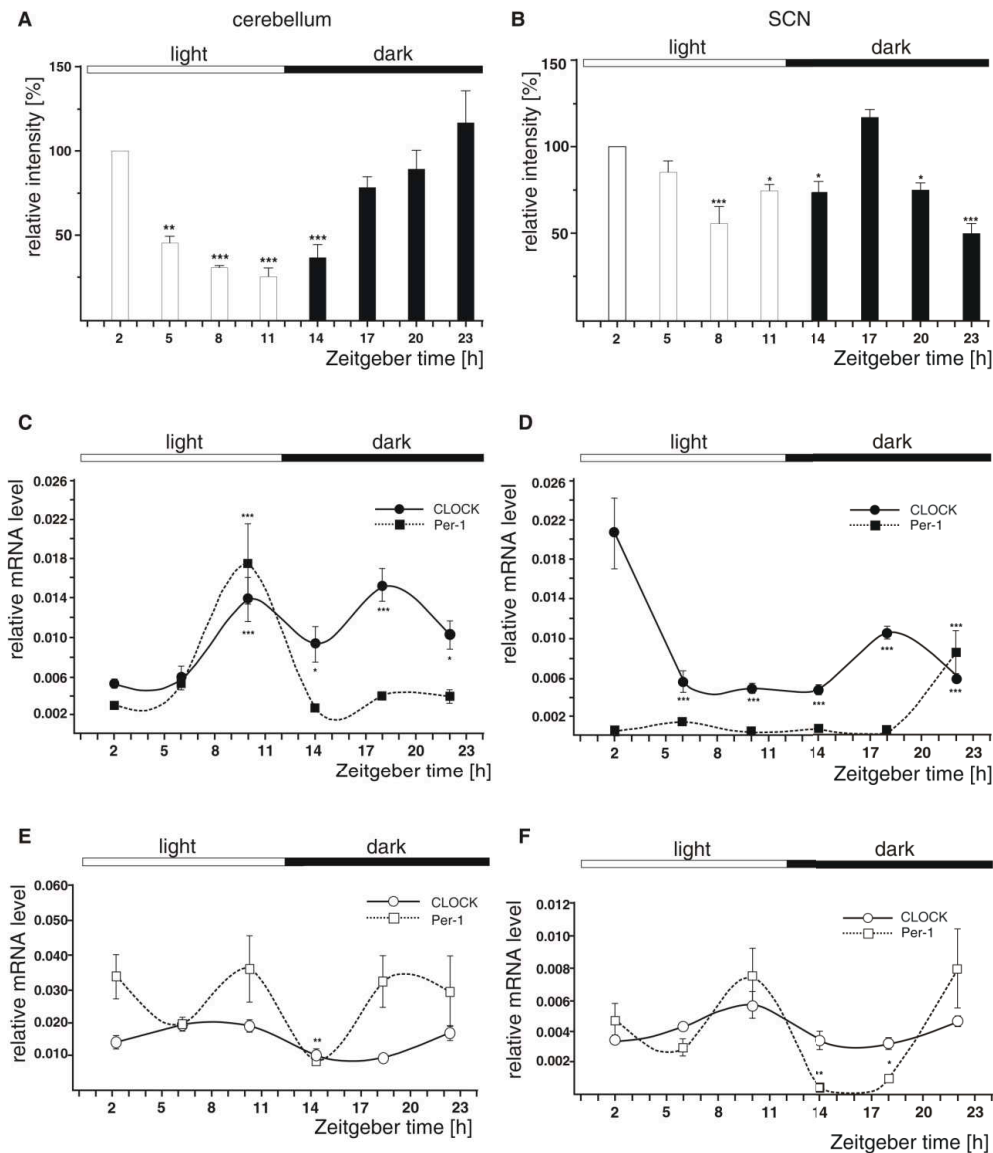


**Figure 32: Variations in nuclear PSA-NCAM levels in cerebellum and SCN affect the expression of CLOCK and Per-1 mRNAs.** (A-B) Nuclear fractions were isolated from cerebellum (A) and SCN (B) of 3 months-old wildtype mice at different ZT points of the 12 h light/12 h dark cycle (ZT0: lights on) and subjected to immunoblot analysis with PSA-specific antibody. Mean values  $\pm$  s.d. from 2 independent experiments with 3 males and 3 females per group (n=12) are shown for the nuclear PSA levels relative to the ZT2 group (set to 100%). Significant differences between groups relative to the ZT2 group are indicated (\* p<0.05, \*\* p<0.01, \*\*\* p<0.001; two-way ANOVA with Dunnett's multiple comparison test). (C-F) RNA was isolated from cerebellum (C, E) and SCN (D, F) of 3 months-old wildtype (NCAM<sup>+/+</sup>) (C, D) and NCAM-deficient (NCAM<sup>-/-</sup>) (E, F) mice at different ZT points of the 12 h light/12 h dark cycle (ZT0: lights on) and subjected to qPCR. Mean values  $\pm$  s.d. from 3 independent experiments with 2 males and 2 females per group (n=12) are shown for the CLOCK and Per-1 mRNA levels relative to the level of reference genes (actin, tubulin and glyceraldehyde 3-phosphate dehydrogenase). Differences in expression levels relative to the levels at ZT2 are indicated (\* p<0.05, \*\* p<0.01, \*\*\* p<0.001; two-way ANOVA with Dunnett's multiple comparison test) (Westphal *et al.*, 2016).

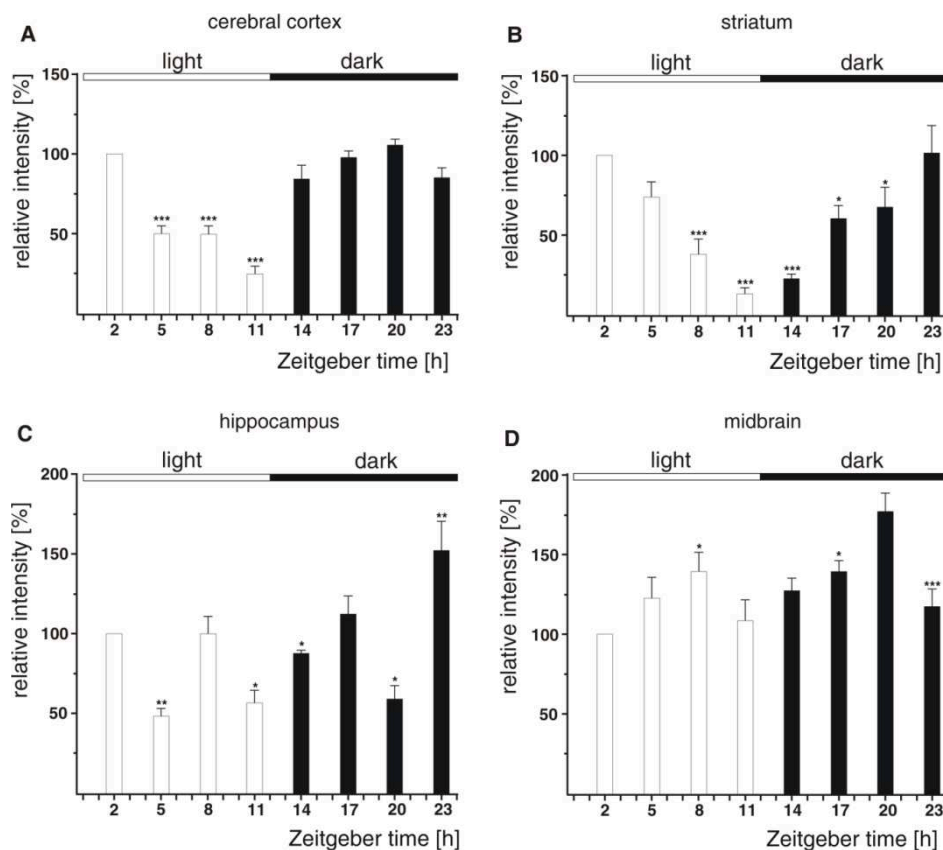


**Figure 33: Nuclear PSA-NCAM levels vary in different brain regions during the circadian rhythm.** (A-D) Nuclear fractions were isolated from the cerebral cortex (A), striatum (B), hippocampus (C) and midbrain (D) of 3 months-old wildtype mice at different ZT points of the 12 h light/12 h dark cycle (ZT0: lights on) and subjected to immunoblot analysis with PSA-specific antibody. Mean values  $\pm$  s.d. from 2 independent experiments with 3 males and 3 females per group ( $n=12$ ) are shown for the nuclear PSA levels relative to the ZT2 group (set to 100%). Significant differences between groups relative to the ZT2 group are indicated (\*  $p<0.05$ , \*\*  $p<0.01$ , \*\*\*  $p<0.001$ ; two-way ANOVA with Dunnett's multiple comparison test) (Westphal *et al.*, 2016).

### 5.12 PSA-carrying NCAM co-localizes with histone H1 *in vivo* during the light/dark cycle

To further demonstrate that the presence of the nuclear PSA-NCAM fragment varies during the circadian rhythm *in vivo*, cerebellum tissue sections of adult wildtype and NCAM-deficient mice were collected at early ZT2 and late ZT10 of the 12 h light/ 12h dark cycle. Since high and low levels of nuclear PSA-NCAM were found at ZT2 and ZT10, respectively, in the cerebella tissue, it was examined whether the interaction of PSA-NCAM with its nuclear binding partner histone H1 is affected during the light/dark cycle. Cerebellar sections were analyzed by proximity ligation assay using PSA-specific and histone H1-specific antibody.

At the early light phase at ZT2 many fluorescent spots were detectable in cerebellar nuclei of wildtype mice revealing a prominent interaction of PSA with histone H1 at this point of time (**Figure 34**). Less fluorescence spots indicating the interaction of PSA with histone H1 were observed at the end of the light phase at ZT10. This result verifies that the nuclear PSA levels are altered during the circadian rhythm. No fluorescence spots indicating an interaction of PSA with histone H1 were detected in cerebella of NCAM-deficient mice.

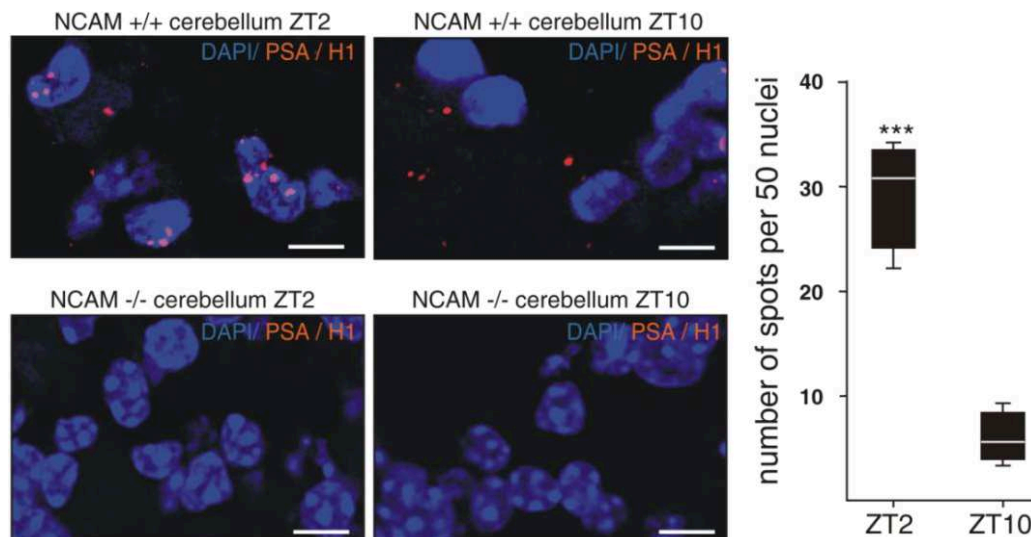


**Figure 34: Level of nuclear co-localization of PSA and histone H1 in cerebellar tissue depends on the circadian rhythm.** Cerebella were isolated from 3 months-old wildtype (NCAM+/+) and NCAM-deficient (NCAM-/-) mice at the early (ZT2) and late (ZT10) light phase of the 12 h light/12h dark cycle (ZT0: lights on) and subjected to proximity ligation assay with PSA-specific mouse antibody and histone H1-specific rabbit antibody. Nuclei were stained with DAPI (blue). Spots of intense fluorescent signals (red) indicate close interactions between PSA and histone H1. Representative confocal images of neuronal nuclei in the cerebellum from mice at ZT2 and ZT10 are shown. Scale bars: 10  $\mu$ m. A boxplot is shown for the quantification of nuclear PSA/histone H1-positive spots in NCAM (+/+) cerebellar tissue. PSA/histone H1-positive red spots were counted in 50 nuclei in three images taken from two animals per time point. (\*\*\*)  $p < 0.001$ ; Student's *t*-test) (Westphal *et al.*, 2016).

The alteration of nuclear PSA levels during the circadian rhythm could further be confirmed by immunogold electron microscopy with PSA antibody. High PSA-immunoreactivity at the early light phase at ZT2 and low PSA-immunoreactivity at the late light phase at ZT10 was observed in cerebellar sections from wildtype mice (**Figure 35**).

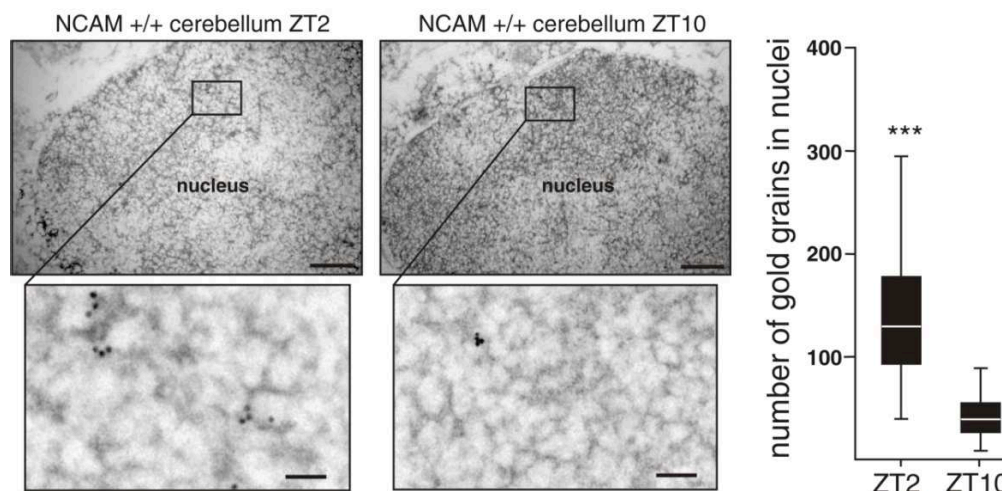


**Figure 35: Nuclear localization of PSA in cerebellar tissue.** Cerebella were isolated from 3 months old wildtype mice at the early (ZT2) and late (ZT10) light phase of the 12 h light/12h dark cycle (ZT0: lights on) and subjected to immunoelectron microscopy with PSA-specific antibody and gold-conjugated secondary antibody. Representative immunoelectron microscopic images of neuronal nuclei in cerebellum from mice at ZT2 and ZT10 are shown (upper images scale bar: 500 nm). Boxes indicate areas shown at higher magnification (lower images). A boxplot is shown for the number of gold particles in neuronal nuclei (\*\* $p < 0.001$ ; Student's  $t$ -test). Immunoelectron microscopic images were taken by David Lutz, Institute for Structural Neurobiology, ZMNH (Westphal *et al.*, 2016).

To determine whether the PSA-lacking NCAM fragment also shows an altered interaction with histone H1 during the circadian rhythm proximity ligation assay was performed at time points ZT2 and ZT10 with specific antibodies against NCAM and histone H1. No difference in fluorescence signal was seen in cerebellum at ZT2 compared to ZT10 (**Figure 36**). Quantification of the NCAM-positive red spots in nuclei confirmed that the number of NCAM-positive spots was similar in the early and late light phase, indicating that the nuclear NCAM level is not altered during the circadian rhythm.

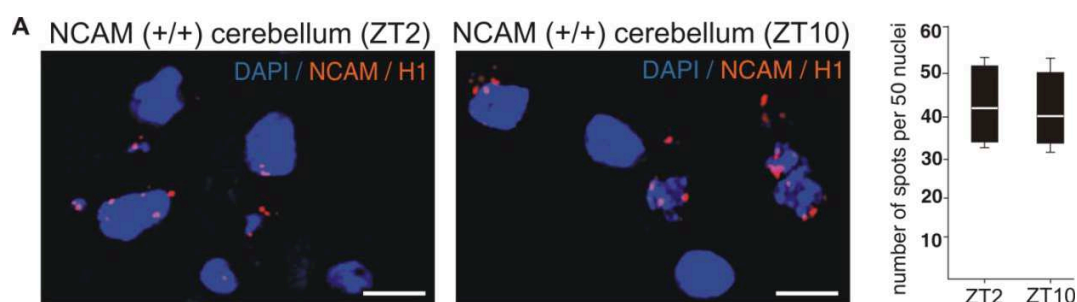


**Figure 36: Nuclear co-localization of NCAM and histone H1 in cerebellar tissue is not altered during time.** Cerebella were isolated from 3 months old wildtype mice at the early (ZT2) and late (ZT10) light phase of the 12 h light/12 h dark cycle (ZT0: lights on) and subjected to proximity ligation assay with NCAM-specific goat antibody and histone H1-specific rabbit antibody. Nuclei were stained with DAPI (blue). Spots of intense fluorescent signals (red) indicate close protein interactions between NCAM and histone H1. Representative confocal images of neuronal nuclei in the cerebellum from mice at ZT2 and ZT10 are shown. Scale bars: 10  $\mu$ m. A boxplot is shown for the quantification of nuclear NCAM/histone H1-positive spots. NCAM/histone H1-positive red spots were counted in 50 nuclei in three images taken from two animals per time point. (\*\* $p < 0.001$ ; Student's  $t$ -test) (Westphal *et al.*, 2016).



To substantiate the nuclear localization of NCAM and PSA in the cerebellum of wildtype and NCAM-deficient mice at ZT2 and ZT10, immunoelectron microscopy was performed with PSA-specific antibody and a secondary antibody coupled to gold particles. The nuclei of wildtype mice showed high numbers of gold clusters indicating nuclear NCAM (**Figure 37 A**) and PSA (**Figure 37 B**) in comparison to no visible gold clusters in nuclei of NCAM-deficient mice. This result showed that nuclear PSA and NCAM are present in the cerebellum of wildtype mice and are not present in cerebellum of NCAM-deficient mice at the early light phase ZT2.

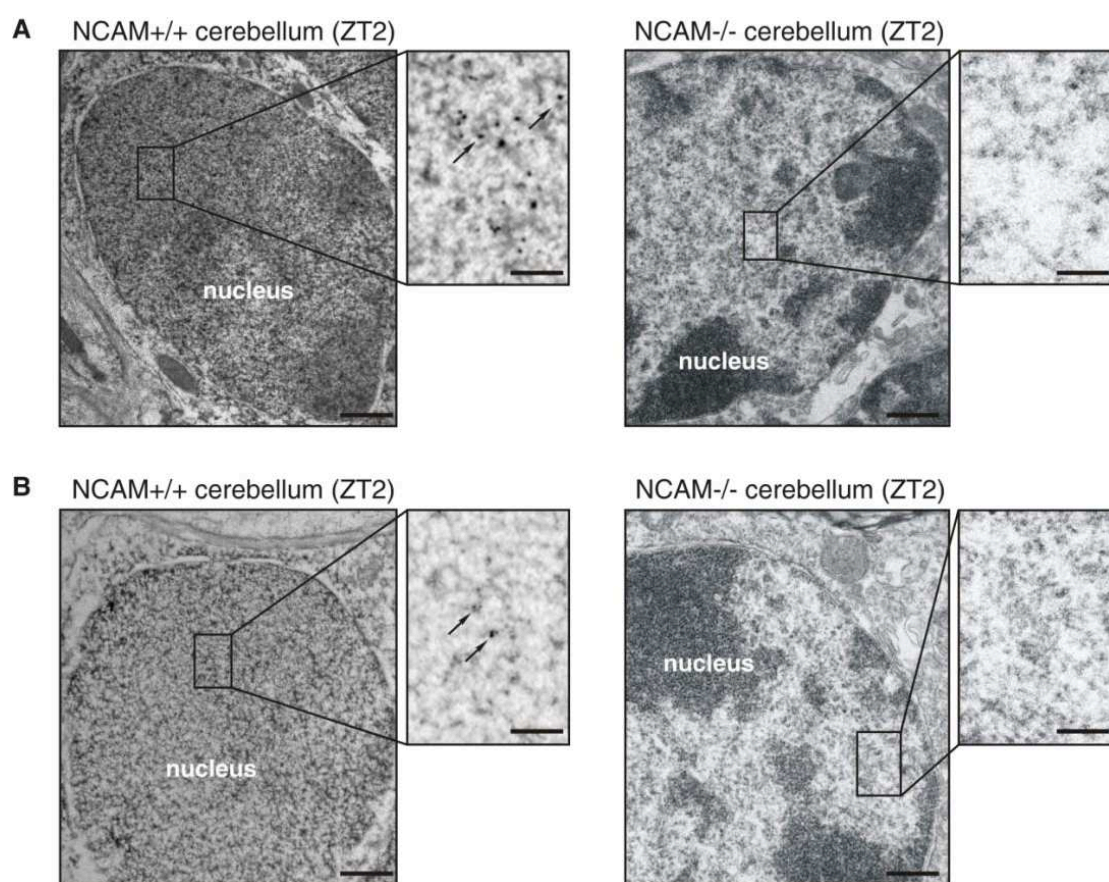


**Figure 37: Nuclear localization of NCAM and PSA in cerebellar tissue.** (A, B) Cerebella were isolated from 3 months old wildtype (NCAM<sup>+/+</sup>) mice and NCAM-deficient (NCAM<sup>-/-</sup>) mice at the early (ZT2) light phase of the 12 h light/12 h dark cycle (ZT0: lights on) and subjected to immunoelectron microscopy with NCAM-specific (A) or PSA-specific (B) antibody. Specific antibodies were coupled to ten (A) or six (B) nm gold particles. Representative immunoelectron microscopic images of neuronal nuclei are shown. Boxes indicate areas shown at higher magnification with (arrows) nuclear NCAM (A) and PSA (B) spots. Scale bars: 500 nm. Immunoelectron microscopic images were taken by David Lutz, Institute for Structural Neurobiology, ZMNH (Westphal *et al.*, 2016).

### **5.13 The effect of the PSA-lacking NCAM and PSA-carrying NCAM fragments on the gene expression of distinct genes**

Since the previous experiments revealed an important role of the nuclear PSA-carrying NCAM fragment in the regulation of gene expression of clock-related genes during the circadian rhythm, expression profiling experiments were performed to determine the influence of nuclear PSA-carrying NCAM and nuclear PSA-lacking NCAM on the overall gene expression.

#### **5.13.1 Nuclear NCAM regulates the expression of Lrp2 and $\alpha$ -synuclein whereas nuclear PSA-NCAM regulates the expression of Nr2f6**

The investigation of the effect of PSA-lacking NCAM and PSA-carrying NCAM fragments on gene expression was performed using microarray analysis of wildtype cerebellar neurons treated under different conditions. To distinguish between PSA-specific and NCAM-specific effects on gene expression, cerebellar neurons were mock-treated, treated with NCAM antibody in the presence or absence of EndoN and subjected to RNA isolation followed by mRNA analysis. For the evaluation of the mRNA expression, the following criteria were applied: A PSA-dependent alteration of gene expression in neurons is given when the mRNA levels differ in neurons treated with NCAM antibody compared to mock-treated and NCAM antibody treated and EndoN pretreated neurons. Hence, similar expression level should be observed in mock-treated and NCAM antibody treated and EndoN pretreated cells. A NCAM-mediated change in mRNA expression profile is indicated by a difference in mRNA levels in NCAM antibody treated neurons and NCAM antibody treated and EndoN-pretreated neurons in comparison to mock-treated neurons. In addition, no significant differences in mRNA gene expression between NCAM antibody and NCAM antibody and EndoN pretreated neurons should be detectable.

Several genes which were up- or down-regulated in a PSA-dependent manner were found in the microarray approach and are listed in **Table 6** (upregulated) and **Table 7** (downregulated). The nuclear receptor subfamily 2 group F member 6 (Nr2f6), also known as Ear2, was upregulated by the factor of  $1.320 \pm 0.023$  in neurons treated with NCAM antibody versus mock-treated cells. Further, no increase in mRNA levels of Nr2f6 was observed in neurons treated with NCAM antibody after EndoN pretreatment versus mock-treated neurons. A number of genes which were either up- or downregulated by the PSA-lacking NCAM fragment were also found and are listed in **Table 8** (down-regulated) and **Table 9** (up-

regulated). The low density lipoprotein receptor-related protein 2 (Lrp2) was up-regulated by the factor of  $1.415 \pm 0.021$  and  $\alpha$ -synuclein was upregulated by the factor of  $1.251 \pm 0.010$  after NCAM antibody treatment. In addition, a difference in gene expression of Lrp2 and  $\alpha$ -synuclein by a factor of  $1.267 \pm 0.011$  and of  $1.249 \pm 0.021$ , respectively, was seen in neurons treated with NCAM antibody compared to neurons treated with NCAM antibody and pretreated with EndoN

**Table 6: NCAM-mediated PSA-dependent upregulation of gene expression.** Shown are relative changes of mRNA levels in untreated cerebellar neurons (mock-treated) or in neurons treated with chicken NCAM antibody after pretreatment without (Ab treated) or with EndoN (EndoN/Ab).

Gene ID	Ab treated vs mock-treated	Ab treated vs EndoN/Ab	Gene name
Abi1	1.155±0.013	1.215±0.012	Abelson interactor 1
Actl6a	1.286±0.009	1.235±0.009	actin-like 6A
Arfgap1	1.270±0.012	1.229±0.009	ADP-ribosylation factor GTPase activating protein 1
Asb6	1.216±0.005	1.228±0.004	ankyrin repeat and SOCS box-containing 6
Asxl1	1.236±0.021	1.247±0.019	additional sex combs like 1
Atg4c	1.268±0.020	1.249±0.020	autophagy-related 4C
Cnm2	1.234±0.018	1.262±0.017	cyclin M2
CNOT10	1.349±0.008	1.259±0.009	CCR4-NOT transcription complex, subunit 10
CPPED1	1.373±0.009	1.212±0.009	calcineurin-like phosphoesterase domain containing 1
Heatr5b	1.267±0.020	1.238±0.022	HEAT repeat containing 5B
Ints2	1.282±0.013	1.262±0.012	integrator complex subunit 2
Lrrtm3	1.262±0.012	1.375±0.010	leucine rich repeat transmembrane neuronal 3
Mtfr1	1.221±0.016	1.252±0.017	mitochondrial fission regulator 1
Naalad2	1.388±0.016	1.309±0.018	N-acetylated alpha-linked acidic dipeptidase 2
Napa	1.254±0.007	1.266±0.007	N-ethylmaleimide sensitive fusion protein attachment protein $\alpha$
Npat	1.276±0.018	1.227±0.021	nuclear protein in the AT region
Nr2f6	1.320±0.023	1.349±0.025	nuclear receptor subfamily 2, group F, member 6
Pcdh10	1.422±0.012	1.408±0.012	OL-protocadherin isoform
Pggt1b	1.210±0.021	1.226±0.020	protein geranylgeranyltransferase type I, beta subunit

**Continuation; Table 6: NCAM-mediated PSA-dependent upregulation of gene expression.**

Pggt1b	1.210±0.021	1.226±0.020	protein geranylgeranyltransferase type I, beta subunit
Pias2	1.296±0.027	1.274±0.028	protein inhibitor of activated STAT 2
Pigt	1.256±0.020	1.218±0.023	phosphatidylinositol glycan anchor biosynthesis, class T
Pitrm1	1.221±0.022	1.267±0.019	pitrilysin metalloproteinase 1
Scn3b	1.281±0.017	1.244±0.020	sodium channel, voltage-gated, type III, $\beta$ , transcript variant 1
Sfi1	1.314±0.011	1.240±0.011	Sfi1 homolog, spindle assembly associated
Slc25a16	1.236±0.021	1.244±0.020	solute carrier family 25, member 16
SLC25A39	1.314±0.017	1.270±0.018	solute carrier family 25, member 39
Tm2d2	1.205±0.006	1.209±0.020	TM2 domain containing 2
TSPY13	1.247±0.070	1.273±0.006	TSPY-like 3
Tsr2	1.234±0.012	1.255±0.012	pre-rRNA-processing protein TSR2 homolog
Ttc7b	1.240±0.018	1.256±0.021	tetratricopeptide repeat domain 7B, transcript variant 1
UCK2	1.316±0.015	1.410±0.015	uridine-cytidine kinase 2
Zbtb45	1.303±0.050	1.306±0.006	zinc finger and BTB domain containing 45
Zdhhc20	1.279±0.011	1.278±0.012	zinc finger, DHHC domain containing 20
Zfp800	1.381±0.022	1.452±0.018	zinc finger protein 800
Zfyve1	1.366±0.002	1.200±0.002	zinc Finger, FYVE domain containing 1
Zfyve26	1.247±0.024	1.287±0.024	zinc finger, FYVE domain containing 26
Zzz3	1.241±0.010	1.219±0.010	zinc finger, ZZ domain containing 3



**Table 7: NCAM-mediated PSA-dependent downregulation of gene expression.** Shown are relative changes of mRNA levels in untreated cerebellar neurons (mock-treated) or in neurons treated with chicken NCAM antibody after pretreatment without (Ab treated) or with EndoN (EndoN/Ab).

Gene ID	Ab treated vs mock-treated	Ab treated vs EndoN/Ab	Gene name
Abcc5	1.308±0.010	1.202±0.010	ATP-binding cassette protein
Bcr	1.324±0.026	1.220±0.023	breakpoint cluster region
Cds2	1.371±0.046	1.315±0.040	CDP-diacylglycerol synthase 2
Chst3	1.276±0.012	1.241±0.011	chondroitin 6/keratan sulfotransferase 3
Ddef2	1.225±0.005	1.264±0.005	development and differentiation enhancing factor 2
Diap1	1.226±0.027	1.201±0.026	diaphanous homolog 1
Dnase1	1.217±0.024	1.248±0.023	deoxyribonuclease I
EBPL	1.250±0.017	1.237±0.020	emopamil binding protein-like
Eif4ebp2	1.319±0.039	1.301±0.027	eukaryotic translation initiation factor 4E binding protein 2
Elavl3	1.291±0.015	1.230±0.013	RNA-binding protein mHuC-S
Gats	1.210±0.011	1.247±0.011	opposite strand transcription unit to Stag3
Gnas	1.386±0.018	1.306±0.018	guanine nucleotide binding protein, $\alpha$ stimulating complex locus
Gpr39	1.310±0.024	1.249±0.026	G protein-coupled receptor 39
Hnrnp1	1.449±0.023	1.370±0.025	heterogeneous nuclear ribonucleoprotein L
Iqgap1	1.204±0.022	1.227±0.021	IQ motif containing GTPase activating protein 1
Kctd10	1.377±0.026	1.226±0.020	potassium channel tetramerisation domain containing 10
Kirrel3	1.255±0.014	1.482±0.013	Kin of IRRE like 3
L1cam	1.254±0.019	1.270±0.018	L1 cell adhesion molecule
Mapt	1.500±0.053	1.314±0.040	microtubule binding protein tau
NUDT7	1.270±0.022	1.269±0.018	nudix (nucleoside diphosphate linked moiety) type motif 7
Pik3r1	1.311±0.015	1.202±0.012	phosphatidylinositol 3-kinase, regulatory subunit, polypeptide 1
Ppara	1.233±0.029	1.215±0.032	peroxisome proliferator activated receptor alpha

**Continuation; Table 7: NCAM-mediated PSA-dependent downregulation of gene expression.**

Ppt1	1.311±0.026	1.252±0.022	palmitoyl-protein thioesterase
Prpf6	1.265±0.034	1.350±0.037	PRP6 pre-mRNA splicing factor 6 homolog
Rbm9	1.418±0.036	1.332±0.037	RNA binding motif protein 9
RHAMM	1.233±0.029	1.284±0.028	hyaluronan mediated motility receptor (RHAMM)
Rsrc2	1.250±0.023	1.367±0.021	arginine/serine-rich coiled-coil 2
Slc39a10	1.270±0.008	1.212±0.007	solute carrier family 39, member 10
Slc6a6	1.315±0.030	1.257±0.042	sodium-dependent taurine transporter
Smad5	1.226±0.029	1.210±0.028	MAD homolog 5
Usp7	1.259±0.011	1.229±0.024	ubiquitin specific peptidase 7
xpo7	1.221±0.026	1.258±0.026	exportin 7
Zbtb46	1.289±0.023	1.215±0.023	zinc finger and BTB domain containing 46
Zfp597	1.330±0.005	1.204±0.006	zinc finger protein 597

**Table 8: NCAM-mediated PSA-independent downregulation of gene expression.** Shown are relative changes of mRNA levels in untreated cerebellar neurons (mock-treated) or in neurons treated with chicken NCAM antibody after pretreatment without (Ab treated) or with EndoN (EndoN/Ab).

<b>Gene ID</b>	<b>Ab treated vs mock-treated</b>	<b>EndoN/Ab vs mock-treated</b>	<b>Gene name</b>
Arsk	1.282±0.023	1.372±0.036	arylsulfatase K
B4galt5	1.384±0.013	1.319±0.020	UDP-Gal:βGlcNAc β1,4-galactosyltransferase 5
Bach1	1.333±0.020	1.352±0.033	BTB and CNC homology 1
Bcl11b	1.365±0.038	1.350±0.052	B-cell leukemia/lymphoma 11B
Crip1	1.476±0.064	1.470±0.056	cysteine-rich protein 1
Dleu7	1.380±0.039	1.542±0.015	deleted in lymphocytic leukemia 7
Fam55c	1.482±0.026	1.373±0.012	family with sequence similarity 55, member C
Golt1b	1.325±0.013	1.304±0.021	Golgi transport 1 homolog B
Ifi30	1.473±0.066	1.306±0.002	interferon gamma inducible protein 30
Narf	1.401±0.014	1.421±0.021	nuclear prelamin A recognition factor
Nup133	1.285±0.037	1.311±0.032	nucleoporin 133
Phf17	1.422±0.024	1.244±0.029	PHD finger protein 17

**Continuation; Table 8: NCAM-mediated PSA-independent downregulation of gene expression.**

Rnf114	1.398±0.014	1.280±0.023	zinc finger protein 313
Sel11	1.392±0.035	1.324±0.027	Sel-1 suppressor of lin-12-like
Sucla2	1.336±0.032	1.263±0.015	succinate coenzyme A ligase, ADP-forming, $\beta$ subunit

**Table 9: NCAM-mediated PSA-independent upregulation of gene expression.** Shown are relative changes of mRNA levels in untreated cerebellar neurons (mock-treated) or in neurons treated with chicken NCAM antibody after pretreatment without (Ab treated) or with EndoN (EndoN/Ab).

Gene ID	Ab treated vs mock-treated	EndoN/Ab vs mock-treated	Gene name
Ccdc88c	1.154±0.005	1.309±0.027	coiled-coil domain containing 88C
Csmd1	1.174±0.002	1.289±0.015	CUB and Sushi multiple domains 1
Dlgap1	1.245±0.011	1.199±0.007	discs, large homolog-associated protein 1
Lrp2	1.415±0.021	1.267±0.011	low density lipoprotein receptor-related protein 2
Snca	1.251±0.010	1.249±0.021	synuclein, alpha
Trappc9	1.282±0.013	1.225±0.007	trafficking protein particle complex 9
Zfp40	1.329±0.014	1.157±0.004	zinc finger protein 40

An independent expression profiling experiment was performed in the group of Melitta Schachner. Cerebellar neurons were treated with rabbit NCAM and rat L1 antibodies in absence and presence of the serine protease inhibitor aprotinin which inhibits the generation of the PSA-lacking NCAM fragment and of the 70 kDa L1 fragment. From these samples the mRNA was isolated and the gene expression levels were determined. Among the genes differentially regulated by NCAM antibody stimulation also Nr2f6, Lrp2 and  $\alpha$ -synuclein were found. The mRNA levels of Nr2f6, Lrp2 and  $\alpha$ -synuclein were increased in cerebellar neurons upon treatment with NCAM antibody relative to the treatments with L1, CHL1 and non-immune control antibodies (**Table 10**). The data for Nr2f6, Lrp2 and  $\alpha$ -synuclein from the previous (marked in blue) and the current (marked in red) microarray study are summarized in **Table 10**. It is noteworthy to mention that Lrp2 and  $\alpha$ -synuclein levels were

not altered by NCAM antibody treatment in the presence of the serine protease inhibitor aprotinin, indicating a PSA-lacking NCAM fragment-dependent gene regulation.

**Table 10: Differential gene expression by PSA-lacking and -carrying NCAM fragments. Shown are the relative changes of Nr2f6, Lrp2 and  $\alpha$ -synuclein mRNA levels in cerebellar neurons after different treatments.** Aprotinin, (apro); rabbit NCAM antibody (rbNCAM-Ab); rabbit L1 antibody (rbL1-Ab); rat L1 antibody (rL1-Ab); rabbit CHL1 antibody (rbCHL1-Ab); non-immune rabbit control antibody (rbIg); non-immune rat control antibody (rIg); chicken NCAM antibody (chNCAM-Ab); chicken NCAM antibody after EndoN pretreatment (EndoN/chNCAM-Ab). Data obtained from the current microarray are marked in red and data derived from the previous microarray are marked in blue.

Treatment	Nr2f6	Lrp2	$\alpha$ -synuclein
chNCAM-Ab vs untreated	1.320±0.023	1.415±0.021	1.251±0.010
chNCAM-Ab vs EndoN/chNCAM-Ab	1.349±0.025	–	–
EndoN/chNCAM-Ab vs untreated	–	1.267±0.011	1.249±0.021
rbNCAM-Ab vs rbCHL1-Ab	1.425±0.183	1.965±0.247	1.275±0.025
rbNCAM-Ab vs rbL1-Ab	1.595±0.098	1.524±0.215	1.505±0.132
rbNCAM-Ab vs rIg	2.205±0.256	1.313±0.379	1.284±0.022
rbNCAM-Ab vs rL1-Ab	1.915±0.154	1.639±0.060	1.228±0.098
rbNCAM-Ab vs rL1-Ab+apro	2.112±0.366	1.496±0.179	1.248±0.071
rbNCAM-Ab vs rbNCAM-Ab+apro	0.908±0.079	1.800±0.039	1.246±0.070

For the validation of the PSA-specific enhancement of Nr2f6 gene expression as well as the NCAM-specific enhancement of Lrp2 and  $\alpha$ -synuclein gene expression, qPCR with specific primer pairs was performed. Cerebellar neurons of wildtype mice were cultured for 24 h (cells exhibiting basal nuclear PSA-NCAM fragment levels) and 30 h (cells expressing high nuclear PSA-NCAM fragment levels) and were treated with NCAM antibody and pretreated without and with EndoN followed by RNA isolation. The RNA was subjected to qPCR and the mRNA levels of Nr2f6, Lrp2 and  $\alpha$ -synuclein were measured relative to reference genes. Neurons cultured for 30 h and then treated with NCAM antibody after pretreatment without or with EndoN showed a significant increase in relative mRNA levels for both  $\alpha$ -synuclein and Lrp2 in contrast to mRNA levels of mock-treated neurons (**Figure 38 A, B**). Moreover, no difference in the mRNA levels of Lrp2 and  $\alpha$ -synuclein were observed between neurons cultured for 24 h that were mock-treated and NCAM antibody treated without and with EndoN pretreatment. This result indicated that the nuclear NCAM fragment specifically enhanced mRNA levels of Lrp2 and  $\alpha$ -synuclein in neurons cultured for

30 h. Also, no change in mRNA levels of Nr2f6 was determined in cerebellar neurons cultured for 24 h after mock-treatment and NCAM antibody treatment in the presence or absence of EndoN (**Figure 38 C**). However, a significant alteration in mRNA levels of Nr2f6 was detected in neurons cultured for 30 h followed by NCAM antibody treatment compared to mock-treated and NCAM antibody treated and EndoN pretreated neurons. These data confirmed the results from the microarray analysis. Thus the expression of Nr2f6 depends on the nuclear expression of PSA-NCAM, whereas Lrp2 and Snca gene expression did not depend on the nuclear PSA-carrying NCAM fragment but depend on the PSA-lacking NCAM fragment.

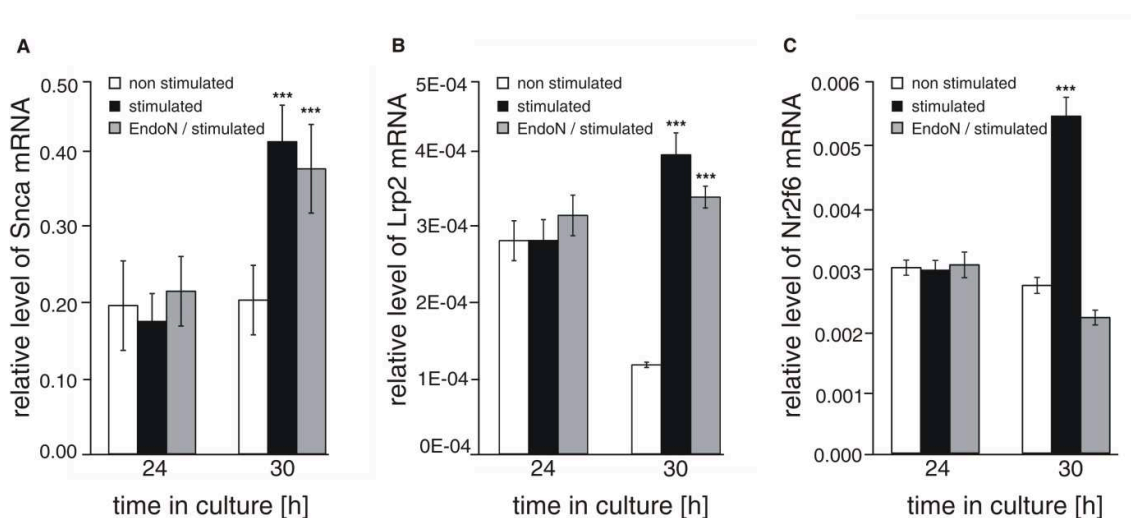


**Figure 38: Nuclear PSA and NCAM affect the expression levels of  $\alpha$ -synuclein, LRP2 and Nr2f6 mRNA in cultured cerebellar neurons.** (A-C) Wildtype cerebellar neurons were maintained in culture for 24 h and 30 h and mock treated (unstimulated) or treated with chicken NCAM antibody (stimulated) and pretreated with EndoN subsequent to treatment with NCAM antibody. RNA was isolated and subjected to qPCR. Mean values  $\pm$  s.d. from 3 independent experiments are shown for the levels of  $\alpha$ -synuclein (Snca) (A), Lrp2 (B) and Nr2f6 (C) mRNA relative to reference genes (actin, tubulin and glyceraldehyde 3-phosphate dehydrogenase). Differences between groups are indicated (\*\*\*)  $p < 0.001$ ; two-way ANOVA with Bonferroni post-hoc test).

Furthermore, cerebellar neurons of wildtype mice were treated with NCAM antibody in the presence and absence of the serine protease inhibitor aprotinin, to block the generation of the PSA-lacking NCAM-fragment, and MMP-2 inhibitor, which inhibits the generation of the PSA-carrying NCAM-fragment. As a control, neurons of NCAM-deficient mice were treated without and with NCAM antibody. The mRNA levels of Lrp2 and  $\alpha$ -synuclein were significantly upregulated in neurons treated with NCAM antibody and in neurons treated with NCAM antibody in the presence of MMP-2 inhibitor relative to mock-treated and NCAM antibody treated neurons in the presence of aprotinin (**Figure 39 A, B**). The mRNA levels of Lrp2 and  $\alpha$ -synuclein in neurons of NCAM-deficient mice were not affected by the NCAM antibody treatment compared to mock-treated neurons. Enhanced mRNA levels of Nr2f6 were

observed in NCAM antibody treated neurons in the presence of aprotinin but not in presence of MMP-2 inhibitor, relative to mock-treated neurons (**Figure 39 C**). Also no differences in mRNA levels were found in NCAM-deficient neurons. These results affirmed that the gene regulation of *Nr2f6* depends on nuclear PSA-carrying NCAM, while the mRNA expression of *Lrp2* and  $\alpha$ -synuclein is affected by nuclear PSA-lacking NCAM.

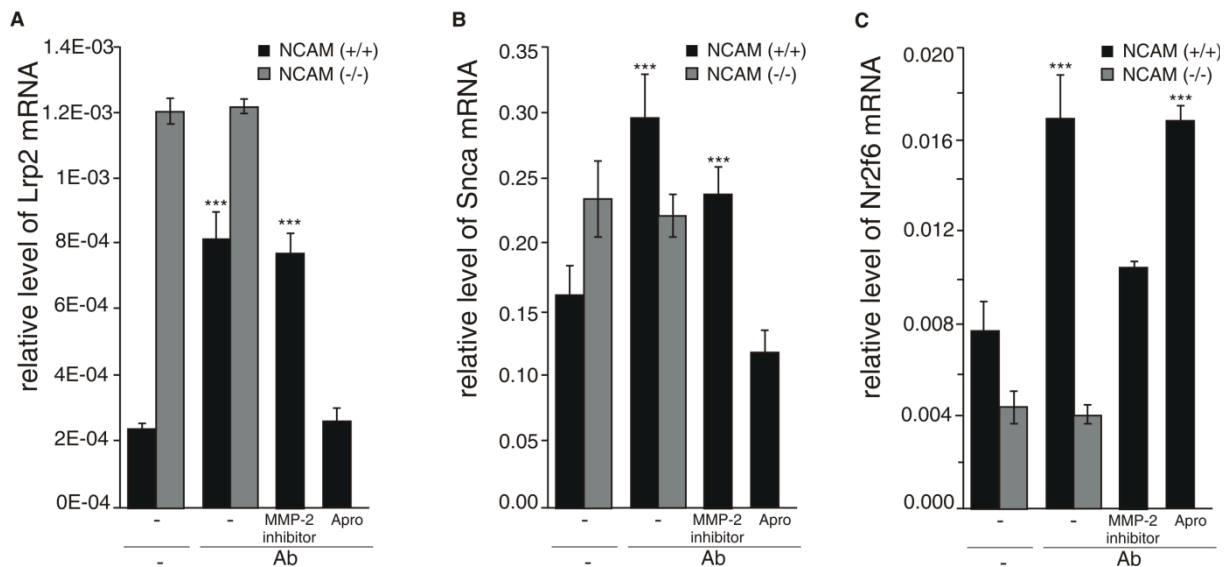


**Figure 39: Nuclear PSA and NCAM affect the expression levels of *Lrp2*,  $\alpha$ -synuclein and *Nr2f6* mRNA in cultured cerebellar neurons.** (A-C) Wildtype (NCAM<sup>+/+</sup>) and NCAM-deficient (<sup>-/-</sup>) cerebellar neurons were maintained in culture for 30 h and were mock-treated (unstimulated) or treated with chicken NCAM antibody (stimulated). Wildtype cerebellar neurons were also pretreated with MMP-2 inhibitor and serine protease inhibitor (Apro) and subsequently treated with chicken NCAM antibody (Ab). RNA was isolated and subjected to qPCR. Mean values  $\pm$  s.d. from 3 independent experiments are shown for the level of *Lrp2* (A),  $\alpha$ -synuclein (*Snca*) (B) and *Nr2f6* (C) mRNA relative to reference genes (actin, tubulin and glyceraldehyde 3-phosphate dehydrogenase). Differences between groups are indicated (\*\*\*)  $p < 0.001$ ; two-way ANOVA with Bonferroni post-hoc test).

### 5.13. Nuclear PSA-NCAM regulates the expression of *Nr2f6* differentially during the circadian rhythm *in vitro* and *in vivo*

Furthermore, it is important to note that *Nr2f6* (*Ear2*) plays a role in the functionality of the forebrain clock and the regulation of daytime feeding behavior (Warnecke *et al.*, 2005). Since my observations show that the expression profile of *Nr2f6* is regulated by PSA-NCAM and that nuclear PSA-NCAM regulates the expression of genes dependent on the circadian rhythm, it is deemed possible that the expression level of *Nr2f6* is regulated differentially by nuclear PSA-NCAM during the circadian rhythm and that thereby *Nr2f6* mRNA levels alternate in the mouse brain during the circadian rhythm. To test this hypothesis, wildtype

cerebellar neurons were cultured for different time periods and the Nr2f6 mRNA levels of NCAM antibody treated neurons were compared to levels in mock-treated or NCAM antibody treated neurons with EndoN pretreatment. At the same time, cerebellar neurons of wildtype mice were treated with NCAM antibody and the relative level of nuclear PSA-NCAM from immunoblot analysis with PSA-specific antibody was compared to mock-treated cells. The nuclear PSA-NCAM level was significantly increased in neurons cultured for 30 h and 42 h and treated with NCAM antibody in contrast to the level in neurons cultured for 24 h, 36 h and 48 h and treatment with NCAM antibody as well as relative to the level in mock-treated cells (**Figure 40 B**). The enhanced nuclear PSA-NCAM level coincided with increased levels of Nr2f6 mRNA (**Figure 40 A**). Upon NCAM antibody treatment, the mRNA levels of Nr2f6 were increased in neurons cultured for 30 h and 42 h, while mRNA levels of Nr2f6 were not altered in mock-treated neurons and NCAM antibody treated and EndoN pretreated neurons at all time points. The correlation analysis by scatter plot indicated a strong positive correlation ( $r^2 = 0.9347$ ) between nuclear PSA levels and Nr2f6 mRNA levels in neurons treated with NCAM antibody. Moreover, the gene expression profile of Nr2f6 was not altered in NCAM-deficient mice at all conditions.

In addition, the PSA-NCAM level was quantified in nuclear fractions from cerebella of wildtype mice by immunoblot with PSA-specific antibody at different Zeitgeber time (ZT) during the 12h light/ 12h dark cycle. During the light phase, the level of nuclear PSA-NCAM fragment declined until the end of the light phase and increased until the end of the dark phase (**Figure 40 C** and **Figure 32 A**). This nuclear PSA-NCAM fragment level corresponded to the Nr2f6 mRNA expression pattern in wildtype cerebellum (**Figure 40 D**). The mRNA levels of Nr2f6 were significantly downregulated from the beginning until the end of the light phase and increased to the basal level in the middle of the dark phase corresponding to the 12h light/ 12h dark cycle. In contrast, in NCAM-deficient mice the expression of Nr2f6 remained high and showed no oscillation during the light and dark cycle. In cerebellum tissue a positive correlation ( $r^2 = 0.7144$ ) between nuclear PSA-NCAM levels and mRNA levels of Nr2f6 was observed (**Figure 40 C, D**). Together, these results confirm the relevance of the nuclear PSA-NCAM fragment for circadian rhythmicity and moreover show that PSA-NCAM regulates the oscillating gene expression of Nr2f6.

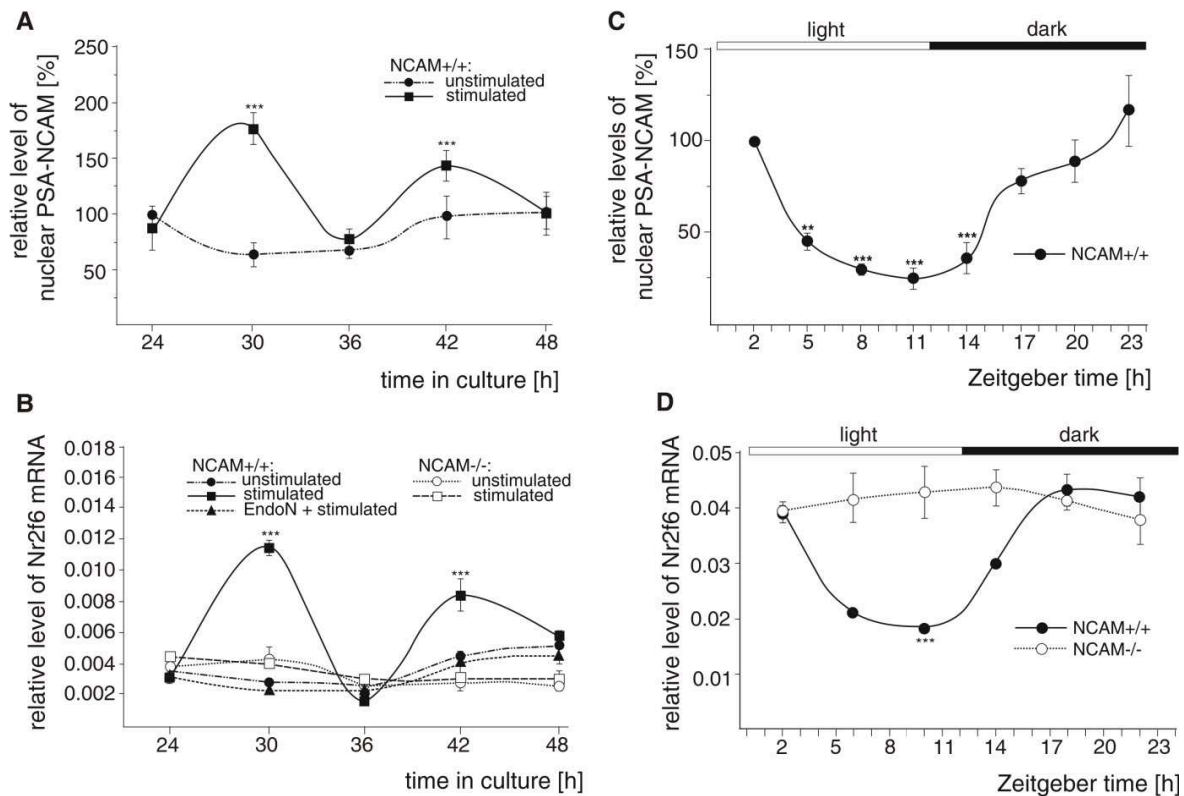


**Figure 40: Nuclear PSA-NCAM affects mRNA levels of Nr2f6 in cultured cerebellar neurons and in cerebellar tissue.** (A, B) Cerebellar neurons of wildtype (NCAM+/+) and NCAM-deficient (NCAM-/-) mice were maintained in culture for different time periods (as indicated) and treated with chicken NCAM antibody (stimulated) with and without EndoN pretreatment (EndoN + stimulated) or mock treated (unstimulated) and subjected either to subcellular fractionation followed by immunoblot analysis with PSA specific antibody of nuclear fractions (A) or to RNA isolation followed by RT-qPCR (B). (C, D) Nuclear fractions were isolated from cerebella of 3 months old wildtype (NCAM+/+) (C, D) and NCAM-deficient (-/-) (D) mice at different ZT points of the 12 h light/12 h dark cycle (ZT0: lights on) by subcellular fractionation and subjected to immunoblot analysis with PSA-specific antibody (C) or to RNA isolation followed by RT-qPCR (D). Mean values  $\pm$  from three independent experiments are shown for nuclear PSA signal by densitometry (A, C). Differences between groups are indicated as (\*\*  $p < 0.01$ , \*\*\*  $p < 0.001$ ; two-way ANOVA with Bonferroni post-hoc test). (B, D) Mean values  $\pm$  from three independent experiments for mRNA level of Nr2f6 relative to mRNA level of reference genes (actin, tubulin and glyceraldehyde 3-phosphate dehydrogenase). Differences in expression levels relative to the levels at ZT2 are indicated (\*  $p < 0.05$ , \*\*  $p < 0.01$ , \*\*\*  $p < 0.001$ ; two-way ANOVA with Dunnett's multiple comparison test).

The combined results not only confirm the nuclear localization of the PSA-carrying NCAM fragment *in vivo*, but also show that the nuclear PSA-NCAM fragment level varies during the light/dark cycle and also varies distinctly in different brain regions, suggesting that PSA-NCAM in neuronal cell nuclei plays an important role in the maintenance of the circadian rhythm *in vivo*.



## 6. DISCUSSION

---

In the present study I show for the first time that a proteolytically processed transmembrane PSA-carrying NCAM fragment is present in the nucleus of neuronal cells. Full length PSA-NCAM is cleaved at the plasma membrane by the matrix metalloproteases MMP-9 and/or MMP-2 upon treatment of cerebellar neurons with surrogate NCAM and PSA ligands. The resulting transmembrane PSA-carrying NCAM fragment is internalized into the cell, transported to endosomes, translocated from the endosomes into the cytoplasm in a calmodulin-dependent manner and imported into the nucleus. The nuclear import is mediated by cofilin and PC4 which were here identified as novel PSA binding partners. The generation of the PSA-carrying NCAM fragment requires the preceding phosphorylation of MARCKS and is mediated by the activation of FGF-receptor dependent signal transduction pathways. Furthermore, the generation and nuclear import of the PSA-NCAM fragment depends on calmodulin-mediated activation of NOS or on the activation of PLD and PI3K, depending on the NCAM and/or PSA ligand used for the treatment of the cells. The nuclear PSA-carrying NCAM fragment participates in the regulation of the expression of the clock-related genes CLOCK and Per-1 as well as of the Nr2f6 gene and has regulatory functions in the circadian rhythm.

### **5.1 PSA-carrying NCAM is cleaved at the plasma membrane by MMP-2 and/or MMP-9 upon treatment of cerebellar neurons with surrogate NCAM ligands**

Homophilic and heterophilic interactions of cell surface proteins can activate cell surface receptors that drive intracellular signaling cascades leading to extracellular cleavage of transmembrane cell surface glycoproteins as shown for NCAM and L1 (Kleene *et al.*, 2010a; Lutz *et al.*, 2012). The proteolytic cleavage of NCAM by a serine protease at the cell surface and the import of a 50 kDa transmembrane PSA-lacking NCAM fragment into the cell nucleus has been shown to occur upon treatment of cerebellar neurons and NCAM-expressing CHO cells with function-triggering NCAM antibody (Kleene *et al.*, 2010a). Since NCAM is the major carrier of PSA, PSA probably enters the nucleus attached to NCAM. The presence of nuclear PSA in cerebellar neurons upon treatment of neurons with function-triggering NCAM antibody and NCAM-Fc as surrogate physiological NCAM ligands was demonstrated in the present study. In nuclear fractions derived from NCAM-Fc stimulated cerebellar neurons that were subjected to PSA immunoprecipitation and subsequent removal of N-glycans including PSA, a 50 kDa NCAM fragment was observed using antibodies against the

intracellular domain or the extracellular domain of NCAM. These results indicate that PSA enters the nucleus attached to a transmembrane NCAM fragment containing the intracellular and transmembrane domains of NCAM and part of the extracellular NCAM domain. Moreover, in PSA immunoprecipitates from non-nuclear membrane fractions of NCAM-Fc treated cerebellar neurons reduced levels of N-deglycosylated NCAM forms of approximately 120 and 180 kDa were observed after digestion of N-glycans, suggesting that the 50 kDa NCAM fragment derives from full-length transmembrane NCAM forms at the plasma membrane.

Since serine proteases are known to cleave NCAM (Endo *et al.*, 1998; Endo *et al.*, 1999) and moreover to generate the transmembrane NCAM fragment (Kleene *et al.*, 2010), it was examined whether the PSA-carrying NCAM fragment is generated by cleavage of full-length PSA-NCAM by a serine protease. The nuclear PSA-NCAM level was similar in cerebellar neurons treated with NCAM antibody in the absence and presence of aprotinin, which is a function blocking serine protease inhibitor. This finding suggests that the nuclear PSA-carrying NCAM fragment is not generated from full length PSA-NCAM by a serine protease which is in contrast to the generation of the PSA-lacking NCAM fragment which is cleaved by a serine protease.

It has been shown that NCAM is not only a target for serine proteases but also for matrix metalloproteases: NCAM is a substrate of MMP-2 *in vitro* (Hübschmann *et al.*, 2005; Hinkle *et al.*, 2006; Dean and Overall, 2007) and MMP-9 is involved in the proteolytic cleavage of NCAM180 *in vivo* (Schichi *et al.*, 2011). Here, I showed that the nuclear PSA-NCAM levels were diminished in cerebellar neurons after treatment with NCAM antibody in the presence of MMP-2 and of MMP-9 inhibitor, indicating that the PSA-NCAM fragment is indeed generated by MMP-2 and/or MMP-9. In isolated nuclear fractions of MMP-2 or MMP-9 inhibitor-treated and NCAM-Fc-stimulated cerebellar neurons that were subjected to PSA immunoprecipitation followed by digestion of N-glycans a reduced level of the 50 kDa NCAM fragment was observed. This finding shows that MMP-2 and/or MMP-9 are involved in the generation of the PSA-NCAM fragment and strengthen the notion that the nuclear PSA-NCAM fragment is generated from cell surface full-length PSA-NCAM.

## **5.2 The PSA binding partners BDNF and histone H1 do not induce the generation and the nuclear import of the PSA-carrying NCAM fragment**

PSA is not only detectable in nuclear fractions of cerebellar neurons upon treatment with surrogate NCAM ligands but was also found in nuclear fractions of adult wildtype mice, suggesting that the extracellular proteolytic cleavage through MMP-2 and MMP-9 is induced by a natural physiological trigger. For this reason, I searched for physiological NCAM and/or PSA ligands which can induce the generation of this PSA-NCAM fragment. BDNF and the BDNF receptor TrkB interact with NCAM via its extracellular or intracellular domains (Muller *et al.*, 2000; Cassens *et al.*, 2010). BDNF triggers the TrkB-mediated enhancement of tyrosine phosphorylation of NCAM and NCAM-dependent neurite outgrowth (Cassens *et al.*, 2010; Kleene *et al.*, 2010b). Previous studies showed that PSA interacts with BDNF in the extracellular space (Vutskits *et al.*, 2001) and that a complex of BDNF and PSA can bind to TrkB leading to downstream signaling (Kanato *et al.*, 2006). Based on these findings it was likely that binding of BDNF to PSA triggers a downstream signaling cascade which could lead to the generation and nuclear import of the transmembrane PSA-carrying NCAM fragment. Since no enhanced levels of the nuclear PSA-NCAM fragment were observed in cerebellar neurons upon treatment with BDNF compared to levels in mock-treated neurons, it can be concluded that BDNF does not influence the generation and nuclear import of the PSA-carrying NCAM fragment.

The direct extracellular interaction was not only shown for PSA with BDNF (Vutskits *et al.*, 2001) but also for PSA with histone H1 *in vitro* and *in vivo* (Mishra *et al.*, 2010). Histone H1 is a nuclear protein which is also expressed on the cell surface of neural tissues (Bolton and Perry, 1997) and promotes PSA-NCAM-mediated functions of the nervous system (Mishra *et al.*, 2010). Application of histone H1 to cultured cerebellar neurons and Schwann cells stimulates PSA-dependent neuritogenesis, process formation, proliferation and migration of cells and improves regeneration after injury in mice (Mishra *et al.*, 2010). Thus, it was tested if histone H1 acts as a physiological trigger to regulate a signaling pathway leading to the generation and nuclear import of the PSA-NCAM fragment. No enhanced nuclear PSA-NCAM level was found upon treatment of cerebellar neurons with histone H1. Although histone H1 could not trigger the generation and nuclear import of the PSA-NCAM fragment after binding to extracellular PSA-NCAM, histone H1 was found to interact with PSA and NCAM in the nucleus of cerebellar neurons. Proximity ligation assay of NCAM antibody treated cerebellar neurons showed the close vicinity of the PSA moiety of PSA-NCAM and

histone H1 as well as of the NCAM core protein and histone H1 in the nucleus of cerebellar neurons. Moreover, a co-localization of PSA and NCAM with histone H1 was shown in brain slices of wildtype mice. These results suggest that histone H1 interacts with the PSA-NCAM fragment in the nuclei of stimulated neurons *in vitro* as well as in brains of wildtype mice *in vivo*. Since histone H1 is required for packaging of chromatin and plays a role in the regulation of transcription (Brown *et al.* 1996), it is possible that the nuclear PSA-NCAM fragment is involved in histone H1-mediated nuclear events like regulation of transcription.

### **5.3 The generation and nuclear import of the PSA-carrying NCAM fragment is triggered by FGF-2 and by myristoylated alanine-rich C-kinase substrate (MARCKS-ED peptide through a FGF-receptor mediated signaling cascade**

Besides BDNF and histone H1 the direct interaction of PSA with FGF-2 has been shown (Ono *et al.*, 2012). The PSA and FGF-2 interaction induces FGF-mediated FGF-receptor signaling (Ono *et al.*, 2012). In contrast, the interaction of FGF-2 with the extracellular domain of NCAM induces NCAM-dependent reduction of FGF-receptor signaling (Francavilla *et al.*, 2007; Kochoyan *et al.*, 2008). Here, FGF-2 was identified as novel physiologic trigger that induces signaling pathways leading to the generation and nuclear import of the PSA-carrying NCAM fragment. Nuclear PSA-NCAM fragment levels were enhanced in cerebellar neurons treated with FGF-2 indicating that FGF-2 triggers a signal pathway which leads to the cleavage of full-length PSA-NCAM and the generation as well as the nuclear import of the PSA-NCAM fragment.

Besides FGF-2, the MARCKS-ED peptide was identified as trigger which mediates the generation and nuclear import of the PSA-NCAM fragment. Interestingly, the generation and nuclear import of the PSA-carrying NCAM fragment upon MARCKS-ED peptide treatment was found to be MMP-2-dependent, but not MMP-9-dependent. The level of nuclear PSA-NCAM was lower in cerebellar neurons treated with MARCKS-ED peptide in the presence of MMP-2 inhibitor but not in the presence of MMP-9 inhibitor. These findings demonstrate that PSA-NCAM is cleaved by MMP-2 after treatment of neurons with MARCKS-ED peptide while the cleavage of PSA-NCAM after treatment of neurons with NCAM antibody involves MMP-2 and MMP-9. These observations suggest different novel signaling cascades which lead to the generation and nuclear import of the PSA-NCAM fragment.

Since FAK plays a role in the generation and nuclear import of the PSA-lacking NCAM fragment (Kleene *et al.*, 2010a), it was tested whether the signaling pathway leading to the

generation of the nuclear PSA-carrying NCAM fragment involves activation of FAK. The nuclear PSA-NCAM levels were similar in cerebellar neurons treated with the NCAM antibody or FGF-2 in absence and presence of a FAK, indicating that FAK plays no role in the generation and nuclear import of the PSA-NCAM fragment.

The idea whether the FGF-receptor plays a role in the signaling pathway leading to generation of the nuclear PSA-NCAM fragment were examined. Since polysialylation of NCAM changes the adhesive properties of NCAM and moreover leads to conformational changes of the NCAM protein backbone, it is likely that the binding between PSA and FGF-2 influences the interaction of NCAM to the FGF-receptor and therefore changes NCAM-mediated FGF-receptor signaling. The nuclear PSA-NCAM fragment levels were reduced in cerebellar neurons treated with NCAM antibody or FGF-2 in the presence of a FGF-receptor inhibitor. Moreover, reduced nuclear PSA-NCAM fragment levels were also observed in cerebellar neurons treated with MARCKS-ED peptide in the presence of a FGF-receptor inhibitor. These results provide evidence that FGF-2, the function-triggering NCAM antibody as well as the MARCKS-ED peptide trigger a FGF-receptor dependent downstream signaling pathway. The binding of the FGF-receptor to NCAM is known to induce a NCAM-mediated increase of intracellular  $Ca^{2+}$  levels (Williams *et al.*, 1994b; Doherty and Walsh, 1996) and free cytoplasmic  $Ca^{2+}$  is known to regulate the binding between MARCKS-ED and calmodulin. Moreover, the binding between MARCKS-ED and calmodulin is highly regulated by PKC and is disturbed upon phosphorylation of MARCKS by PKC (Gallant *et al.*, 2005). Phosphorylation of MARCKS has been shown to play an important role in calcium-calmodulin-dependent signaling pathways (McNamara *et al.*, 1998; McIllroy *et al.*, 1991). Thus, the phosphorylation state of MARCKS can provide information about the amount of free calmodulin and may indicate whether calmodulin is involved in the FGF-receptor-mediated signaling pathways. Here, the phosphorylation of MARCKS was enhanced in neurons upon treatment with NCAM antibody, FGF-2 or MARCKS-ED peptide relative to the total MARCKS amount. These findings indicate that the generation and nuclear import of the PSA-NCAM fragment depend on a FGF-receptor-mediated signal pathway which requires phosphorylation of MARCKS.

### **5.3.1 Generation of the transmembrane PSA-NCAM fragment through a FGF-receptor-mediated calmodulin/NOS-dependent signaling pathway upon treatment of cerebellar neurons with NCAM antibody or FGF-2**

The activation of PLC is required to induce the PKC-mediated phosphorylation of MARCKS which subsequently leads to dissociation of calmodulin from MARCKS (**Figure 41**) (Gallant *et al.*, 2005; Morash *et al.*, 2005; Verghese *et al.*, 1994). The nuclear level of the PSA-NCAM fragment was not enhanced in cerebellar neurons after treatment with NCAM antibody or FGF-2 in the presence of PLC and PKC inhibitor in contrast to cells treated with NCAM antibody or FGF-2 alone which showed enhanced levels of the nuclear PSA-NCAM fragment. Thus, PLC and PKC activity are required for the signaling cascade which leads to the generation and nuclear import of the PSA-NCAM fragment. This finding supports the assumption that the activity of PKC leads to phosphorylation of MARCKS and dissociation of calmodulin from MARCKS. Free calmodulin can bind and activate NOS and activated NOS produces NO which is released from the cell into the extracellular space (Su *et al.*, 1995). The generation and nuclear import of the PSA-NCAM fragment was blocked in cerebellar neurons upon NCAM antibody or FGF-2 treatment in the presence of calmodulin or NOS inhibitors, demonstrating that a calmodulin- and NOS-dependent signaling pathway leads to generation and nuclear import of the PSA-NCAM fragment. Moreover, the extracellular level of NO was enhanced in supernatants of NCAM antibody or FGF-2 treated neurons. Neuronal and exogenous NO can induce S-nitrosylation of cysteine thiols in MMP-9 which leads then to the activation of MMP-9 (Gu *et al.*, 2002; Manabe *et al.*, 2005; Ridnour *et al.*, 2007). Since my results indicated that MMP-9 is S-nitrosylated in supernatants of cerebellar neurons after treatment with NCAM antibody, I propose that calmodulin/NOS-mediated release of NO leads to S-nitrosylation of MMP-9 and activation of MMP-9 and MMP-2.

Of note, MMP-2 was not S-nitrosylated and it remains unclear how MMP-2 is activated but it can be speculated that MMP-9 is required for the proteolytic activation of MMP-2 and that MMP-2 is the protease which cleaves PSA-NCAM.

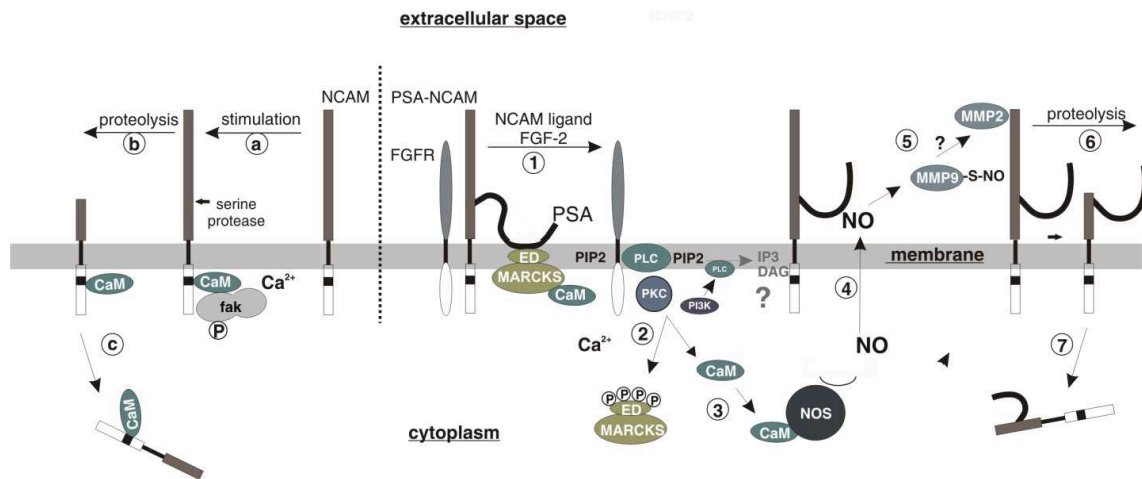


**Figure 41: Schematic presentation of the signaling pathway leading to the internalization of a PSA-lacking and PSA-carrying NCAM fragment after treatment of cerebellar neurons with surrogate PSA-NCAM ligands. (a-c)** Treatment of NCAM with a function triggering NCAM antibody leads to the recruitment of full length NCAM to lipid rafts, intracellular increase of calcium and interaction of PSA-lacking NCAM with calmodulin and phosphorylated FAK (a). PSA-lacking NCAM is cleaved extracellularly by a serine protease (b) and a transmembrane 55 kDa NCAM fragment is internalized into the cell (c). (1-7) PSA interacts with the effector domain (ED) of MARCKS in the MARCKS-calmodulin complex at the plasma membrane. Treatment of PSA-carrying NCAM with NCAM antibody or FGF-2 leads to the binding of NCAM to the FGF-receptor followed by activation of PLC (1). The activation of PLC triggers the activation of PKC which in turn stimulates the dissociation of PSA-NCAM from MARCKS through phosphorylation of the MARCKS-ED. PI3K serves as co-activator of PLC with converts PIP2 to IP3 and DAG (2). Phosphorylation of MARCKS-ED leads to the dissociation of calmodulin from MARCKS and the free calmodulin can bind and activate NOS (3). Activation of NOS promotes the production of free NO which is released into the extracellular space (4). MMP-9 is activated by S-nitrosylation by free NO and is then able to activate MMP-2 (5) leading to the cleavage of PSA-carrying NCAM (6) and internalization of PSA-carrying NCAM fragment (7).

### 5.3.2 Generation of the transmembrane PSA-NCAM fragment through the FGF-receptor-mediated PLD/PI3K signaling cascade upon treatment of cerebellar neurons with MARCKS-ED peptide

Surprisingly, the treatment of cerebellar neurons with MARCKS-ED peptide was found to trigger a FGF-receptor-mediated but calmodulin- and NOS-independent signaling pathway. Since the MARCKS-ED peptide triggered generation and nuclear import of the PSA-NCAM fragment was not affected by application of calmodulin and NOS inhibitors and the extracellular NO level was not altered after treatment of neurons with MARCKS-ED peptide, I suppose that NOS remains inactive after treatment of neurons with MARCKS-ED peptide. All NOS isoforms bind calmodulin for enzymatic activity and several studies showed that phosphorylation of calmodulin can alter its ability to activate NOS (Greif *et al.*, 2004; Piazza *et al.*, 2012). Therefore it is conceivable that calmodulin is phosphorylated upon MARCKS-ED peptide treatment and that this phosphorylation prevents NOS activation (Figure 42).

PI3K and PLD besides PLC and PKC were shown to play a role in the signaling pathway which leads to the generation and nuclear import of the PSA-NCAM fragment upon treatment of cerebellar neurons with MARCKS-ED peptide. Interestingly, PLD is not required for the generation of the PSA-NCAM fragment after treatment of cerebellar neurons with NCAM antibody or FGF-2. PLD might be directly activated by MARCKS-ED or MARCKS could influence the ability of PKC to activate PLD by so far unknown mechanisms (Morash *et al.*, 2005). Moreover activated PLD can regulate PI3K via phosphatidic acid. PI3K serves as positive regulator of PLD and co-activator of PLC and PI3K has been shown to regulate and activate MMP-2 together with PLD (Ispanovic and Haas, 2006; Reich *et al.*, 1995). These observations suggest that MMP-2 is activated through a FGF-receptor-mediated PLD/PI3K signaling pathway upon treatment of cerebellar neurons with MARCKS-ED peptide. In this signaling pathway MMP-2 seems to be directly activated and is not dependent on the previous activation of MMP-9 as observed for the signaling pathway upon NCAM antibody or FGF-2 treatment.

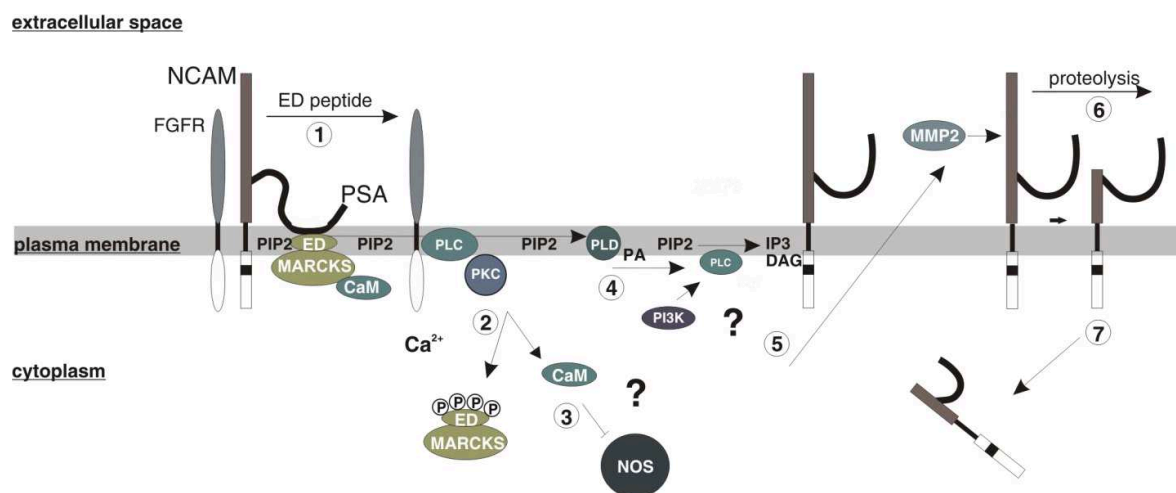


**Figure 42: Schematic presentation of MARCKS-ED peptide triggered pathways leading to the generation and internalization of a PSA-carrying NCAM fragment. (1-7)** PSA interacts with MARCKS-calmodulin at the plasma membrane through binding of PSA with the effector domain (ED) of MARCKS. PIP2 is also associated with MARCKS within the plasma membrane. The treatment of PSA-carrying NCAM with MARCKS-ED peptide (1) leads to the activation of the FGF-receptor-mediated PLC/PIP2 downstream signaling pathway which activates PKC. Activated PKC induces the phosphorylation of MARCKS which triggers the dissociation of MARCKS from the plasma membrane (2). Calmodulin dissociates from MARCKS upon MARCKS phosphorylation and is phosphorylated which could influence the ability of calmodulin to activate NOS (3). PLD activates PI3K via generation of phosphatidic acid. PI3K serves as positive regulator of PLD and co-activator of PLC with converts PIP2 to IP3 and DAG (4). PI3K and PLD activates MMP-2 by an unknown mechanism (5) leading to the cleavage of full length PSA-carrying NCAM by MMP-2 (6). A transmembrane proteolytic PSA-carrying NCAM fragment is internalized by endocytosis (7).



#### **5.4 Translocation of the transmembrane PSA-carrying NCAM fragment from the endosomes into the cytoplasm is calmodulin-dependent whereas PC4 and cofilin are involved in the import of the fragment into the nucleus**

The transmembrane PSA-lacking NCAM fragment was shown to be internalized into the cell, transported into the ER, translocated from the ER into the cytoplasm and to be imported into the nucleus in a calmodulin-dependent manner (Kleene *et al.*, 2010a). In contrast, a transmembrane L1 fragment has been shown to be transported from the plasma membrane to late endosomes, to be released from endosomes into the cytoplasm and to be translocated into the nucleus in a pathway that depends on importin and chromatin-modifying protein 1 (Lutz *et al.*, 2012). The results from electron microscopy and subcellular fractionation revealed that the PSA-carrying NCAM fragment is located in endosomes and is not present in the ER after endocytosis upon treatment of cerebellar neurons with NCAM antibody (**Figure 43**). The release of the PSA-NCAM fragment from endosomes into the cytoplasm was blocked in the presence of a calmodulin inhibitor and by a calmodulin antibody. This result suggests that the release of the PSA-carrying NCAM fragment from the endosomes into the cytoplasm is calmodulin-dependent. Since the release of PSA-carrying NCAM and PSA-lacking NCAM fragments from organelles depends on calmodulin and calmodulin plays a role in the nuclear import of the PSA-lacking fragment, I supposed that calmodulin is required for the nuclear import of the PSA-carrying NCAM fragment. My results from the nuclear import assay indicated that the import of the PSA-NCAM fragment was not blocked using the calmodulin inhibitor or a calmodulin antibody and showed that calmodulin does not seem to play a role in the nuclear import of the PSA-NCAM fragment.

By ELISA I could demonstrate the direct binding of cofilin and PC4 with colominic acid, the bacterial homologue of PSA. Moreover, ELISA results indicate that only full-length PC4 binds to PSA. An interaction of PSA with cofilin and PC4 was shown in the nucleus of neurons by proximity ligation assay and by co-immunoprecipitation from nuclear fractions of NCAM antibody treated cerebellar neurons. The actin severing protein cofilin is transported through a nuclear localization signal and is a nuclear import carrier for actin (Pendleton *et al.*, 2003, Munsie *et al.*, 2012). Cofilin acts as an actin polymerization factor and is associated with RNA polymerase II (pol II) and plays an important role in pol II transcription (Calvo *et al.*, 2005; Ono, 2007; Obrdlik and Percipalle, 2011). Active genes were shown to be free of actin in immunoprecipitates of cofilin silenced cells and histone H3 acetylation levels on lysine 9 were shown to be lower in absence of cofilin and actin. Histone acetylation is an

indicator for transcriptional activation and therefore it is likely that nuclear cofilin is involved in gene silencing and required for pre-mRNA synthesis (Obrdlik and Percipalle, 2011). Yeast Sub1, the homolog of PC4 is thought to be a part of the promotor-bound pre-initiation complex of pol II and acts as an activator of pol II-mediated transcription (Sikorski *et al.*, 2011). PC4 interacts directly with DNA and is important for chromatin compaction and decompaction by cooperation or competition with histone H1 (Das *et al.*, 2010). Since this study revealed not only the interaction of PSA with PC4 and cofilin but also the interaction of PSA with histone H1 in the nucleus, it could be possible that nuclear PSA-NCAM is involved in the pol II-mediated transcription machinery and that PSA might play a role in PC4-dependent chromatin compaction and decompaction.

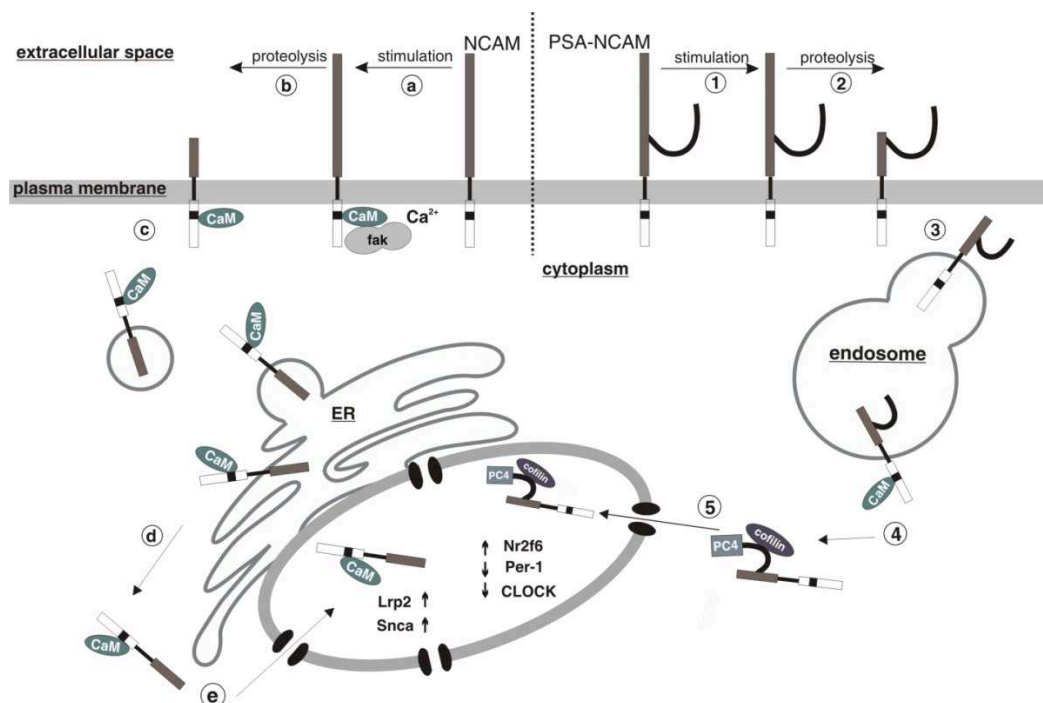


**Figure 43: Schematic presentation of the trafficking of a PSA-lacking and PSA-carrying NCAM fragment into the nucleus and their role in modulation of gene expression. (a-e)** Treatment of NCAM with a function triggering NCAM antibody leads to the recruitment of full length NCAM to lipid rafts (a). PSA-lacking NCAM is cleaved extracellularly by a serine protease (b) and a transmembrane 55 kDa NCAM fragment is internalized by endocytosis into endosomes and translocated to the ER (c). From the ER the NCAM fragment is translocated into the cytoplasm (d) and transported into the nucleus in a calmodulin-dependent manner (e). In the nucleus, the NCAM fragment is involved in the regulation of Lrp2 and  $\alpha$ -synuclein (Snca) mRNA expression. (1-5) Treatment of PSA-carrying NCAM with surrogate PSA-NCAM ligands (2) leads to the proteolytic cleavage of PSA-carrying NCAM (2) and the internalization of a transmembrane PSA-NCAM fragment by endocytosis (3). The PSA-NCAM fragment is transported to endosomes and released into the cytoplasm in a calcium and calmodulin-dependent manner (4). The fragment is then transported from the cytoplasm into the nucleus together with PC4 and cofilin (5). In the nucleus, the PSA-carrying NCAM fragment is involved in the regulation of Nr2f6 and clock-related genes CLOCK and Per1 mRNA expression.

### **5.5 Nuclear PSA-NCAM plays a role in the circadian rhythm and is involved in the gene expression of the clock-related genes Per-1, CLOCK and Nr2f6**

The circadian rhythm was used as read out system to study the functional role of nuclear PSA-NCAM. Since PSA is located in the SCN and participates in regulating photic and non-photic inputs during the light/dark cycle (Glass *et al.*, 2003; Golombek *et al.*, 2010), it was assumed that the generation and nuclear import of transmembrane PSA-NCAM upon treatment of cerebellar neurons with surrogate NCAM and/or PSA ligands might act as stimuli of photic or non-photic inputs to control the circadian rhythm. It is known that the circadian rhythm persists in cultured cerebellar granule cells and that the expression of clock-related genes still exists (Kaeffer and Pardini, 2005). My results revealed that the generation and nuclear import of the PSA-NCAM fragment upon treatment of cerebellar neurons with NCAM antibody is time-dependent and fluctuates during the circadian rhythm.

The circadian clocks are expressed by different tissues but the SCN comprises the master circadian clock and regulates the entrainment of circadian rhythmicity in mammals (Glass *et al.*, 1994; Shen *et al.*, 1999; Glass *et al.*, 2000; Shen *et al.*, 2001; Fedorkova *et al.*, 2002). Removal of PSA by microinjection of EndoN into the murine SCN has been shown to lead to an impairment of the circadian rhythm (Fedorkova *et al.*, 2002). I could show that the level of nuclear PSA varies during the light/dark cycle not only in the SCN but also in the subordinated clocks in the cerebellum, striatum, cortex, hippocampus and midbrain. The oscillation pattern of the nuclear PSA-NCAM fragment was distinct in each brain region.

CLOCK or Per-1 are key players in regulating circadian clocks and are controlled by complex transcriptional-translational feedback loops. Since nuclear PSA-NCAM plays a role in the regulation of their transcription, I supposed that nuclear PSA-NCAM is involved in the regulation of clock-related genes. The level of the nuclear PSA-NCAM fragment correlated with mRNA levels of the clock-related genes Per-1 and CLOCK in cerebellar neurons after treatment with NCAM antibody. Moreover, my results showed that Per-1 and CLOCK are differently regulated depending on the nuclear PSA-NCAM fragment levels in the cerebellum and SCN of wildtype mice. In correlation analysis of mRNA levels of CLOCK and Per-1 with nuclear PSA-NCAM fragment levels only moderate correlations between CLOCK mRNA levels and nuclear PSA-NCAM fragment levels in the SCN and between Per-1 mRNA levels and nuclear PSA-NCAM fragment levels in the cerebellum were found. Since my results showed a correlation between nuclear PSA-NCAM fragment levels and the transcription of Per-1 in the cerebellum and since it is reported that the transcription of Per-1 in the SCN is

induced by photic stimuli and is involved in the light-input pathway of the circadian rhythm (Wjinen and Young, 2006), I speculate that nuclear PSA mimics non-photoc stimuli to regulate the gene expression pattern of Per-1 in the cerebellum.

The transcription factor Nr2f6 is involved in the regulation of the transcriptional repression and hormonal response during the development of the locus coeruleus (LC) and a strong defect in LC development has been reported in Nr2f6-deficient mice. The LC has an important function in light- and restricted food-driven entrainment during the circadian rhythm. The Nr2f6-deficient mice show besides altered entrainment of the light/dark cycle also an altered oscillation of the expression pattern of the clock-related gene Per-1, indicating a deficit in the function of the forebrain circadian clock (Warnecke *et al.*, 2005).

Microarray analysis revealed that mRNA levels of Nr2f6 were altered in cerebellar neurons upon treatment with NCAM antibody. After verification of the expression profile of Nr2f6 by qPCR I could demonstrate that the upregulation of the mRNA level of Nr2f6 depended on the levels of the nuclear PSA-NCAM fragment. My results demonstrate that Nr2f6 has a higher expression in cerebellar neurons of wildtype mice compared to neurons of NCAM-deficient mice. The mRNA level of Nr2f6 in the cerebellum of wildtype mice and also in NCAM antibody treated cerebellar neurons varies during the 12 h light/12 h dark cycle in strong correlation with nuclear PSA-NCAM fragment levels. These results indicate that the gene expression of Nr2f6 is influenced by nuclear PSA-NCAM fragment levels and has an important function in the cerebellum in regulating the circadian rhythm.

### **5.6 Nuclear PSA-lacking NCAM is involved in the gene expression of Lrp2 and $\alpha$ -synuclein**

Besides upregulated mRNA levels of Nr2f6, altered mRNA levels of Lrp2 and  $\alpha$ -synuclein were identified in NCAM antibody-treated cerebellar neurons by microarray analysis. Lrp2, also known as megalin, is a membrane protein and member of the LDL receptor family of lipoprotein receptors, acts as a multi-ligand endocytic receptor for vitamins, hormones bound to protein complexes and lipoproteins and plays a role in cholesterol transport (May *et al.*, 2007; Marzolo and Farfan 2011). Lrp2 is highly expressed and plays an important role in proper forebrain development and plays a functional role in neuronal survival and regeneration in the adult nervous system (Fleming *et al.*, 2009). By qPCR, I could demonstrate that the higher mRNA level of Lrp2 in cerebellar neurons after NCAM antibody treatment depended on nuclear NCAM fragment levels and not on nuclear

PSA-NCAM fragment levels. Genetic studies have shown that a reduced gene expression of Lrp2 is associated with Alzheimer's disease (Vargas *et al.*, 2010). Moreover, forebrain abnormalities, called Donnai-Barrow syndrome, are found in humans with Lrp2 gene defects. The symptoms observed in these patients include the agenesis of the corpus callosum and impairments in brain development, hearing and seeing (Kantarci *et al.*, 2007; Marzolo and Farfan, 2011). These investigations underscore the importance of proper Lrp2 mRNA expression for brain development and function. Of note, a higher overall mRNA level of Lrp2 was observed in cerebellar neurons of NCAM-deficient mice compared to mock-treated neurons of wildtype mice. There are many known regulators for Lrp2 mRNA expression which are partly ligands of Lrp2, for instance clusterin. The glycoprotein clusterin plays a role in anti-apoptotic events as well as in cancer and Alzheimer's disease and is a well-known ligand and positive regulator of Lrp2 gene and protein expression (Marzolo and Farfan, 2011). I conclude that in the absence of NCAM another glycoprotein, like clusterin, could be involved in the regulation of the Lrp2 mRNA level.

My research showed that the gene expression of  $\alpha$ -synuclein was altered in cerebellar neurons after treatment with NCAM antibody.  $\alpha$ -synuclein is highly expressed in neural tissues and mainly located at the presynapses but it also present in the nuclei and axons of neurons.  $\alpha$ -synuclein is implicated in presynaptic signaling and synaptic transmission and plays a role in physiological functions like calcium regulation, mitochondrial homeostasis, gene expression, protein phosphorylation and fatty acid binding (Bensky *et al.*, 2016). In synapses,  $\alpha$ -synuclein regulates particularly vesicular trafficking and endocytosis and operates as negative regulator of synaptic transmission. Furthermore, it is involved in the release, transport and reuptake of dopamine. Increased mRNA levels of  $\alpha$ -synuclein and accumulations in Lewy bodies and Lewy neuritis have been reported to cause neuronal dysfunctions which are linked to Parkinson's disease (PD) (Linnertz *et al.*, 2009; Soldner *et al.*, 2016). qPCR analysis revealed that the upregulated mRNA levels of  $\alpha$ -synuclein depends on nuclear NCAM-fragment levels. Recent studies showed that  $\alpha$ -synuclein overexpression and aggregation results in a decreased expression of the dopamine receptor and alterations in the glutaminergic transmission in the striatum and frontal cortex in rats. Furthermore,  $\alpha$ -synuclein seems to have a regulatory effect on the distribution of the dopamine transporter in striatum and substantia nigra in mice in the early pathogenesis of PD (Belluci *et al.*, 2015). The combined studies reveal the important functions of  $\alpha$ -synuclein and demonstrate that altered gene expression levels are strongly associated with the development of neuronal dysfunction

## 7. SUMMARY

---

The membrane-associated glycoprotein NCAM is the main carrier of the unusual glycan  $\alpha$ 2,8-linked polysialic acid (PSA) in the mammalian nervous system. PSA-NCAM is involved in the regulation of differentiation and migration of neuronal precursor cells, axonal outgrowth, synaptogenesis, physiological and morphological synaptic plasticity in the early embryonic stage during brain development. In the adulthood, PSA-NCAM is upregulated after injury of the central and peripheral nervous system and enhances axon regrowth in the peripheral nervous system and sprouting in the central nervous system. Moreover, PSA-NCAM plays an important role in the control of the circadian rhythm. PSA-NCAM can participate in homophilic and/or heterophilic interactions which can mediate signal transduction pathways. These NCAM-mediated signal transduction pathways can be modified by PSA due to its biophysical characteristics. Several proteins have been reported to interact with the extracellular or intracellular domain of NCAM while only a few binding partners are known to interact with PSA.

In the present study the generation and nuclear import of a transmembrane PSA-carrying NCAM fragment has been shown upon treatment of cerebellar neurons with surrogate NCAM ligands, e.g. function-triggering NCAM antibody or NCAM-Fc, with the PSA ligand FGF-2 or with a peptide comprising the effector domain (ED) of MARCKS. The results of immunoblot analysis and cell surface biotinylation have revealed that this PSA-carrying NCAM fragment is proteolytically cleaved from full length NCAM at the plasma membrane by the matrix metalloproteases MMP2 and/or MMP9. Treatment of cerebellar neurons with surrogate NCAM and/or PSA ligands leads to activation of a FGF-receptor-mediated PLC-dependent and PKC-dependent signal transduction pathway as well as phosphorylation of MARCKS. Interestingly, the generation and nuclear import of the PSA-carrying NCAM fragment by NCAM antibody and FGF-2 was shown to depend on calmodulin-mediated activation of NOS, which enhanced production and release of NO and led to NO-dependent S-nitrosylation of MMP9 and activation of MMP2, while the MARCKS-ED peptide triggered generation and nuclear import of the PSA-carrying NCAM fragment depends on the activation of PLD- and PI3K-mediated signaling pathways which activate MMP2.

To unravel the pathway by which the PSA-NCAM fragment reaches the nucleus, immunoelectron microscopy and subcellular fractionation of stimulated cells after cell surface biotinylation were performed. The results demonstrated that the PSA-carrying NCAM fragment is transported to endosomes after internalization. Moreover, this fragment is

translocated from the endosomes into the cytoplasm in a calmodulin-dependent manner and the import into the nucleus was shown to depend on cofilin and PC4, but not calmodulin. In this study, cofilin and PC4 were identified as novel binding partners of PSA by performing immunoprecipitation with PSA antibody and ELISA. Moreover, the nuclear co-localization of PSA with cofilin and PC4 and histone H1 was confirmed by proximity ligation assay.

The nuclear PSA-NCAM levels varied in different brain regions depending on the 12 h light/ 12 h dark cycle. Nuclear PSA was shown to be involved in the regulation of mRNA levels of the clock-related genes circadian locomotor output cycles kaput (CLOCK) and period-1 (Per-1) during the circadian rhythm. Moreover, microarray analysis revealed an influence of the nuclear PSA-carrying as well as PSA-lacking NCAM fragment on the regulation of mRNA levels of nuclear receptor subfamily 2 group F member 6 (Nr2f6) or of low density lipoprotein receptor-related protein 2 (Lrp2) and  $\alpha$ -synuclein. The upregulation of Nr2f6 was found to depend on nuclear PSA-NCAM levels, while the upregulation of Lrp2 and  $\alpha$ -synuclein depended on nuclear NCAM levels.

Together, these findings demonstrate the relevance of the nuclear PSA-NCAM fragment in transcription and affirmed that nuclear PSA-NCAM plays an important role in the circadian rhythm, indicating a functional relevance of nuclear PSA-NCAM in the nervous system.

## 8. ZUSAMMENFASSUNG

---

Das neurale Zelladhäsionsmolekül (NCAM) ist ein Glykoprotein des Nervensystems und der Hauptträger der Polysialinsäure (PSA), welche durch eine  $\alpha 2,8$ -Bindung an den NCAM-Proteinteil geknüpft wird. Während der Entwicklung des Nervensystems ist PSA-NCAM an einer Vielzahl von Prozessen, wie der Differenzierung und Migration von Vorläuferzellen, dem Auswachsen von Axonen sowie bei der Synaptogenese und physiologischer und morphologischer synaptischer Plastizität, beteiligt. Im Erwachsenenalter spielt PSA-NCAM eine wichtige Rolle bei der Aufrechterhaltung des Nervensystems und ist in der Regulation des Tag-Nacht-Rhythmus involviert. Darüber hinaus kann PSA-NCAM das Wachstum von Axonen nach Verletzungen im peripheren und zentralen Nervensystem fördern. Durch homophile Interaktionen und/oder heterophile Interaktionen von PSA-NCAM mit anderen Liganden können Signaltransduktionswege durch NCAM vermittelt werden. Das NCAM-Protein kann aufgrund der biophysikalischen Eigenschaften von PSA jedoch so modifiziert werden, dass die Bindung von NCAM an andere Liganden und folglich die NCAM-induzierte Signaltransduktion gestört wird. Mehrere Proteine sind in der Lage mit der extrazellulären oder intrazellulären Domäne von NCAM zu interagieren, wohingegen nur wenige Bindungspartner bekannt sind, die mit PSA interagieren.

In dieser Studie konnte ich zeigen, dass in Kleinhirnneuronen ein transmembranes und PSA-tragendes NCAM-Fragment an der Plasmamembran generiert und in den Zellkern transportiert wird. Dieser Vorgang wurde durch Stimulation von Kleinhirnneuronen mit einem gegen NCAM gerichteten funktionsstimulierenden Antikörper, mit NCAM-Fc, dem NCAM- und PSA-Liganden FGF-2 sowie durch ein MARCKS-Peptid, welches die MARCKS-Effektordomäne enthält, induziert. Mit Hilfe von Western-blot-Analysen und Oberflächenbiotinylierung konnte die proteolytische Spaltung von PSA-NCAM an der Plasmamembran durch die Matrixmetalloproteasen 2 (MMP-2) und/oder 9 (MMP9) nachgewiesen werden. Der Signal-transduktionsweg, der durch Stimulation von Kleinhirnneuronen mit den beschriebenen Liganden ausgelöst wird, führt zu einer über den FGF-Rezeptor vermittelten Aktivierung von PLC und PKC. Darüber hinaus erfordert die Signalweiterleitung die Phosphorylierung von MARCKS. Interessanterweise werden unterschiedliche FGF-Rezeptor-basierte Signaltransduktionswege induziert, in Abhängigkeit vom Liganden der zur Behandlung der Kleinhirnneuronen genutzt wird. Im Rahmen dieser Arbeit konnte außerdem gezeigt werden, dass die durch Zugabe von NCAM-Antikörper oder



FGF-2 stimulierte Entstehung des PSA-NCAM-Fragments von einer Calmodulin-abhängigen Aktivierung von NOS und von der damit verbundenen Produktion und Freisetzung von NO in den extrazellulären Raum abhängt. Extrazelluläres NO ist in der Lage MMP-9 durch S-Nitrosylierung zu aktivieren, wodurch die Aktivität von MMP-2 gesteigert wird, was dann die Spaltung von PSA-NCAM und den Import des PSA-NCAM-Fragments in den Zellkern bewirkt. Im Unterschied dazu kann die Stimulation von Neuronen mit dem MARCKS-ED-Peptid eine PLD- und PI3K-induzierte Aktivierung von MMP-2 und eine MMP-2-abhängige Spaltung von PSA-NCAM in Kleinhirnneuronen vermitteln.

Immunelektronenmikroskopie und subzelluläre Fraktionierung von Oberflächenbiotinylierten und durch NCAM-Antikörper stimulierten cerebellaren Neuronen wurde verwendet, um den Transport des PSA-tragenden NCAM-Fragments von der Plasmamembran in den Zellkern zu untersuchen. Das PSA-NCAM-Fragment wird in Endosomen transportiert und mit Hilfe von Calmodulin aus den Endosomen in das Zytoplasma freigesetzt. Beim Import vom Zytoplasma in den Zellkern spielt Calmodulin jedoch keine Rolle und ich konnte feststellen, dass das PSA-NCAM-Fragment in Abhängigkeit von PC4 und Cofilin in den Zellkern transportiert wird. Im Rahmen dieser Arbeit konnte die Interaktion von PSA mit PC4 und Cofilin mittels ELISA und Immunpräzipitation mit einem Antikörper, der gegen PSA gerichtet ist, charakterisiert werden. Mit Hilfe des *proximity ligation assay* wurde die Interaktion von PSA mit PC4 und Cofilin auch im Zellkern nachgewiesen.

Ein wichtiger neuer Befund meiner Arbeit war, dass die Mengen des nukleären PSA-NCAM-Fragments in Abhängigkeit vom Tag-Nacht-Rhythmus oszillieren. Des Weiteren zeigten die Ergebnisse, dass die Regulation der mRNA-Mengen der zirkadianen Uhr zugehörigen Gene *circadian locomotor output cycles kaput* (CLOCK) und *period-1* (Per-1) durch das nukleäre PSA-NCAM Fragment beeinflusst waren. Mittels *microarray analysis* wurde der Einfluss des PSA-NCAM- bzw. des NCAM-Fragmentes, welches kein PSA trägt, auf die Regulation der nukleären mRNA-Mengen des *nuclear receptor subfamily 2 group F member 6* (Nr2f6) bzw. des *low density lipoprotein receptor-related protein 2* (Lrp2) sowie von  $\alpha$ -Synuclein festgestellt. Die Untersuchungen mit qPCR zeigten eine vermehrte Genexpression von Nr2f6, welche durch nukleäres PSA und eine vermehrte Genexpression von Lrp2 und  $\alpha$ -synuclein welche durch nukleäres NCAM induziert wurden.

## 9. ABBREVIATIONS

---

Ab	antibody
AA	arachidonic acid
ADAM	a disintegrin and metalloprotease
AMPA	$\alpha$ -amino-3-hydroxy-5-methyl-4-isoxazolepropionic acid
ATP	adenosine triphosphate
BDNF	brain derived neurotrophic factor
BSA	bovine serum albumine
CaCl <sub>2</sub>	calcium chloride
CaM	almodulin
cAMP	cyclic adenosine monophosphate
cDNA	Complementary deoxyribonucleic acid
cGMP	cyclic guanosine monophosphatase
CHO	chinese hamster ovary
CO <sub>2</sub>	carbon dioxide
COCK	circadian Locomoter Output Cycles Kaput
CREB	cAMP response element-binding protein
Ct	cycle threshold
DAG	diacylglycerol
DAN	diamine 2,3-diaminonaphthalene
DAPI	2-(4-Amidinophenyl)-1 <i>H</i> -indole-6-carboxamidine
dH <sub>2</sub> O	ultrapure water
DMF	dimethylformamide
DMSO	dimethyl sulfoxide
dNTP	deoxy nucleoside triphosphate
DTT	dithiothreitol
ECD	extracellular domain
ED	effector domain
EDTA	ethylenediaminetetraacetic acid
EGFR	epidermal growth factor receptor
ELISA	enzyme-linked immunosorbent assay
EM	immunolectron microcopy
EndoN	endoneuraminidase N
ER	endoplasmatic reticulum
ER	endoplasmatic reticulum
ERK	extracellular signal-regulated kinase
FAK	focal adhesion kinase
FGF-2	fibroblast growth factor-2
FGFR	fibroblast growth factor receptor
FN	fibronectine
GAPDH	glyceraldehyde 3-phosphate dehydrogenase
GDNF	glia-derived neurotrophic factor
GMEM	Glasgow minimal essential medium

## ABBREVIATIONS

GPI	glycosylphosphatidylinositol
GST	glutathione S- transferase
HCL	hydrochloride acid
HEPES	4-(2-hydroxyethyl)-1-piperazineethanesulfonic acid
HIS	polyhistidine
HRP	horse radish peroxidase
IB	immunoblot
ICD	intracellular domain
IgG	immunoglobulin G
IP	immunoprecipitation
IP <sub>3</sub>	inositol-1,4,5-trisphosphate
KCL	potassium chloride
kDa	kilo dalton
KH <sub>2</sub> PO <sub>4</sub>	potassium dihydrogen phosphate
Kir3.3	inwardly rectifying K <sup>+</sup> channel
Lrp2	low Density Lipoprotein Receptor-Related Protein 2
LTP	long term potentiation
MAPK	mitogen-activated protein kinase
MARCKS	myristoylated alanine-rich C-kinase substrate
Mg(CH <sub>3</sub> COO) <sub>2</sub>	magnesium acetate
MgCl <sub>2</sub>	magnesium chloride
MMP-2	matrix metalloprotease-2
MMP2/9	matrix metalloprotease-2/9
MMP-9	matrix metalloprotease-9
MMTS	methyl methanethiosulfonate
Na <sub>2</sub> HPO <sub>4</sub>	sodium hydrogen phosphate
Na <sub>4</sub> P <sub>2</sub> O <sub>7</sub>	tetrasodium diphosphate
NaCl	sodium chloride
NaHCO <sub>3</sub>	sodium hydrogen carbonate
NaOH	sodium hydroxide
NCAM	neural cell adhesion molecule
NI	nuclear import assay
NMDA	N-methyl-D-aspartate
NO	nitric oxide
NO <sub>2</sub> <sup>-</sup>	nitrite
NO <sub>3</sub> <sup>-</sup>	nitrate
NOS	nitric oxide synthase
NP-40	nonyl phenoxypolyethoxylethanol.
Nr2f6	nuclear Receptor Subfamily 2 Group F Member 6
OPD	o-phenylenediamine dihydrochloride
PC4	positive transcription factor 4
PCR	polymerase chain reaction
PEG	polyethylene glycol
PEG	polyethylene glycol
Per	period 1

## ABBREVIATIONS

PI3K	protein 3-kinase
PIP <sub>2</sub>	phosphatidylinositol-1,4,5-bisphosphate
PKC	protein kinase C
PLA	proximity ligation assay
PLC	phospholipase C
PLD	phospholipase D
PLL	poly-l-lysine
PMSF	phenylmethanesulfonyl fluoride
PNGase F	peptide-N-glycosidase F
PSA	polysialic acid
RFU	relative fluorescence units
RNA	ribonucleic acid
RPTPalpha	receptor-like protein-tyrosine phosphatase alpha
RT	room temperature
SCN	suprachiasmatic nucleus
SDS	sodium dodecyl sulfate
sGC	soluble guanylyl cyclase
SNCA	$\alpha$ synuclein
ST8SiaII and IV	polysialyltransferases II and IV
SYBR	N',N'-dimethyl-N-[4-[(E)-(3-methyl-1,3-benzothiazol-2-ylidene)methyl]-1-phenylquinolin-1-ium-2-yl]-N-propylpropane-1,3-diamine
TA	translocation assay
TACE	tumor necrosis factor alpha converting enzyme
Taq	Taq polymerase
TIMP-1	tissue metalloprotease-1
Tris	2-Amino-2-hydroxymethyl-propane-1,3-diol
TrkB	tyrosine receptor kinase B
ZT	Zeitgeber

## 10. REFERENCES

---

- Albach, C.; Damoc, E.; Denzinger, T.; Schachner, M.; Przybylski, M.; Schmitz, B. (2004) Identification of N-glycosylation sites of the murine neural cell adhesion molecule NCAM by MALDI-TOF and MALDI-FTICR mass spectrometry. *Analytical and bioanalytical Chemistry* 378 (4), pp. 1129–1135.
- Allen, S. J.; Dawbarn, D. (2006) Clinical relevance of the neurotrophins and their receptors. *Clinical Science* 110 (2), pp. 175–191.
- Angata, K.; Long, J. M.; Bukalo, O.; Lee, W.; Dityatev, A.; Wynshaw-Boris, A.; Schachner, M.; Fukuda, M.; Marth, J. D. (2004) Sialyltransferase ST8Sia-II assembles a subset of polysialic acid that directs hippocampal axonal targeting and promotes fear behavior. *Journal of Biological Chemistry* 279 (31), pp. 32603–32613.
- Aonurm-Elm, A.; Jaako, K.; Jurgenson, M.; Zharkovsky, A. (2016) Pharmacological approach for targeting dysfunctional brain plasticity: Focus on neural cell adhesion molecule (NCAM). *Pharmacological Research*. 113 (PtB), pp.731-738.
- Aonurm-Helm, A.; Anier, K.; Zharkovsky, T.; Castren, E.; Rantamaki, T.; Stepanov, V.; Järv, J.; Zharkovsky, A. (2015) NCAM-deficient mice show prominent abnormalities in serotonergic and BDNF systems in brain - Restoration by chronic amitriptyline. *Journal of the European College of Neuropsychopharmacology* 25 (12), pp. 2394–2403.
- Arbuzova, A.; Murray, D.; McLaughlin, S. (1998) MARCKS, membranes, and calmodulin: kinetics of their interaction. *Biochimica et Biophysica acta* 1376 (3), pp. 369–379.
- Arbuzova, A.; Schmitz, A. A. P.; Vergeres, G. (2002) Cross-talk unfolded: MARCKS proteins. *Biochemical Journal* 362 (Pt 1), pp. 1–12.
- Balsalobre, A.; Marcacci, L.; Schibler, U. (2000): Multiple signaling pathways elicit circadian gene expression in cultured Rat-1 fibroblasts. In *Current Biology* 10 (20), pp. 1291–1294..
- Becker, C. G.; Artola, A.; Gerardy-Schahn, R.; Becker, T.; Welzl, H.; Schachner, M. (1996) The polysialic acid modification of the neural cell adhesion molecule is involved in spatial learning and hippocampal long-term potentiation. *Journal of Neuroscience Research* 45 (2), pp. 143–152.
- Beggs, H. E.; Baragona, S. C.; Hemperly, J. J.; Maness, P. F. (1997) NCAM140 interacts with the focal adhesion kinase p125(fak) and the SRC-related tyrosine kinase p59(fyn). *Journal of Biological Chemistry* 272 (13), pp. 8310–8319.
- Bellucci, A.; Navarria, L.; Falarti, E.; Zaltieri, M.; Bono, F.; Collo, G.; Spillantini, M. G.; Missale, C.; Spano, P. (2011) Redistribution of DAT/ $\alpha$ -synuclein complexes visualized by "in situ" proximity ligation assay in transgenic mice modelling early Parkinson's disease. *PLoS One* 6 (12), e27959.
- Benskey, M. J.; Perez, R. G.; Manfredsson, F. P. (2016) The contribution of alpha synuclein to neuronal survival and function - Implications for Parkinson's disease. *Journal of Neurochemistry* 137 (3), pp. 331–359.
- Benson, D. L.; Colman, D. R.; Huntley, G. W. (2001): Molecules, maps and synapse specificity. *Nature Review Neuroscience* 2 (12), pp. 899–909.
- Berridge, M. J. (1993) Cell signalling. A tale of two messengers. *Nature* 365 (6445), pp. 388–389.
- Bhat, S.; Silberberg, D. H. (1988) Developmental expression of neural cell adhesion molecules of oligodendrocytes in vivo and in culture. *Journal of Neurochemistry* 50 (6), pp. 1830–1838.
- Bodrikov, V.; Leshchyn'ska, I.; Sytnyk, V.; Overvoorde, J.; den Hertog, J.; Schachner, M. (2005) RPTPalph is essential for NCAM-mediated p59fyn activation and neurite elongation. *Journal of Cell Biology* 168 (1), pp. 127–139.
- Bolton, S. J.; Perry, V. H. (1997) Histone H1; a neuronal protein that binds bacterial lipopolysaccharide. *Journal Neurocytology* 26(12), pp.823-831.

- Bonfanti, L.; Theodosis, D. T. (2009) Polysialic acid and activity-dependent synapse remodeling. *Cell Adhesion & Migration* 3 (1), pp. 43–50.
- Bouzioukh, F.; Tell, F.; Jean, A.; Rougon, G. (2001) NMDA receptor and nitric oxide synthase activation regulate polysialylated neural cell adhesion molecule expression in adult brainstem synapses. *Journal of Neuroscience* 21 (13), pp. 4721–4730.
- Breitsprecher, D.; Koestler, S. A.; Chizhov, I.; Nemethova, M.; Mueller, J.; Goode, B. L.; Small, J. V.; Rottner, (2011): Cofilin cooperates with fascin to disassemble filopodial actin filaments. *Journal of Cell Science* 124 (Pt 19), pp. 3305–3318.
- Brenneman, L. H.; Kochlamazashvili, G.; Stoenica, L.; Nonneman, R. J.; Moy, S. S.; Schachner, M.; Dityatev, A.; Maness, P. F. (2011) Transgenic mice overexpressing the extracellular domain of NCAM are impaired in working memory and cortical plasticity. *Neurobiology of Disease* 43 (2), pp. 372–378.
- Brockstedt, U.; Dobra, K.; Nurminen, M.; Hjerpe, A. (2002): Immunoreactivity to cell surface syndecans in cytoplasm and nucleus: tubulin-dependent rearrangements. *Experimental Cell Research* 274 (2), pp. 235–245.
- Brown, D. T.; Alexander B. T.; Sittman, D. B. (1996) Differential effect of H1 variant overexpression on cell cycle progression and gene expression. *Nucleic Acids Research* 24 (3), pp. 486–93.
- Brummendorf, T.; Rathjen, F. G. (1995) Cell adhesion molecules 1: immunoglobulin superfamily. *Protein Profile* 2 (9), pp. 963–1108.
- Calvo, O.; Manley, J. L. (2005) The transcriptional coactivator PC4/Sub1 has multiple functions in RNA polymerase II transcription. *The EMBO Journal* 24 (5), pp. 1009–1020.
- Cassens, C.; Kleene, R.; Xiao, M.-F.; Friedrich, C.; Dityateva, G.; Schafer-Nielsen, C.; Schachner, M. (2010). Binding of the Receptor Tyrosine Kinase TrkB to the Neural Cell Adhesion Molecule (NCAM) Regulates Phosphorylation of NCAM and NCAM-dependent Neurite Outgrowth. *Journal of Biological Chemistry* 285 (37), pp. 28959–28967.
- Chen, S.; Mantei, N.; Dong, L.; Schachner, M. (1999) Prevention of neuronal cell death by neural adhesion molecules L1 and CHL1. *Journal of Neurobiology* 38 (3), pp. 428–439.
- Chuong, C. M.; Edelman, G. M. (1984) Alterations in neural cell adhesion molecules during development of different regions of the nervous system. *Journal of Neuroscience* 4 (9), pp. 2354–2368.
- Cole, G. J.; Loewy, A.; Glaser, L. (1986) Neuronal cell-cell adhesion depends on interactions of N-CAM with heparin-like molecules. *Nature* 320 (6061), pp. 445–447.
- Conesa, C.; Acker, J. (2010) Sub1/PC4 a chromatin associated protein with multiple functions in transcription. *RNA Biology* 7 (3), pp. 287–290.
- Covault, J.; Liu, Q.-Y.; El-Deeb, S. (1991) Calcium-activated proteolysis of intracellular domains in the cell adhesion molecules NCAM and N-cadherin. *Molecular Brain Research* 11 (1), pp. 11–16.
- Cremer, H.; Lange, R.; Christoph, A.; Plomann, M.; Vopper, G.; Roes, J.; Brown, R.; Baldwin, S.; Kraemer, P.; Scheff, S.; Barthels, D.; Rajewsky, K.; Wille, W. (1994) Inactivation of the N-CAM gene in mice results in size reduction of the olfactory bulb and deficits in spatial learning. *Nature* 367 (6462), pp. 455–459.
- Cunningham, B. A.; Hemperly, J. J.; Murray, B. A.; Prediger, E. A.; Brackenbury, R.; Edelman, G. M. (1987) Neural cell adhesion molecule: structure, immunoglobulin-like domains, cell surface modulation, and alternative RNA splicing. *Science* 236 (4803), pp. 799–806.
- Curreli, S.; Arany, Z.; Gerardy-Schahn, R.; Mann, D.; Stamatou, N. M. (2007) Polysialylated neuropilin-2 is expressed on the surface of human dendritic cells and modulates dendritic cell-T lymphocyte interactions. *The Journal of Biological Chemistry* 282 (42), pp. 30346–30356.
- Czech, M. P. (2000) PIP2 and PIP3: complex roles at the cell surface. *Cell* 100 (6), pp. 603–606.

- Dai, S.; Sarmiere, P. D.; Wiggan, O.; Bamburg, J. R.; Zhou, D. (2004) Efficient Salmonella entry requires activity cycles of host ADF and cofilin. *Cellular Microbiology* 6 (5), pp. 459–471.
- Das, C.; Gadad, S. S.; Kundu, T. K. (2010) Human positive coactivator 4 controls heterochromatinization and silencing of neural gene expression by interacting with REST/NRSF and CoREST. *Journal of Molecular Biology* 397 (1), pp. 1–12.
- Dean, R. A.; Overall, C. M. (2007) Proteomics Discovery of Metalloproteinase Substrates in the Cellular Context by iTRAQ™ Labeling Reveals a Diverse MMP-2 Substrate Degradome. *Molecular & Cellular Proteomics* 6 (4), pp. 611–623.
- Denninger, J. W.; Marletta, M. A. (1999) Guanylate cyclase and the NO/cGMP signaling pathway. *Bioenergetics* 1411 (2–3), pp. 334–350.
- Doherty, P.; Walsh, F. S. (1996) CAM-FGF receptor interactions: a model for axonal growth. *Molecular and Cellular Neurosciences* 8 (2-3), pp. 99–111.
- Eckhardt, M.; Mühlenhoff, M.; Bethe, A.; Koopman, J.; Frosch, M.; Gerardy-Schahn, R. (1995) Molecular characterization of eukaryotic polysialyltransferase-1. *Nature* 373 (6516), pp. 715–718.
- El Maarouf, A.; Rutishauser, U. (2010) Use of PSA-NCAM in repair of the central nervous system. *Advances in Experimental Medicine and Biology* 663, pp. 137–147.
- Endo, A.; Nagai, N.; Urano, T.; Ihara, H.; Takada, Y.; Hashimoto, K.; Takada, A. (1998) Proteolysis of highly polysialylated NCAM by the tissue plasminogen activator-plasmin system in rats. *Neuroscience Letters* 246 (1), pp. 37–40.
- Endo, A.; Nagai, N.; Urano, T.; Takada, Y.; Hashimoto, K.; Takada, A. (1999) Proteolysis of neuronal cell adhesion molecule by the tissue plasminogen activator–plasmin system after kainate injection in the mouse hippocampus. *Neuroscience Research* 33 (1), pp. 1–8.
- Fedorkova, L.; Rutishauser, U.; Prosser, R.; Shen, H.; Glass, J. D. (2002) Removal of polysialic acid from the SCN potentiates nonphotic circadian phase resetting. *Physiology & Behavior* 77 (2–3), pp. 361–369.
- Finne, J. (1982) Occurrence of unique polysialosyl carbohydrate units in glycoproteins of developing brain. *Journal of Biological Chemistry* 257 (20), pp. 11966–11970.
- Fleming, C. E.; Mar, F. M.; Franquinho, F.; Saraiva, M. J.; Sousa, M. M. (2009) Transthyretin internalization by sensory neurons is megalin mediated and necessary for its neurotogenic activity. *Journal of Neuroscience* 29 (10), pp. 3220–3232.
- Francavilla, C.; Loeffler, S.; Piccini, D.; Kren, A.; Christofori, G.; Cavallaro, U. (2007) Neural cell adhesion molecule regulates the cellular response to fibroblast growth factor. *Journal of Cell Science*. 120 (24), p. 4388.
- Franz, Colin K.; Rutishauser, Urs; Rafuse, Victor F. (2005) Polysialylated neural cell adhesion molecule is necessary for selective targeting of regenerating motor neurons. *The Journal of Neuroscience* 25 (8), pp. 2081–2091.
- Gallant, C.; You, J. Y.; Sasaki, Y.; Grabarek, Z.; Morgan, K. G. (2005) MARCKS is a major PKC-dependent regulator of calmodulin targeting in smooth muscle. *Journal of Cell Science* 118 (Pt 16), pp. 3595–3605.
- Gambhir, A.; Hangyas-Mihalyne, G.; Zaitseva, I.; Cafiso, D. S.; Wang, J.; Murray, D.; Pentylala, S. N.; Smith, S. O.; McLaughlin, S. (2004) Electrostatic sequestration of PIP<sub>2</sub> on phospholipid membranes by basic/aromatic regions of proteins. *Biophysical Journal* 86 (4), pp. 2188–2207.
- Gascon, E.; Vutskits, L.; Kiss, J. Z. (2007) Polysialic acid–neural cell adhesion molecule in brain plasticity: From synapses to integration of new neurons. In *Brain Research Reviews* 56 (1), pp. 101–118.
- Gennarini, G.; Rougon, G.; Deagostini-Bazin, H.; Hirn, M.; Goridis, C. (1984) Studies on the transmembrane disposition of the neural cell adhesion molecule N-CAM. A monoclonal antibody recognizing a cytoplasmic

- domain and evidence for the presence of phosphoserine residues. *European Journal of Biochemistry* 142 (1), pp. 57-64.
- Geyer, H.; Bahr, U.; Liedtke, S.; Schachner, M.; Geyer, R. (2001) Core structures of polysialylated glycans present in neural cell adhesion molecule from newborn mouse brain. *European Journal of Biochemistry* 268 (24), pp. 6587-6599.
- Giuliano, K. A.; Khatib, F. A.; Hayden, S. M.; Daoud, E. W.; Adams, M. E.; Amorese, D. A.; Bernstein, B. W.; Bamburg, J. R. (1988) Properties of purified actin depolymerizing factor from chick brain. *Biochemistry* 27 (25), pp. 8931-8938.
- Glass, J. D.; Lee, W.; Shen, H.; Watanabe, M. (1994) Expression of immunoreactive polysialylated neural cell adhesion molecule in the suprachiasmatic nucleus. *Neuroendocrinology* 60 (1), pp. 87-95.
- Glass, J. D.; Watanabe, M.; Fedorkova, L.; Shen, H.; Ungers, G.; Rutishauser, U. (2003) Dynamic regulation of polysialylated neural cell adhesion molecule in the suprachiasmatic nucleus. *Neuroscience* 117 (1), pp. 203-211.
- Glass, J. D.; Shen, H.; Fedorkova, L.; Chen, L.; Tomasiewicz, H.; Watanabe, M. (2000) Polysialylated neural cell adhesion molecule modulates photic signaling in the mouse suprachiasmatic nucleus. *Neuroscience Letters* 280 (3), pp. 207-210.
- Goetz, R.; Mohammadi, M. (2013) Exploring mechanisms of FGF signalling through the lens of structural biology. *Nature Reviews Molecular Cell Biology* 14(3), pp. 166-80.
- Golombek, D. A.; Rosenstein, R. E. (2010) Physiology of Circadian Entrainment. *Physiological Reviews* 90 (3), pp. 1063-1102.
- Greif, D. M.; Sacks, D. B.; Michel, T. (2004) Calmodulin phosphorylation and modulation of endothelial nitric oxide synthase catalysis. *Proceedings of the National Academy of Sciences* 101 (5), pp. 1165-1170.
- Gu, Z.; Kaul, M.; Yan, B.; Kridel, S. J.; Cui, J.; Strongin, A.; Smith, J. W.; Liddington, R. C.; Lipton, S. A. (2002) S-nitrosylation of matrix metalloproteinases: signaling pathway to neuronal cell death. *Science* 297 (5584), pp. 1186-1190.
- Hammond, M. S. L.; Sims, C.; Parameshwaran, K.; Suppiramaniam, V.; Schachner, M.; Dityatev, A. (2006) Neural cell adhesion molecule-associated polysialic acid inhibits NR2B-containing N-methyl-D-aspartate receptors and prevents glutamate-induced cell death. *The Journal of Biological Chemistry* 281 (46), pp. 34859-34869.
- Hart G. W.; West C. M. (2009): Nucleocytoplasmic Glycosylation. Chapter 17: Essentials of Glycobiology. Varki A.; Cummings R. D.; Esko J. D.; Freeze H. H.; Stanley P.; Bertozzi C. R.; Etzler M. E. 2nd. Cold Spring Harbor (NY): Cold Spring Harbor Laboratory Press.
- He, H. T.; Barbet, J.; Chaix, J. C.; Goridis, C. (1986) Phosphatidylinositol is involved in the membrane attachment of NCAM-120, the smallest component of the neural cell adhesion molecule. *The EMBO Journal* 5 (10), pp. 2489-2494.
- He, Q.; Meiri, K. F. (2002) Isolation and characterization of detergent-resistant microdomains responsive to NCAM-mediated signaling from growth cones. *Molecular and Cellular Neurosciences* 19 (1), pp. 18-31.
- Hinkle, C. L.; Diestel, S.; Lieberman, J.; Maness, P. F. (2006) Metalloprotease-induced ectodomain shedding of neural cell adhesion molecule (NCAM). *Journal of Neurobiology* 66 (12), pp.1378-1395.
- Horstkorte, R.; Schachner, M.; Magyar, J. P.; Vorherr, T.; Schmitz, B. (1993) The fourth immunoglobulin-like domain of NCAM contains a carbohydrate recognition domain for oligomannosidic glycans implicated in association with L1 and neurite outgrowth. *The Journal of Cell Biology* 121 (6), pp. 1409-1421.
- Hübschmann, M. V.; Skladchikova, G.; Bock, E.; Berezin, V. (2005) Neural cell adhesion molecule function is regulated by metalloproteinase-mediated ectodomain release. *Journal of Neuroscience Research* 80 (6), pp. 826-837.



- Ispanovic, E.; Haas, T. L. (2006) JNK and PI3K differentially regulate MMP-2 and MT1-MMP mRNA and protein in response to actin cytoskeleton reorganization in endothelial cells. *Cell physiology* 291 (4), C579-C588.
- Jaffrey, S. R.; Erdjument-Bromage, H.; Ferris, C. D.; Tempst, P.; Snyder, S. H. (2001) Protein S-nitrosylation: a physiological signal for neuronal nitric oxide. *Nature Cell Biology* 3 (2), pp. 193–197.
- Johnson, C. P.; Fujimoto, I.; Rutishauser, U.; Leckband, D. E. (2005) Direct evidence that neural cell adhesion molecule (NCAM) polysialylation increases intermembrane repulsion and abrogates adhesion. *The Journal of Biological Chemistry* 280 (1), pp. 137–145.
- Kaeffer, B.; Pardini, L. (2005) Clock genes of Mammalian cells: practical implications in tissue culture. *In Vitro Cellular & Developmental Biology - Animal* 41 (10), pp. 311–320.
- Kalus, I.; Bormann, U.; Mzoughi, M.; Schachner, M.; Kleene, R. (2006) Proteolytic cleavage of the neural cell adhesion molecule by ADAM17/TACE is involved in neurite outgrowth. *Journal of Neurochemistry* 98 (1), pp. 78–88.
- Kanato, Y.; Kitajima, K.; Sato, C. (2008) Direct binding of polysialic acid to a brain-derived neurotrophic factor depends on the degree of polymerization. *Glycobiology* 18 (12), pp. 1044–1053.
- Kantarci, S.; Al-Gazali, L.; Hill, R. S.; Donnai, D.; Black, G. C.; Bieth, E.; Chassaing, N.; Lacombe, D.; Devriendt, K.; Teebi, A.; Loscertales, M.; Robson, C.; Liu, T.; MacLaughlin, D. T.; Noonan, K. M.; Russell, M. K.; Walsh, C. A.; Donahoe, P. K.; Pober, B. R. (2007) Mutations in LRP2, which encodes the multiligand receptor megalin, cause Donnai-Barrow and facio-oculo-acoustico-renal syndromes. *Nature Genetics* 39 (8), pp. 957–959.
- Kiryushko, D.; Korshunova, I.; Berezin, V.; Bock, E. (2006) Neural cell adhesion molecule induces intracellular signaling via multiple mechanisms of Ca<sup>2+</sup> homeostasis. *Molecular Biology of the Cell* 17 (5), pp. 2278–2286.
- Kiselyov, V. V.; Soroka, V.; Berezin, V.; Bock, E. (2005) Structural biology of NCAM homophilic binding and activation of FGFR. *Journal of Neurochemistry* 94 (5), pp. 1169–1179.
- Kiss, J. Z.; Rougon, G. (1997) Cell biology of polysialic acid. In *Current Opinion in Neurobiology* 7 (5), pp. 640–646.
- Kleene, R.; Mzoughi, M.; Joshi, G.; Kalus, I.; Bormann, U.; Schulze, C.; Xiao, M. F.; Dityatev, A.; Schachner, M. (2010a) NCAM-induced neurite outgrowth depends on binding of calmodulin to NCAM and on nuclear import of NCAM and fak fragments. *The Journal of Neuroscience* 30 (32), pp. 10784–10798.
- Kleene, R.; Cassens, C.; Bähring, R.; Theis, T.; Xiao, M.-F.; Dityatev, A.; Schäfer-Nielsen, C.; Döring, F.; Wischmeyer, E.; Schachner, M. (2010b) Functional consequences of the interactions among the neural cell adhesion molecule NCAM, the receptor tyrosine kinase TrkB, and the inwardly rectifying K<sup>+</sup> channel KIR3.3. *Journal of Biological Chemistry* 285 (37), pp. 28968–28979.
- Kleene, R.; Schachner, M. (2004) Glycans and neural cell interactions. *Nat Rev Neurosci* 5 (3), pp. 195–208.
- Klingenberg, O.; Wiedlocha, A.; Rapak, A.; Khnykin, D.; Citores, L.; Olsnes, S. (2000) Requirement for C-terminal end of fibroblast growth factor receptor 4 in translocation of acidic fibroblast growth factor to cytosol and nucleus. *Journal of Cell Science* 113 (Pt 10), pp. 1827–1838.
- Klint, P.; Claesson-Welsh, L. (1999) Signal transduction by fibroblast growth factor receptors. *Frontiers in Bioscience* 4, D165-D177.
- Ko, C. H.; Takahashi, J. S. (2006) Molecular components of the mammalian circadian clock. *Human Molecular Genetics* 15 (2), pp. 271–277.
- Kochoyan, A.; Poulsen, F. M.; Berezin, V.; Bock, E.; Kiselyov, V. V. (2008) Structural basis for the activation of FGFR by NCAM. *Protein Science* 17 (10), pp. 1698–1705.

- Kolkova, K. (2010) Biosynthesis of NCAM. *Advances in Experimental Medicine and Biology* 663, pp. 213–225.
- Leshchyn'ska, I.; Sytnyk, V.; Morrow, J. S.; Schachner, M. (2003) Neural cell adhesion molecule (NCAM) association with PKC $\beta$ 2 via beta1 spectrin is implicated in NCAM-mediated neurite outgrowth. *The Journal of Cell Biology* 161 (3), pp. 625–639.
- Liao, H.-J.; Carpenter, G.; Schmid, S. (2007) Role of the Sec61 translocon in EGF receptor trafficking to the nucleus and gene expression. *Molecular Biology of the Cell* 18 (3), pp. 1064–1072.
- Lin, S. Y.; Makino, K.; Xia, W.; Matin, A.; Wen, Y.; Kwong, K. Y.; Bourguignon, L.; Hung, M. C. (2001) Nuclear localization of EGF receptor and its potential new role as a transcription factor. *Nature Cell Biology* 3 (9), pp. 802–808.
- Linnertz, C.; Saucier, L.; Ge, D.; Cronin, K. D.; Burke, J. R.; Browndyke, J. N.; Hulette, C. M.; Welsh-Bohmer K. A.; Chiba-Falek O. (2009) Genetic regulation of alpha-synuclein mRNA expression in various human brain tissues. *PLoS One* 4(10), e7480.
- Litosch, I. (2016) Decoding Galphaq signaling. *Life Sciences* 152, pp. 99–106.
- Lobaugh, L. A.; Blackshear, P. J. (1990) Neuropeptide Y stimulation of myosin light chain phosphorylation in cultured aortic smooth muscle cells. *The Journal of Biological Chemistry* 265 (30), pp. 18393–18399.
- Lutz, D.; Wolters-Eisfeld, G.; Joshi, G.; Djogo, N.; Jakovcevski, I.; Schachner, M.; Kleene, R. (2012) Generation and nuclear translocation of sumoylated transmembrane fragment of cell adhesion molecule L1. *Journal of Biological Chemistry* 287 (21), pp. 17161–17175.
- Manabe, S.-I.; Gu, Z.; Lipton, S. A. (2005) Activation of matrix metalloproteinase-9 via neuronal nitric oxide synthase contributes to NMDA-induced retinal ganglion cell death. *Investigative Ophthalmology & Visual Science* 46 (12), pp. 4747–4753.
- Maness, P. F.; Schachner, M. (2007) Neural recognition molecules of the immunoglobulin superfamily: signaling transducers of axon guidance and neuronal migration. *Nature Neuroscience* 10 (1), pp. 19–26.
- Marzolo, M.-P.; Farfan, P. (2011) New insights into the roles of megalin/LRP2 and the regulation of its functional expression. *Biological Research* 44 (1), pp. 89–105.
- May, P.; Woldt, E.; Matz, R. L.; Boucher, P. (2007) The LDL receptor-related protein (LRP) family: an old family of proteins with new physiological functions. *Annals of Medicine* 39 (3), pp. 219–228.
- McIlroy, B. K.; Walters, J. D.; Blackshear, P. J.; Johnson, J. D. (1991) Phosphorylation-dependent binding of a synthetic MARCKS peptide to calmodulin. *Journal of Biological Chemistry* 266 (8), pp. 4959–4964.
- McNamara, R. K.; Stumpo, D. J.; Morel, L. M.; Lewis, M. H.; Wakeland, E. K.; Blackshear, P. J.; Lenox, R. H. (1998) Effect of reduced myristoylated alanine-rich C kinase substrate expression on hippocampal mossy fiber development and spatial learning in mutant mice: transgenic rescue and interactions with gene background. *Proceedings of the National Academy of Sciences* 95 (24), pp. 14517–14522.
- Milev, P.; Friedlander, D. R.; Sakurai, T.; Karthikeyan, L.; Flad, M.; Margolis, R. K.; Grumet, M.; Margolis, R. U. (1994) Interactions of the chondroitin sulfate proteoglycan phosphacan, the extracellular domain of a receptor-type protein tyrosine phosphatase, with neurons, glia, and neural cell adhesion molecules. *Journal of Cell Biology* 127 (6 Pt 1), pp. 1703–1715.
- Mishra, B.; von der Ohe, M.; Schulze, C.; Bian, S.; Makhina, T.; Loers, G.; Kleene, R.; Schachner, M. (2010) Functional role of the interaction between polysialic acid and extracellular histone H1. *Journal of Neuroscience* 30 (37), pp. 12400–12413.
- Morash, S. C.; Douglas, D.; McMaster, C. R.; Cook, H. W.; Byers, D. M. (2005) Expression of MARCKS effector domain mutants alters phospholipase D activity and cytoskeletal morphology of SK-N-MC neuroblastoma cells. *Neurochemical Research* 30 (11), pp. 1353–1364.

- Mühlenhoff, M.; Eckhardt, M.; Bethe, A.; Frosch, M.; Gerardy-Schahn, R. (1996) Autocatalytic polysialylation of polysialyltransferase-1. *EMBO Journal* 15 (24), pp. 6943–6950.
- Mühlenhoff, M.; Eckhardt, M.; Gerardy-Schahn, R. (1998) Polysialic acid: three-dimensional structure, biosynthesis and function. *Current Opinion in Structural Biology* 8 (5), pp. 558–564.
- Muller, D.; Djebbara-Hannas, Z.; Jourdain, P.; Vutskits, L.; Durbec, P.; Rougon, G.; Kiss, J. Z. (2000) Brain-derived neurotrophic factor restores long-term potentiation in polysialic acid-neural cell adhesion molecule-deficient hippocampus. *Proceedings of the National Academy of Sciences* 97 (8), pp. 4315–4320.
- Muller, D.; Wang, C.; Skibo, G.; Toni, N.; Cremer, H.; Calaora, V. Rougon, G.; Kiss, J. Z. (1996) PSA-NCAM is required for activity-induced synaptic plasticity. *Neuron* 17 (3), pp. 413–422.
- Munsie, L. N.; Desmond, C. R.; Truant, R. (2012) Cofilin nuclear-cytoplasmic shuttling affects cofilin-actin rod formation during stress. *Journal of Cell Science* 125 (Pt 17), pp. 3977–3988.
- Navarria, L.; Zaltieri, M.; Longhena, F.; Spillantini, M. G.; Missale, C.; Spano, P.; Bellucci, A. (2015) Alpha-synuclein modulates NR2B-containing NMDA receptors and decreases their levels after rotenone exposure. *Neurochemistry International* 85-86, pp. 14-23.
- Nelson, R. W.; Bates, P. A.; Rutishauser, U. (1995) Protein determinants for specific polysialylation of the neural cell adhesion molecule. *Journal of Biological Chemistry* 270 (29), pp. 17171–17179.
- Niethammer, P.; Delling, M.; Sytnyk, V.; Dityatev, A.; Fukami, K.; Schachner, M. (2002) Cosignaling of NCAM via lipid rafts and the FGF receptor is required for neuritogenesis. *Journal of Cell Biology* 157 (3), pp. 521–532.
- Obrdlík, A.; Percipalle, P. (2011) The F-actin severing protein cofilin-1 is required for RNA polymerase II transcription elongation. *Nucleus* 2 (1), pp. 72–79.
- von der Ohe, M.; Wheeler, S. F.; Wührer, M.; Harvey, D. J.; Liedtke, S.; Mühlenhoff, M.; Gerardy-Schahn R.; Geyer, H.; Dwek, R. A.; Geyer, R.; Wing, D. R.; Schachner, M. (2002) Localization and characterization of polysialic acid-containing N-linked glycans from bovine NCAM. *Glycobiology* 12 (1), pp. 47–63.
- Oltmann-Norden, I.; Galuska, S. P.; Hildebrandt, H.; Geyer, R.; Gerardy-Schahn, R.; Geyer, H.; Mühlenhoff, M. (2008) Impact of the polysialyltransferases ST8SiaII and ST8SiaIV on polysialic acid synthesis during postnatal mouse brain development. *Journal of Biological Chemistry* 283 (3), pp. 1463–1471.
- Ono, S.; Hane, M.; Kitajima, K.; Sato, C. (2012) Novel regulation of fibroblast growth factor 2 (FGF2)-mediated cell growth by polysialic acid. *Journal of Biological Chemistry* 287 (6), pp. 3710–3722.
- Ono, S. (2007) Mechanism of depolymerization and severing of actin filaments and its significance in cytoskeletal dynamics. *International Review of Cytology* 258, pp. 1–82.
- Paratcha, G.; Ledda, F.; Ibanez, C. F. (2003) The neural cell adhesion molecule NCAM is an alternative signaling receptor for GDNF family ligands. *Cell* 113 (7), pp. 867–879.
- Park, C.; Shin, K. S.; Ryu, J. H.; Kang, K.; Kim, J.; Ahn, H.; Huh, Y. (2004) The inhibition of nitric oxide synthase enhances PSA-NCAM expression and CREB phosphorylation in the rat hippocampus. *Neuroreport* 15 (2), pp. 231–234.
- Parseghian, M. H.; Luhrs, K. A. (2006) Beyond the walls of the nucleus: the role of histones in cellular signaling and innate immunity. *Biochemistry and Cell Biology* 84 (4), pp. 589–604.
- Patterson, S. L.; Abel, T.; Deuel, T. A.; Martin, K. C.; Rose, J. C.; Kandel, E. R. (1996) Recombinant BDNF rescues deficits in basal synaptic transmission and hippocampal LTP in BDNF knockout mice. *Neuron* 16 (6), pp. 1137–1145.
- Pendleton, A.; Pope, B.; Weeds, A.; Koffer, A. (2003) Latrunculin B or ATP depletion induces cofilin-dependent translocation of actin into nuclei of mast cells. *The Journal of Biological Chemistry* 278 (16), pp. 14394–14400.

- Persohn, E.; Pollerberg, G. E.; Schachner, M. (1989) Immunoelectron-microscopic localization of the 180 kD component of the neural cell adhesion molecule N-CAM in postsynaptic membranes. *Journal of Comparative Neurology* 288 (1), pp. 92–100.
- Piazza, M.; Futrega, K.; Spratt, D. E.; Dieckmann, T.; Guillemette, J. G. (2012) Structure and dynamics of calmodulin (CaM) bound to nitric oxide synthase peptides: effects of a phosphomimetic CaM mutation. *Biochemistry* 51(17), pp. 3651-3661.
- Planque, N. (2006) Nuclear trafficking of secreted factors and cell-surface receptors: new pathways to regulate cell proliferation and differentiation, and involvement in cancers. *Cell Communication and Signaling* 4 (1), pp. 1–18.
- Ponimaskin, E.; Dityateva, G.; Ruonala, M. O.; Fukata, M.; Fukata, Y.; Kobe, F.; Wouters, F. S.; Delling, M.; Bredt, D. S.; Schachner, M.; Dityatev, A. (2008) Fibroblast growth factor-regulated palmitoylation of the neural cell adhesion molecule determines neuronal morphogenesis. *Journal of Neuroscience* 28 (36), pp. 8897–8907.
- Probstmeier, R.; Bilz, A.; Schneider-Schaulies, J. (1994) Expression of the neural cell adhesion molecule and polysialic acid during early mouse embryogenesis. *Journal of Neuroscience Research* 37 (3), pp. 324–335.
- Prosser, R. A.; Rutishauser, U.; Ungers, G.; Fedorkova, L.; Glass, J. D. (2003) Intrinsic role of polysialylated neural cell adhesion molecule in photic phase resetting of the mammalian circadian clock. *The Journal of Neuroscience* 23 (2), pp. 652–658.
- Rauch, M. E.; Ferguson, C. G.; Prestwich, G. D.; Cafiso, D. S. (2002) Myristoylated alanine-rich C kinase substrate (MARCKS) sequesters spin-labeled phosphatidylinositol 4,5-bisphosphate in lipid bilayers. *Journal of Biological Chemistry* 277 (16), pp. 14068–14076.
- Reich, R.; Blumenthal, M.; Liscovitch, M. (1995) Role of phospholipase D in laminin-induced production of gelatinase A (MMP-2) in metastatic cells. *Clinical & Experimental Metastasis* 13 (2), pp. 134–140.
- Reilly, J. F.; Maher, P. A. (2001) Importin beta-mediated nuclear import of fibroblast growth factor receptor: role in cell proliferation. *Journal of Cell Biology* 152 (6), pp. 1307-1312.
- Rho, J. K.; Lee, H.; Park, C.-S.; Choi, C.-M.; Lee, J. C. (2013) Sensitive detection of EML4-ALK fusion oncoprotein of lung cancer by in situ proximity ligation assay. *Clinical Chemistry and Laboratory Medicine* 51 (9), pp. 1843–1848.
- Ridnour, L. A.; Windhausen, A. N.; Isenberg, J. S.; Yeung, N.; Thomas, D. D.; Vitek, M. P.; Roberts, D. D.; Wink, D. A. (2007) Nitric oxide regulates matrix metalloproteinase-9 activity by guanylyl-cyclase-dependent and -independent pathways. *Proceedings of the National Academy of Sciences* 104 (43), pp. 16898–16903.
- Rutishauser, U. (2008) Polysialic acid in the plasticity of the developing and adult vertebrate nervous system. *Nature Review Neuroscience* 9 (1), pp. 26–35.
- Saffell, J. L.; Doherty, P.; Tiveron, M. C.; Morris, R. J.; Walsh, F. S. (1995) NCAM requires a cytoplasmic domain to function as a neurite outgrowth-promoting neuronal receptor. *Molecular and Cellular Neurosciences* 6 (6), pp. 521–531.
- Sato, C.; Hane, M.; Kitajima, K. (2016) Relationship between ST8SIA2, polysialic acid and its binding molecules, and psychiatric disorders. *Biochimica et Biophysica Acta* 1860 (8), pp. 1739–1752.
- Schmidt, C. M.; McKillop, I. H.; Cahill, P. A.; Sitzmann, J. V. (1999) The role of cAMP-MAPK signalling in the regulation of human hepatocellular carcinoma growth in vitro. *European Journal of Gastroenterology & Hepatology* 11 (12), pp. 1393–1399.
- Schnaar, R. L.; Gerardy-Schahn, R.; Hildebrandt, H. (2014) Sialic acids in the brain: gangliosides and polysialic acid in nervous system development, stability, disease, and regeneration. *Physiological Reviews* 94 (2), pp. 461–518.

- Seki, T. (2003) Microenvironmental elements supporting adult hippocampal neurogenesis. *Anatomical Science International* 78 (2), pp. 69–78.
- Shapiro, L.; Love, J.; Colman, D. R. (2007) Adhesion molecules in the nervous system: structural insights into function and diversity. *Annual Review of Neuroscience* 30, pp. 451–474.
- Shen, H.; Glass, J. D.; Seki, T.; Watanabe, M. (1999) Ultrastructural analysis of polysialylated neural cell adhesion molecule in the suprachiasmatic nuclei of the adult mouse. *Anatomical Report* 256 (4), pp. 448–457.
- Shen, H.; Watanabe, M.; Tomasiewicz, H.; Glass, J. D. (2001) Genetic deletions of NCAM and PSA impair circadian function in the mouse. *Physiology & Behavior* 73 (1–2), pp. 185–193.
- Shen, H.; Watanabe, M.; Tomasiewicz, H.; Rutishauser, U.; Magnuson, T.; Glass, J. D. (1997) Role of Neural Cell Adhesion Molecule and Polysialic Acid in Mouse Circadian Clock Function. *Journal of Neuroscience* 17 (13), pp. 5221–5229.
- Sheppard, A.; Wu, J.; Rutishauser, U.; Lynch, G. (1991) Proteolytic modification of neural cell adhesion molecule (NCAM) by the intracellular proteinase calpain. *Protein Structure and Molecular Enzymology* 1076 (1), pp. 156–160.
- Shichi, K.; Fujita-Hamabe, W.; Harada, S.; Mizoguchi, H.; Yamada, K.; Nabeshima, T.; Tokuyama, S. (2011) Involvement of matrix metalloproteinase-mediated proteolysis of neural cell adhesion molecule in the development of cerebral ischemic neuronal damage. *Journal of Pharmacology and Experimental Therapeutics* 338 (2), pp. 701–710.
- Sikorski, T. W.; Ficarro, S. B.; Holik, J.; Kim, T.; Rando, O. J.; Marto, J. A.; Buratowski, S. (2011) Sub1 and RPA associate with RNA polymerase II at different stages of transcription. *Molecular Cell* 44 (3), pp. 397–409.
- Soldner, F.; Stelzer, Y.; Shivalila, C. S.; Abraham, B. J.; Latourelle, J. C.; Barrasa, M. I.; Goldmann, J.; Myers, R. H.; Young, R. A.; Jaenisch, R. (2016) Parkinson-associated risk variant in distal enhancer of  $\alpha$ -synuclein modulates target gene expression. *Nature* 5, 533(7601), 95–99.
- Storms, S. D.; Rutishauser, U. (1998) A role for polysialic acid in neural cell adhesion molecule heterophilic binding to proteoglycans. *The Journal of biological chemistry* 273 (42), pp. 27124–27129.
- Su, Z.; Blazing, M. A.; Fan, D.; George, S. E. (1995) The calmodulin-nitric oxide synthase interaction. Critical role of the calmodulin latch domain in enzyme activation. *Journal of Biological Chemistry* 270 (49), pp. 29117–29122.
- Theis, T.; Mishra, B.; von der Ohe, M.; Loers, G.; Prondzynski, M.; Pless, O.; Blackshear, P. J.; Schachner, M.; Kleene, R. (2013) Functional role of the interaction between polysialic acid and yristoylated alanine-rich C kinase substrate at the plasma membrane. *Journal of Biological Chemistry* 288 (9), pp. 6726–6742.
- Vaithianathan, T.; Matthias, K.; Bahr, B.; Schachner, M.; Suppiramaniam, V.; Dityatev, A.; Steinhäuser, C. (2004) Neural cell adhesion molecule-associated polysialic acid potentiates alpha-amino-3-hydroxy-5-methylisoxazole-4-propionic acid receptor currents. *Journal of Biological Chemistry* 279 (46), pp. 47975–47984.
- Vargas, T.; Bullido, M. J.; Martinez-Garcia, A.; Antequera, D.; Clarimon, J.; Rosich-Estrago, M.; Martin-Requero, A.; Mateo, I.; Rodriguez-Rodriguez, E.; Vilella-Cuadrada, E.; Frank A.; Lleo, A.; Molina-Porcel, L.; Blesa, R.; Combarros, O.; Gomez-Isla, T.; Bermejo-Pareja F.; Valdivieso, F.; Carro, E. (2010) A megalin polymorphism associated with promoter activity and Alzheimer's disease risk. *Neuropsychiatric* 153B (4), pp. 895–902.
- Vergheze, G. M.; Johnson, J. D.; Vasulka, C.; Haupt, D. M.; Stumpo, D. J.; Blackshear, P. J. (1994) Protein kinase C-mediated phosphorylation and calmodulin binding of recombinant myristoylated alanine-rich C kinase substrate (MARCKS) and MARCKS-related protein. *Journal of Biological Chemistry* 269 (12), pp. 9361–9367.

- Vutskits, L.; Djebbara-Hannas, Z.; Zahng, H.; Paccaud, J. P.; Durbec, P.; Rougon, G.; Muller, D.; Kiss, J. Z. (2001) PSA-NCAM modulates BDNF-dependent survival and differentiation of cortical neurons. *European Journal of Neuroscience* 13 (7), pp. 1391-402.
- Walsh, F. S.; Doherty, P. (1996) Cell adhesion molecules and neuronal regeneration. *Current Opinion in Cell Biology* 8 (5), pp. 707-713.
- Wang, Y.; Barnes, E. O.; Laborda, E.; Molina, A.; Compton, R. G. (2012): Differential pulse techniques in weakly supported media: Changes in the kinetics and thermodynamics of electrode processes resulting from the supporting electrolyte concentration. *Journal of Electroanalytical Chemistry* 673, pp. 13-23.
- Warnecke, M.; Oster, H.; Revelli, J.-P.; Alvarez-Bolado, G.; Eichele, G. (2005) Abnormal development of the locus coeruleus in Ear2(Nr2f6)-deficient mice impairs the functionality of the forebrain clock and affects nociception. *Genes & Development* 19 (5), pp. 614-625.
- Werneburg, S.; Buettner, F. F.; Mühlenhoff, M.; Hildebrandt, H. (2015) Polysialic acid modification of the synaptic cell adhesion molecule SynCAM 1 in human embryonic stem cell-derived oligodendrocyte precursor cells. *Stem Cell Research* 14 (3), pp. 339-346.
- Wijnen, H.; Young, M. W. (2006) Interplay of circadian clocks and metabolic rhythms. *Annual Review of Genetics* 40, pp. 409-448.
- Williams, E. J.; Furness, J.; Walsh, F. S.; Doherty, P. (1994a) Activation of the FGF receptor underlies neurite outgrowth stimulated by L1, N-CAM, and N-cadherin. *Neuron* 13 (3), pp. 583-594.
- Williams, E. J.; Walsh, F. S.; Doherty, P. (1994b) The production of arachidonic acid can account for calcium channel activation in the second messenger pathway underlying neurite outgrowth stimulated by NCAM, N-Cadherin, and L1. *Journal of Neurochemistry* 62 (3), pp.1231-1234.
- Ziembra, B. P.; Burke, J. E.; Masson, G.; Williams, R. L.; Falke, J. J. (2016) Regulation of PI3K by PKC and MARCKS: Single-Molecule Analysis of a Reconstituted Signaling Pathway. *Biophysical Journal* 110 (8), pp. 1811-1825.
- Zong, F.; Fthenou, E.; Wolmer, N.; Hollósi, P.; Kovalszky, I.; Szilák, L.; Mogler, C.; Nilsonne, G.; Tzanakakis, G.; Dobra K. (2009) Syndecan-1 and FGF-2, but not FGF receptor-1, share a common transport route and co-localize with heparanase in the nuclei of mesenchymal tumor cells. *PLoS One* 4 (10), e7346.

## 11. ACKNOWLEDGEMENTS

---

This study has been performed in the Institute for Biosynthesis of Neuronal Structures of the Centre of Molecular Neurobiology Hamburg (ZMNH). I would like to heartily thank Prof. Dr. Melitta Schachner for providing me the interesting research project and for writing my thesis in her lab. I am grateful for the fruitful discussions and for constant support and guidance during these years which have helped to expand my knowledge and skills in the field of molecular neuroscience. Moreover I am grateful to Prof. Dr. Melitta Schachner and Prof. Dr. Thorsten Burmester for the reviewing and co-supervision of my thesis.

I am very thankful to Dr. Ralf Kleene for introducing me into this interesting project and for his excellent supervision during my work. The suggestions and the valuable time that he rendered for planning the experiments with me and for discussion of my results at all times were of immense help.

I am very grateful to Dr. Gabriele Loers for her introduction into primary cell culture and into basic biochemical techniques. She always helped me to overcome some experimental problems and provided me with a lot of beneficial advices.

I have to thank Ralf and Gaby for providing me with a big source of ideas for this research and for their suggestions during the writing and for their time and effort they had spend in the correction of my thesis.

I specially thank Dr. David Lutz for his support and knowledge in immunoelectron microscopy and for the analyzing of my samples. Many to thank Dr. Igor Jakovcevsk and Dr. Jelena Katic for introducing me into morphological techniques.

I would like to thank Dr. Sabine Fleischer, Dr. Irm Hermans-Borgmeyer, Dr. Uwe Borgmeyer and Dr. Stefan Kindler from the ZMNH PhD program for their time and discussions with me.

I am grateful to my previous and current colleagues Dr. Thomas Theis, Kristina Kraus, Agnieszka Kotarska, Jelena Brasanac, Gaston Castillo, Maria Girbes-Minguez and Mina Yakoub for their support and the nice working atmosphere in the lab. Specially I am thankful to Ute Bork for her technical assistance and her support and commitment in the lab.

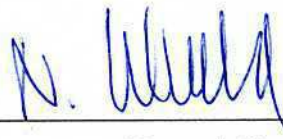
Last but never the least my heartiest thanks go to my parents, brother and my friends which supports me with a lot of energie and care. My special thank goes to my dearest boyfriend Marian who was giving me encourage, power and love the hole time.

## EIDESSTATTLICHE VERSICHERUNG

Sehr geehrte Damen und Herren,

Hiermit erkläre ich an Eides statt, dass ich die vorliegende Dissertation selbstständig verfasst und keine anderen als die angegebenen Quellen und Hilfsmittel genutzt habe.

Hamburg, den 01. Januar 2017



---

Unterschrift





Zentrum für Molekulare Neurobiologie Hamburg (ZMNH)  
Institut für Synaptische Physiologie

Dr. Christine Gee  
Institut für Synaptische Physiologie

ZMNH, Falkenried 94  
20251 Hamburg

Telefon: +49 (0) 40 7410-57190

Fax: +49 (0) 40 7410-58364

[christine.gee@zmnh.uni-hamburg.de](mailto:christine.gee@zmnh.uni-hamburg.de)

Universitätsklinikum Hamburg-Eppendorf | ZMNH | Institute für Synaptische Physiologie  
Falkenried 94 | 20251 Hamburg

**English Language Thesis Certification – Nina Westphal**

Hamburg, 16.12.2016

As a native english speaker, I can certify that the quality of English in the thesis “Functional role of a polysialic acid-carrying proteolytic fragment of the neural cell adhesion molecule NCAM in the nervous system” is of a high standard and that the thesis is fully understandable.

Sincerely yours,

Christine Gee